Chromatin reader Dido3 regulates the genetic network of B cell differentiation

Fernando Gutiérrez del Burgo[1], Tirso Pons[1], Enrique Vázquez de Luis[2], Carlos Martínez-A[1] & Ricardo Villares[1,*]

[1] Centro Nacional de Biotecnología/CSIC, Darwin 3, Cantoblanco, E-28049, Madrid, Spain

[2] Centro Nacional de Investigaciones Cardiovasculares, Instituto de Salud Carlos III, Melchor Fernández Almagro 3, Madrid 28029, Spain.

[*]email: rvillares@cnb.csic.es

ABSTRACT

The development of hematopoietic lineages is based on a complex balance of transcription factors whose expression depends on the epigenetic signatures that characterize each differentiation step. The B cell lineage arises from hematopoietic stem cells through the stepwise silencing of stemness genes and balanced expression of mutually regulated transcription factors, as well as DNA rearrangement. Here we report the impact on B cell differentiation of the lack of DIDO3, a reader of chromatin status, in the mouse hematopoietic compartment. We found reduced DNA accessibility in hematopoietic precursors, leading to severe deficiency in the generation of successive B cell differentiation stages. The expression of essential transcription factors and differentiation markers is affected, as is the somatic recombination process.

One Sentence Summary: Epigenetic control of early hematopoiesis

INTRODUCTION

B cells originate from hematopoietic stem cells (HSC) through a process defined by the activation or silencing of key transcription factors and parallel DNA recombination events. HSC can develop into multipotent progenitors (MPP) that are able to give rise to B cells by passing through lymphoid progenitor cell stages known as lymphoid-primed multi-potential progenitor (LMPP), common lymphoid progenitor (CLP), prepro-B, pro-B, pre-B, and immature B cells[1]. It is currently considered that B cell differentiation is initiated by interaction of a PU.1-, IKAROS-, and IL7R-expressing progenitor cell with stromal cells and IL7[2]. IKAROS complexes might initially suppress myeloid gene expression in lymphoid progenitors and then participate in B and T cell specification by respectively silencing T and B cell-specific loci[3]. Progenitor progression to the B cell lineage is then controlled by the transcription factors E2A (E12/47), EBF1, FOXO1, and PAX5[4]. E2A and EBF1 specify the B cell lineage by activating B lymphoid gene expression in prepro-B cells[5]. PAX5 subsequently controls B cell commitment at the transition to the pro-B cell stage, and is necessarily maintained to sustain B-lineage identity[6].

In the CLP subpopulation, somatic rearrangements are first detected between the diversity (DH) and joining (JH) gene segments of the heavy chain (HC) locus[7]. CLP can mature into four different cell types: B lymphocytes, T lymphocytes, NK, and dendritic cells[8,9]. In mice, upregulation of B220 expression in a CLP subpopulation allows differentiation to prepro-B cells. Prepro-B cells determined for B cell differentiation are characterized by tyrosine kinase AA4.1 (CD93) expression[10]. Entry into the B lineage is marked by CD19 expression and the end of DH-JH rearrangement in the early pro-B state. IL7R signaling contributes to early pro-B cell survival and transient proliferation[11] and sequential reorganization of Ig genes[12]. Heavy chain recombination culminates in the late pro-B stage with the productive rearrangement of VH heavy chain variable segments with DJH (VH-DJH). Productive rearrangement of *Igh* is essential for pre-BCR signaling, a crucial checkpoint for survival and further differentiation[13].

Post-translational histone modifications constitute one of the epigenetic mechanisms that enables control of chromatin structure, DNA accessibility, and gene expression in a dynamic, cell type-specific manner. Proteins that specifically "read" these modifications must play important roles in development, differentiation, and tumorigenesis[14].

Dido1 is a gene highly conserved throughout evolution; its orthologs have been identified in chordates and insects. The shortest coded protein isoform, DIDO1, includes nuclear location and nuclear export signals (NLS, NES), and a plant Zn-finger homeodomain (PHD);

it interacts with chromatin mainly through di/trimethylated lysine of histone H3 (H3K4me2/3)[15,16], and works as a reader of the chromatin state. DIDO1 nonetheless has yet to be assigned to known complexes. Both PHD and NLS, but not NES, are present in all three natural isoforms. DIDO2 is the least abundant and includes a transcription elongation factor S-II central domain (TFIIS2M), necessary for the nucleolytic activity of RNA polymerase II, and a *Spen* paralog and ortholog C-terminal (SPOC) domain of unknown function, but which is usually found in proteins with transcriptional co-repressor activity. DIDO3 is the main isoform and includes all domains found in DIDO2 as well as a coiled-coil (CC) region that probably has a tertiary or quaternary structural function. There are also proline-, alanine-, and arginine-rich low complexity regions in DIDO3.

All attempts to date to delete *Dido1* have resulted in cell lethality. N-terminal truncation results in a shorter protein, expressed by an internal promoter, that is associated with aneuploidy, centrosome amplification, and DNA damage in the form of centromere-localized breaks[17]. Mice with the *Dido1ΔNT* mutation show hematological myeloid neoplasms, and alterations in *DIDO1* are associated with the myelodysplastic syndrome in humans[18]. Deletion of the *Dido* 3' terminal exon (E16) renders a truncated form of DIDO3. This deficiency leads to embryonic lethality; embryos die by gestation day 8.5[19]. Embryonic stem cells (ESC) derived from these DIDO3 C-terminal mutant embryos do not differentiate correctly, but retain their capacity for self-renewal.

Due to the embryonic lethality of *Dido* exon 16, we studied the effect of DIDO3 deficiency in the hematopoietic lineage using mice bearing a floxed exon 16 of *Dido1*[20] and a Cre recombinase gene under the control of the *Vav1* promoter. In these mice, the B cell population is severely reduced by a primary defect in the pro-B cell stage progression. By analyzing the transcription levels of B cell-characteristic genes at distinct differentiation stages in these DIDO3-deficient mice, we detected a reduction in expression of B cell markers and of transcription factors specifically in prepro-B samples; there was no evident alteration in master regulators such as *Spi1* (PU.1) and *Ikzf1* (Ikaros). This finding suggests that DIDO3 is involved in the chromatin restructuring needed for the B cell differentiation pathway, and thus controls developmental cell plasticity and lineage fate decisions.

RESULTS

To characterize the *Dido1* expression pattern in different human and mouse tissues, cell lines, and cancer types, we retrieved publicly available data from web bio-sources. Publicly accessible expression data using the Genevisible tool (https://genevisible.com/search). The Affymetrix microarray data (Mouse Genome 430 2.0 and Human Genome U133 Plus 2.0) explored with Genevisible web bio-source (https://genevisible.com) indicated the highest *Dido1* mRNA expression in hematopoietic system (Suppl Fig. 1).

Loss of the DIDO3 protein results in anemia and severe peripheral lymphopenia. To examine the *in vivo* role of DIDO3 in hematopoiesis, we deleted exon 16 of *Dido1* in murine HSC early in development. Mice homozygous for the floxed allele (*Dido1*$^{flE16/flE16}$) were crossed with mice carrying one functional and one mutated allele of *Dido1* (*Dido1*$^{\Delta E16}$, which lacks the DIDO3 C terminus) and the *Vav1:iCre* transgene. The resulting *Dido1*$^{flE16/\Delta E16}$;R26R-EYFP;iCre^{Vav1} mice (hereafter *Dido1*ΔE16) were used as experimental subjects, and *Dido1*$^{flE16/+}$;R26R-EYFP;iCre^{Vav1} littermates (hereafter wt) were used as controls, except where otherwise specified. Ablation of *Dido1* exon 16 in early development was confirmed by qPCR on DNA samples from sorted lineage (lin)$^{-}$Kit^{+}Sca1^{+}(LSK) cells derived from bone marrow, which showed >99% reduction in *Dido1*E16 DNA content (Suppl. Fig. 2A). Hematologic analysis showed a significant decrease in cellular components when *Dido1*ΔE16 mice were compared with heterozygous littermate controls. White blood cell numbers dropped to 33% of wt (1.71 ± 1.32 vs. 5.11 ± 1.71 x 10^3 cells/µl, n = 8, $p<0.001$) and red cell numbers to 92% of wt values (9.65 ± 0.36 vs. 10.54 ± 0.51 x 10^6 cells/µl, n = 8, $p<0.01$). Within the leukocyte fraction, the lymphocyte subpopulation was responsible for the defect observed, with a reduction in cell numbers to 27% of wt (1.02 ± 1.20 vs. 3.84 ± 1.61 x 10^3 cells/µl, n = 8, $p<0.0001$)(Suppl. Fig. 2B). Peripheral blood samples from wt and *Dido1*ΔE16 mice were analyzed by flow cytometry for EYFP reporter expression; >97% of circulating cells were EYFP-positive in both lymphoid and myeloid gates, as determined by forward scatter (FS) vs. side scatter (SS) gating (Suppl. Fig. 2B).

We calculated total numbers of various cell subsets in peripheral blood from complete blood count and flow cytometry data. *Dido1*ΔE16 mice had significantly reduced lymphocyte subset counts, including B220 (58 ± 26 vs 2675 ± 423 cells/µl in control samples, n = 6, $p<0.0001$), CD4 (301 ± 123 vs. 749 ± 232 cells/µl, $p<0.01$), CD8 (109 ± 48 vs. 423 ± 87 cells/µl, $p<0.001$), and NK1.1 (50 ± 15 vs. 163 ± 69 cells/µl, $p<0.05$), while monocyte (90 ± 8 vs 90 ±

18 cells/µl) and granulocyte numbers (590 ± 348 vs. 550 ± 161cells/µl) were unaffected (Suppl. Fig. 2C).

Bone marrow analysis

As *Dido1* was previously linked more closely to development and stem cell differentiation functions, we analyzed the B cell lineage in bone marrow. We used flow cytometry to identify $lin^{-}Sca1^{+}Kit^{+}IL7R^{-}$ (LSK) and common lymphoid progenitor $lin^{-}Sca1^{+}Kit^{+}IL7R^{+}$ (CLP) cell populations (Fig. 1A, B), and found no significant differences in the relative proportions of each. *Dido1*ΔE16 mice nonetheless showed reduced total bone marrow cellularity and significantly lower absolute numbers of LSK cells (Fig. 1C). From *Dido1*ΔE16 mice, we obtained $2.85 \pm 0.83 \times 10^4$ lin^{-} cells, vs. $3.93 \pm 0.45 \times 10^4$ from wt mice (n = 6, t-test ** $p<0.01$). The numbers for LSK ($2.09 \pm 0.64 \times 10^4$ vs. $3.34 \pm 1.0 \times 10^4$, t-test * $p<0.05$) and CLP cells ($1.13 \pm 0.50 \times 10^3$ vs. $1.92 \pm 1.17 \times 10^3$, t-test $p>0.05$) were also reduced.

We analyzed the distribution of the distinct B cell precursor subpopulations, namely prepro-B, pro-B, pre-B, and immature B cells (Fig. 2A). The number of $B220^{+}$ cells was substantially lower in *Dido1*ΔE16 mice than in the controls (Fig. 2B). The populations most affected were pre-B and immature B cells, although the number of prepro-B and pro-B cells was similar in mice of both genotypes (Fig. 2C).

Functional analysis of bone marrow precursors

Signaling from the pre-BCR complex promotes the survival and proliferation of cells that have successfully rearranged the *Igh* locus. This is a first checkpoint in which those rearrangements that give rise to a non-functional heavy chain lead to death by apoptosis. In a second checkpoint, immature B cells whose BCR is activated by an autoantigen in the bone marrow can undergo receptor editing to modify its light chain, or they can be deleted by apoptosis. To detect cell death in distinct precursor populations, we used flow cytometry to analyze bone marrow samples from *Dido1*ΔE16 and wt mice, labeled with appropriate antibodies and with annexin V and DAPI. Apoptosis levels were slightly higher, although non-significant, in *Dido1*ΔE16 mice. In the immature B cell population ($EYFP^{+}B220^{+}CD19^{+}IgM^{low}$), both the number of apoptotic cells and the annexin V mean fluorescence intensity (MFI) in bone marrow of *Dido1*ΔE16 mice showed a significant increase relative to controls (Fig. 3A, B). This result suggests that DIDO3 affects the size of the immature B cell population in *Dido1*ΔE16 mice by increasing the number of cells that

undergo apoptotic processes at this stage. Our data support the idea that DIDO3 is necessary to overcome the BCR signaling-dependent checkpoint.

We used BrdU (5-bromo-2'-deoxyuridine) incorporation in DNA *in vivo* to identify and examine proliferating cells, and DAPI to determine DNA content and cell cycle stages. The percentage of cells that incorporated BrdU after 18 h post-intraperitoneal inoculation was quantified for pro-B/pre-B and immature/mature cells. Cells from *Dido1*ΔE16 mice in pro-B/pre-B states showed BrdU incorporation similar to that of control mice (Fig. 3C). In the immature cell population, there was a non-significant increase in the percentage and the MFI of cells that incorporated BrdU (Fig. 3D) (MFI: pro-B/pre-B: *Dido1*ΔE16 = 4.25 ± 1.232 vs. wt = 4.68 ± 0.852; t test: $p = 0.52$; $n = 3$; immature/mature B cells, *Dido1*ΔE16 = 3.92 ± 1.144 vs. wt = 2.05 ± 0.443; t test: $p = 0.09$; $n = 3$). The percentage of S phase cells of the pro-B/pre-B populations of both mice was similar, although an increase in the percentage of *Dido1*ΔE16 mature/immature B cells was observed in this phase (Fig. 3D). The increase in the percentage of immature B cells in the S phase in *Dido1*ΔE-16 compared to control mice and the increase in cells that undergo apoptosis suggest that immature B cells from *Dido1*ΔE16 mice undergo an S phase block that eventually leads to apoptosis.

In vitro differentiation assays were carried out to determine whether the *Dido1*ΔE16 mouse B cell precursors showed alterations in their capacity to differentiate towards the B lineage. We purified cells lacking lineage-specific markers (lin^-) by negative selection and plated them in a semi-solid matrix and medium optimized for B cell development, supplemented with IL7. In cultures from wild type mice, between 25 and 35 colonies were counted in plates seeded with 2 x 10^6 lin^-cells/ml; between 5 and 10 smaller cell groups/plate were also registered. No colonies were found in plates seeded with lin^- precursors from *Dido1*ΔE16 mice, although we detected some clusters consisting of a small number of disaggregated and undifferentiated cells (Suppl. Fig 3). B lineage cells ($B220^+$) from the conditional mutant mice thus showed differentiation defects when stimulated *in vitro*, with blocking of proliferation and maturation towards B precursors in these conditions.

Hematopoietic precursors from *Dido1*ΔE16 mice failed to repopulate the bone marrow of irradiated recipient mice

The small numbers of early hematopoietic precursors in *Dido1*ΔE16 mice and their failure in *in vitro* differentiation assays led us to test whether their function was affected *in vivo* in the absence of DIDO3. As transplant recipients, we used nine lethally irradiated B6-CD45.1 mice

(10 Gy); at day 1 post-irradiation, the mice received a retro-orbital injection of 150 µL of a mixture of total bone marrow cells (3.75 x 10^6) from CD45.2$^+$EYFP$^+$*Dido1*ΔE16 and CD45.2$^+$EYFP$^-$*Dido1*$^+$ donor mice, at a 1:1 ratio (Suppl. Fig. 4).

Peripheral blood was monitored at day 14 post-inoculation; we observed a lower CD45.2$^+$EYFP$^+$*Dido1*ΔE16 cell contribution to circulating blood populations; of the blood cells, 12.78 ± 1.97% were CD45.2$^+$EYFP$^+$*Dido1*ΔE16 and 80.13 ± 3.43% were CD45.2$^+$EYFP$^-$*Dido1*$^+$. A further 6.73 ± 3.45% were endogenous surviving cells (CD45.1$^+$), mainly of the CD3$^+$ phenotype, reported to be thymus-derived radioresistant cells[21] (Fig. 4A). At day 21 post-inoculation, ~25% of circulating leukocytes were B cells, most of which were CD45.2$^+$EYFP$^-$*Dido1*$^+$, with only 0.05% CD45.2$^+$EYFP$^+$*Dido1*ΔE16 and 0.01% CD45.1 B cells. This imbalance was partially anticipated, given the severely biased composition of the transplanted bone marrow, with higher percentages of pre-B and immature B progenitors in wt mice.

At 28 days post-transplant, four mice were sacrificed and their bone marrow analyzed by flow cytometry. The highest percentage of hematopoietic cells observed was CD45.2 (5.91 ± 6.26% CD45.2$^+$EYFP$^+$*Dido1*ΔE16; 55.64 ± 9.42% CD45.2$^+$EYFP$^-$*Dido1*$^+$), with a residual percentage of CD45.1 cells (0.99 ± 0.49%). We also verified that only 3.02 ± 1.96 x 10^4 cells were CD45.2$^+$EYFP$^+$*Dido1*ΔE16 vs. 2.24 ± 1.21 x 10^6 CD45.2$^+$EYFP$^-$ *Dido1*$^+$ cells; 8.45 ± 6.49 x 10^3 CD45.1 cells were also found. This result suggests a lower level of nesting and/or expansion capacity in DIDO3-deficient cells.

At 40 days post-transplant, the five remaining mice were sacrificed and bone marrow populations were analyzed by flow cytometry (Fig. 4B). From 6.04 ± 1.33 x 10^5 lin$^-$ cells/femur, only 1.68 ± 1.13 x 10^4 cells/femur were CD45.2$^+$EYFP$^+$*Dido1*ΔE16, and 1.64 ± 0.41 x 10^4 cells/femur were CD45.1$^+$.

The bone marrow analysis yielded means of 2.25 ± 1.87 x 10^3 LSK and 1.31 ± 1.25 x 10^2 CLP CD45.2$^+$EYFP$^+$*Dido1*ΔE16 cells, significantly lower than the 1.91 ± 0.80 x 10^4 LSK and 8.58 ± 2.34 x 10^2 CLP CD45.2$^+$EYFP$^-$*Dido1*$^+$ cells. B cell precursors were identified by B220 expression and encompass cell populations from the prepro-B phase to immature and mature B cells. Approximately 99% of B220$^+$ cells were CD45.2EYFP$^-$*Dido1*$^+$ (2.15 ± 1.01 x 10^6 cells/femur), and only 2.96 ± 1.90 x 10^4 cells/femur were CD45.2$^+$EYFP$^+$*Dido1*ΔE16 (Fig. 4C). These data indicate that, relative to LSK-wt cells, the LSK-*Dido1*ΔE16 cells and the remainder of the B lineage progenitor cells had a cell-autonomous disadvantage both in nesting and in repopulating the bone marrow of irradiated mice.

Identification of essential regulators of stem cell function and the B cell pathway by ATAC-seq analysis of bone marrow LSK cells

Although the proportion of LSK cells within the lin$^-$ population is similar in wt and *Dido1*ΔE16 mice, adoptive transfer experiments showed a lower repopulation capacity, especially considering that this undifferentiated population was overrepresented in the mutant fraction of the inoculum. As DIDO1 was demonstrated to be a chromatin interactor that recognizes accessible regions of chromatin with H3K4me3 histone marks, we analyzed this population by Omni-ATAC-seq[22]. This technique detects differences in chromatin accessibility, as assessed by sensitivity to DNA digestion by transposase Tn5 in a process termed "tagmentation". The tagmented fragments were subjected to massive sequencing, and two biological replicas with accessible regions in the range of 10^4 were used for differential analysis between wt and *Dido1*ΔE16 LSK cells.

Accessible regions were annotated with the ChIPseeker program[23] by associating the position of the accessible regions in each replica with the structure of the genes (promoter, 5'-UTR, exon, intron, 3'-UTR, or intergenic) in the mouse reference genome assembly GRCm38/UCSC mm10. After filtering low quality reads, an average of 52 million high quality reads were obtained, and 96.1% clean reads were mapped to the GRCm38/UCSC mm10 assembly using Bowtie2 (bowtie-bio.sourceforge.net/bowtie2/) and in parallel BWA-MEM 0.7.15 (http://bio-bwa.sourceforge.net). The largest percentage of accessible regions was concentrated in gene promoters and introns and in intergenic regions, in both LSK-wt and LSK-*Dido1*ΔE16 cells (Fig. 5A). In the *Dido1*ΔE16 samples, however, there was a relative reduction in the number of introns and intergenic regions relative to promoters, which was related to the preferential association of DIDO1 to enhancer sequences over promoters[24].

A Gene Set Enrichment Analysis (GSEA, http://www.gsea-msigdb.org) of the ATAC-seq data was performed. GSEA is a computerized method that determines whether gene sets defined *a priori* show concordant and significant differences between two biological states[25]. In seeking overlaps with genesets in the C2 collection ("curated genesets") of MSigDB, we found that the promoters with the least accessibility in LSK-*Dido1*ΔE16 coincided with (1) genes with mixed epigenetic marks (H3K4me2 and H3K27me3) in mouse embryonic fibroblast (MEF) HCP genes (high-CpG-density promoters), $p<1.79 \times 10^{-49}$; (2) silencing marks (H3K27me3) in embryonic cells, $p<4.88 \times 10^{-31}$; (3) human EED targets (a core subunit of PRC2), $p<3.72 \times 10^{-27}$, and (4) human SUZ12 targets (also a core subunit of PRC2), $p<3.61 \times 10^{-25}$ (Supplementary Table 1). In accordance with these data, our previous microarray data[26]

analyzed here by GSEA, indicate that genes silenced in DIDO3-deficient ESC correlate significantly with those silenced in mouse *Suz12*-deficient ESC; the genes overexpressed in these cells also coincided with those overexpressed in the *Suz12*$^{-/-}$ cells. There thus appears to be a relationship between epigenetic regulation of gene expression by PRC2 and the presence of DIDO3. An online tool (http://bioinformatics.psb.ugent.be/webtools/Venn/) was used to construct a Venn diagram that represents differentially-expressed genes (DEG) associated with distinct genesets by GSEA (Fig. 5B). There was also correlation with (5) genes expressed after p53 activation ($p<1.48 \times 10^{-24}$), in agreement with the *Cdkn2a* alterations observed in *Dido1*ΔE16 mouse samples at later developmental stages (see below).

When analysis was limited to non-promoter regions (intra- or intergenic), using the MSigDB C3 collection ("regulatory target gene sets"), there was significant overlap with (1) the targets of the putative histone-lysine N-methyltransferase PRDM6 ($p<7.5 \times 10^{-24}$), and (2) the set of genes with at least one occurrence of the highly conserved motif M17 AACTTT, a potential binding site for an unknown transcription factor in the region spanning up to 4 kb around their transcription start sites ($p<5.91 \times 10^{-69}$) (Fig. 5C). Within the 79 genes common to the three genesets, we found a number of essential regulators for stem cell function and B cell pathway entrance, including *Akt3, Runx1, Ebf1, Igfr1, Tcf4, Cdk6*, and *Etv6*. GSEA analysis of the few identified sites that show higher accessibility in *Dido1*ΔE16 LSK cells yielded no relevant results.

To validate the expression data in additional samples by RT-qPCR, we selected several genes in the list of regions with different Tn5 accessibility in LSK-wt and LSK-*Dido1*ΔE16 cells: genes related to the Polycomb group (PcG) proteins (*Bmi1, Ezh2*), maintenance and differentiation of stem cells (*Runx1, Nanog, Ikzf2* (Helios), *Tcf12* (Heb)), differentiation towards lineage B (*Klf3, Il7r, Ebf1, Tcf3* (E2A, E12/E47), *Spi1* (PU.1), *Foxo1*) or towards lineage T (*Gata3*), and cell proliferation (*Mycn* (N-myc), *Myc, Cdk6*). The analysis showed that expression of genes related to differentiation towards the B lineage was non-significantly lower in LSK-*Dido1*ΔE16 than in LSK-wt cells. Other genes such as *Gata3* or *Cdk6* were expressed more significantly in LSK-*Dido1*ΔE16 cells, whereas *Nanog* levels were 16 times higher than in LSK-wt cells (Fig. 5D). *Dido1*ΔE16 CLP samples showed reduced *Ebf1* expression, whereas *Nanog* levels were normal.

TLDA analysis of gene expression in B cell precursors.

To analyze expression of several genes related to B cell development in the different precursor subpopulations, we used customized TaqMan Low Density Arrays, tested against preamplified samples of cDNA synthesized from total RNA from sorted subpopulations. The largest number of differences was detected in the prepro-B subpopulation (Fig. 6A), which suggests that a smaller number of cells is able to follow the B cell pathway at this less-differentiated stage. mRNA levels of transcription factors such as *Tcf3*, *Foxo1*, and *Ebf1* (labeled (1) in Fig. 6A) were decreased in *Dido1*ΔE16 compared to wild type mice. These factors are necessary for precursor differentiation towards the B lineage and are crucial for expression of Pax5, an essential factor for maintenance of B line identity. We also observed lower levels of mRNA encoded by genes related to B cell development and maturation (labeled (2) in Fig. 6A), including *Pax5, Igll1*(Igλ5)*, S1pr1, Btk, Blk, Cd79a* (MB-1, Igα)*, Cd79b* (Igβ)*, Irf4, Cr2* (Cd21)*, Pou2af1* (OBF1), and *Cxcr4*. In *Dido1*ΔE16 cells, we detected upregulation of genes (labeled (3) in Fig. 6A) such as *Cebpb*, whose relationship with cancer-driven myelopoiesis is observed in humans[27], and of *Spn* (Cd43), which is downregulated in the wt cells at this stage[28], when V(D)J recombination begins.

As in almost every developmental process, the three "E-proteins" play a fundamental role in hematopoiesis. These transcription factors are characterized by a basic helix-loop-helix (bHLH) domain with capacity to homo- and hetero-dimerize with themselves and other HLH proteins, and to bind to DNA through E-boxes (CACGTG sequences). *Tcf3* (which encodes E2A isoforms E12 and E47) and *Tcf12* (which encodes HEB isoforms HEBcan and HEBalt) have been implicated in B cell development. To test the expression of the distinct isoforms, we designed specific primers for conventional RT-qPCR assays. As already detected in the TLDA assays, *Tcf3* expression was lower in *Dido1*ΔE16 than in wt prepro-B cells; this reduction was due equally to E12 and E47 isoforms (Fig. 6B). However, while the expression of the HEBcan isoform of *Tcf12* (assessed by exon 1/2 levels) was not affected by DIDO3 absence, HEBalt isoform expression (exon X9 levels) dropped to 10% of the wt in *Dido1*ΔE16 prepro-B cells (Fig. 6C).

Tcf3 levels remained low in *Dido1*ΔE16 pro-B cells (Fig. 6D), and we also found low *Bcl2* and high levels of the cell cycle regulator *Cdkn2a* (p16, cyclin-dependent kinase inhibitor 2A). E2A is necessary to maintain *Ebf1* and *Pax5* expression as well as the B cell genetic program, whereas BCL2 is an antiapoptotic factor, and CDKN2A inhibits the kinase-dependent kinase cyclin 4 (CDK4) and therefore blocks the cell cycle in G1.

In the pre-B *Dido1*ΔE16 population, we again detected a pro-apoptotic environment, with low *Bcl2* and high levels of cyclin D2 (*Ccnd2*), which codes for the regulatory subunit of CDK4 and CDK6, necessary for cell cycle G1/S transition. Our data also showed no silencing of genes that encode pre-BCR components such as *Igll1*, *CD79a*, and *CD79b*, or genes that inhibit pro-B cell differentiation such as *Erg* (Fig. 6E).

In immature B-*Dido1*ΔE16 cells, we detected an increase in the mRNA levels of stemness-related transcription factors (*Pou5f1* (Oct-4), *Nanog*, *Kit*, and *Ly6a* (Sca1)), in addition to high levels of pre-BCR surrogate light chain components such as *Vpreb2* and *Vpreb1*, and of cell cycle regulatory genes such as cyclin-dependent kinase inhibitor *Cdkn2b* (p15INK4b). We also observed overexpression of *Id3*, which forms heterodimers with HLH proteins that lead to inhibition of DNA binding and thus, regulation of gene transcription (Fig. 6F). All these results suggested that *Dido1*ΔE16 affects differentiation processes both in mouse hematopoietic precursors and in embryonic stem cells.

RNA-seq analysis of gene expression in pre-B cells

As the first checkpoint in B cell development is dependent on pre-BCR activation and takes place at the pre-B stage[29], where we found the greatest effect of the absence of DIDO3 (seen as lack of progenitor cell progression), we sequenced the transcriptome (RNA-Seq) of cells in this phase.

Using pooled samples (2-3 mice/pool) to obtain sufficient starting material, we sorted pre-B cells by flow cytometry and purified RNA. Two biological replicates were used to construct libraries for massive sequencing. After filtering low quality reads, an average of 24 million clean reads were obtained and 94.91% clean reads were mapped to the mouse genome. A total of 7846 genes with more than three fragments per kilobase of transcript per million mapped reads (FPKM) was used for subsequent analyses. DEG were defined based on the absolute value of their fold change $|FC| \geq 1.5$ ($\log_2 FC > 0.6|$) associated to a false discovery rate (FDR) ≤ 0.05. We found 120 genes with higher expression in wt pre-B cells, and 346 genes upregulated in *Dido1*ΔE16 cells (Supplementary table 2).

The biological significance of DEG was explored using the network tool STRING v.11.0 (https://string-db.org). Gene Ontology (GO) terms with FDR <0.25 included positive regulation of leukocyte differentiation, cellular response to stimulus, positive regulation of lymphocyte activation, positive regulation of lymphocyte differentiation, positive regulation of T cell differentiation, positive regulation of B-cell differentiation, signal transduction, regulation of signaling, immune response, and regulation of leukocyte cell-cell adhesion. After

gene clustering, the highlighted signaling pathways were MTOR, GPCR, Rho-GTPase, interferon, β-catenin, cytokine signaling in the immune system, and antigen processing by ubiquitination and proteosome degradation (Suppl. Fig. 5).

For a second analysis we applied the GSEA tool, using a ranked list of genes with base mean >1, ordered by FC. By analysis against the group of genesets defined as targets of specific transcription factors, we identified the genesets of targets for PRC2 components JARID2 and SUZ12 ($p<0.001$) (Fig. 7). *Aebp2*, a substoichometric PRC2 subunit that stimulates the K9 and K27 methylation of histone $H3^{30}$, was upregulated ($\log_2 FC = 2.61$ FDR = 0.067) in *Dido1*ΔE16 pre-B cells.

The relevance of pre-BCR in the pre-B developmental checkpoint and the PRC2 participation in V(D)J recombination led us to study the effect of DIDO3 deficiency on the transcription of *Igh* and *Igk* loci. Joining (J) and variable (V) regions of the *Igk* locus were not notably affected. There was over-representation of proximal *Igh* V regions (Q52 and 7183 families), whereas intermediate and distal V fragments (mainly J558 and 3609 families) were under-represented in *Dido1*ΔE16 pre-B cells (Fig. 8A and Supplementary table 3). We detected unexpectedly high transcription levels of DNA located between J and D fragments (Fig. 8B). In wt cells, this DNA segment is eliminated by recombination in the previous pro-B stage, or even in prepro-B, by RAG1/2 activity. Finally, we detected expression of the *Igg2b* (γ2b) gene, which suggested that isotype-switched $IgG2b^+$ memory B cells co-purified with pre-B cells ($B220^+CD19^+CD43^-IgM^-$) in numbers substantially higher than in wt samples (Fig. 8C).

DISCUSSION

Although DIDO3, which is expressed ubiquitously in the organism, presumably has a more general function in determining chromatin structure, its profound influence on the B cell population led us to focus our study on this cell lineage. Speculations on the molecular mechanism involved have been treated elsewhere[31,32,20,33]. Here we demonstrate that DIDO3 plays a role in HSC homing and differentiation, as well as in the later B cell differentiation process.

In lymphopoiesis B, Ebf1 is the key transcription factor for B cell specification and compromise[5]. Ectopic expression of Ebf1 in HSC directs differentiation towards the B lineage at the expense of other lineages[34]. *Ebf1*$^{-/-}$ mice maintain a developmental blockade of the B lineage in the prepro-B stage and lack mature B cells[35]. Our mouse model shows partial arrest in B cell development in the prepro- and pro-B populations (B220^{+}CD43^{+}CD19^{-} and B220^{+}CD43^{+}CD19^{+}, respectively), comparable to the phenotype of *Ebf1*$^{+/-}$ mice. Our RT qPCR assays show that *Ebf1* expression in purified *Dido1*ΔE16 CLP is approximately one-third of that observed in wt CLP cells, where the specification process towards the lymphoid lineage begins. Heterozygotic deletion of *Ebf1* resulted in an impaired response to IL7 *in vitro*[36], which provides a possible explanation for the observed stage-specific reduction in cellular expansion. The loss of DIDO3 in the LSK state activates *Nanog* transcription, which negatively modulates *Ebf1*. Decreasing EBF1 levels would reduce the potential of CLP-*Dido1*ΔE16 cells for differentiation into the B lineage.

All the canonical E proteins are important for lymphoid development[37]. HEB (*Tcf12*) and E2 2 (*Tcf4*) are thought to contribute to the total E protein dose needed for B cell development, since the absence of either factor led to a decrease in pro-B cell numbers, but no obvious developmental block[38]. Of the E proteins, E2A is necessary to maintain *Ebf1*, *Foxo1*, and *Pax5* expression, and hence the B cell genetic program. B cell development in Tcf3$^{+/-}$;Tcf12$^{-/-}$ mice is completely blocked at the CLP stage[39]. It is not known, however, whether this arrest is due to the lack of HEBcan, HEBalt, or both isoforms. In our case, neither is completely absent, but whereas HEBcan levels were normal, HEBalt levels dropped in *Dido1*ΔE16 prepro-B cells to 10% of that in wt, which suggests an undescribed function for this isoform. Lack of E2A function results in an inability to rearrange *Igh* gene segments, which can be rescued with a single dose of E2A[40]. Although it remains to be determined whether this effect is dose-dependent, it could explain our results with *Dido1*ΔE16 pre-B cells, in which a substantial number of RNA reads correspond to the segment between D and J fragments, which was deleted efficiently in wt samples.

We also detected abnormal *Igg2b* expression in *Dido1*ΔE16 pre-B cells. CpG DNA stimulates TLR9, with intense expression of activation-induced cytidine deaminase (AICDA) and production of *Igg2b* germ line transcripts in B cell precursors[41], but we did not find *Aicda* or the TLR9-pathway components overexpression. We thus support the possibility of relatively large numbers of isotype-switched memory B cells[42] in *Dido1*ΔE16 bone marrow, as were co-purified in our pre-B cell sorting strategy.

In *Dido1*ΔE16 pro-B cells, we found high levels of *Cdkn2a*, which acts as an inhibitor of the kinase-dependent kinase cyclin 4 (CDK4), and low levels of *Bcl2*, involved in blocking cell death (anti-apoptotic). *Cdkn2a* is a known target of EZH2 in several cell types[43]. *Cdkn2a* codes for p19ARF, which stabilizes p53, as well as p16INK4a, a CDK4 inhibitor[44], both of which could affect the survival and expansion of adaptive lymphoid cells. CDK4 regulates cell progress in G1 and would be inhibited by excess CDKN2A.

EZH2, a core PRC2component, is needed to silence *Cdkn2a* in developing B lymphocytes prior to the preBCR checkpoint[45]. The Cdkn2a/p53 pathway must be repressed until preBCR selection, but also needs to be accessible to protect developing B cells from oncogenic transformation. Indeed, many early B lineage acute leukemias harbor inactivating mutations at the *Cdkn2a* locus. In contrast, germinal center B cell lymphomas have activating *Ezh2* mutations; in these cells, EZH2 might contribute to tumorigenesis, in part through *Cdkn2a* repression. EZH2-dependent repression of *Cdkn2a* is therefore a critical control point for preBCR selection that could be manipulated by lymphoid cells to promote transformation[46].

We found significant association of the transcriptional alterations in *Dido1*ΔE16 cells with a number of PRC2 targets and genes bearing H3K27me3 epigenetic marks, which suggests that DIDO3 is involved in determining specific PRC2 activity in the B cell lineage. Moreover, loss of EZH2 is known to cause impaired distal VH–DJH rearrangement and *Igh* locus contraction[47]. There is thus a preference to use proximal V fragments as in our model, which reinforces the view that DIDO3 acts in coordination with PRC2.

We showed differential expression of the DIDO isoforms in MPD[18], and others reported that BCR-ABL1 translocation (Philadelphia chromosome; Ph) in myelocytic leukemia (CML) might be involved in modulating *DIDO1* expression in a JAK2V617F-independent manner[48]. Disorders in multiple signaling pathways and genetic abnormalities combined with the Ph are essential for the evolution of different types of leukemia; however, why MPD evolve specifically into CML, acute myeloid leukemia, acute leukemia leukocytosis, or mixed-phenotype acute leukemia is currently unclear. BCR-ABL1 kinase hyperactivity leads to the activation of signaling pathways and deregulation of cellular processes[49,50], and

hyperactivation of most of these pathways have been confirmed in CML and ALL mouse models. BCR-ABL1 activity channels mainly through JAK/STAT and PI3K/AKT/mTOR pathways, and through CCAAT/enhancer-binding proteins (C/EBP, which regulate normal myelopoiesis as well as myeloid disorders)[51]. Our Gene Ontology analysis of RNAseq data showed that, in cells lacking DIDO3, the expression of PI3K/mTOR and JAK/STAT pathway components, as well as *Cebpb*, are affected at the transcriptional level. Statistical analysis of DNA methylation showed that target genes of NANOG[52], Polycomb-group target genes, and/or genes with an AACTTT promoter motif can have a methylation profile that seems to indicate predisposition to development of cancer, such as breast cancer[53]. Such aberrant DNA methylation profiles can be seen in advance of any signs or clinical symptoms of cancer.

In all, our data provide evidence of the involvement of DIDO3, a reader of histone post-translational modifications (PTM), in several processes of bone marrow hematopoiesis, including precursor homing, cell cycle progression, apoptosis, and differentiation. DIDO3 deficiency is associated with alterations in DNA accessibility and transcriptional defects of major B cell differentiation master regulators. This association seems to be related, at least in part, to the relationship of DIDO3 with PRC2. Remaining open questions include the DNA methylation and the general histone PTM landscape in DIDO3-deficient cells, as well as the consequences of DIDO3 deficiency in peripheral B cell differentiation and hematopoietic cancer development.

MATERIALS AND METHODS

Mice

In brief, a mouse strain bearing an exon 16 flanked by *loxP* sites was generated and interbred with Cre^{VAV1}-producing mice heterozygous for exon 16 deletion. Hematopoietic populations were isolated from the offspring. Mice were handled according to national and European Union guidelines, and experiments were approved by the Comité Ético de Experimentación Animal, Centro Nacional de Biotecnología, Consejo Superior de Investigaciones Científicas and by the Comunidad de Madrid (PROEX 055-14).

Flow cytometry

Cells from each sample were diluted in a solution of 0.5% PBS-BSA, 0.065% NaN_3. To avoid nonspecific antibody binding, samples were blocked with Fc-Block (CD16/32; BD Pharmingen). Antibodies used were from eBioscience (B220-eF450, CD3-biotin, CD5-percpCy5.5, CD19-AlexaFluor700, CD93-APC, CD127 (IL7R)-PeCy7, Sca1-APC), Beckman Coulter (B220-biotin, B220-PE, CD4-biotin, CD8-PE, CD8-biotin, cKit-APC, Gr1-biotin, Ly6C-biotin), BioLegend (CD4-PeCy7, CD11b-PeCy7, CD45.2-AlexaFluor700), and BD Pharmingen (CD11b-biotin, CD21-APC, CD23-PE, CD43-biotin, CD45.1-PE, IgG1-PE, IgG3-PE, Ly6G-PE, Nk1.1-APC). Biotinylated antibodies were visualized with streptavidin-eF450 (eBioscience), streptavidin-PE (Southern Biotech) or streptavidin-PE-CF594 (eBioscience). Cell death was monitored using annexin V-APC (Immunostep) and DAPI. In *in vivo* assays, the cell cycle was analyzed by measuring BrdU incorporation into cell DNA 18 h after intraperitoneal injection of 200 mg BrdU (Invitrogen). Cells were labeled following the protocol for the BrdU Staining Kit for flow cytometry (Invitrogen). Analytical cytometric data was acquired using a Gallios cytometer (Beckman Coulter).

Competitive bone marrow transplantation

B57.SJL-Ptprca Pepcb/BoyJ (B6-CD45.1) mice were used as transplant recipients. Recipient cells can be distinguished from hematopoietic cells from donor mice that express the CD45.2 alloantigen (present in the C57BL/6 strain). A group of six $CD45.1^+$ mice were irradiated (10 Gy) to inhibit cell division and provoke apoptosis of hematopoietic cells. On day 1 post-irradiation, mice were inoculated retro-orbitally with 150 µl (3.75×10^6 cells) of a 1:1 mixture of bone marrow cells from $CD45.2^+$;$EYFP^+$;*Dido1*ΔE16 and $CD45.2^+$;$EYFP^-$;$Dido1^{+/+}$ mice (Suppl. Fig. 4). Mice were bled at various times to monitor transplant evolution, and were euthanized at 4 weeks. Bone marrow was extracted for flow cytometry analysis.

***In vitro* differentiation of bone marrow cells**

Bone marrow cells from wt and *Dido1*ΔE16 mice (lin⁻: CD3, CD11b, CD19, CD45R (B220), Ly6G/C (Gr1), TER119), were purified with the EasySep Mouse Hematopoietic Progenitor Cell Isolation kit (STEMCELL Technologies) according to the manufacturer's protocol. Isolated cells were grown in a semi-solid methyl cellulose matrix for the Mouse Hematopoietic CFU Assay in Methocult Media 3630 (STEMCELL Technologies), following the manufacturer's instructions. The medium is supplemented with IL7, which promotes growth of B lymphocyte progenitor cells as pre-B colony-forming units (CFU-pre-B).

RT-qPCR

RNA was extracted from sorted cell samples with the RNeasy Plus Mini Kit (50; Qiagen) according to manufacturer's instructions; quality was determined by electropherogram (Agilent 2100 Bionalyzer). To obtain cDNA, the SuperScriptIII First-Strand Synthesis System for RT-PCR kit (Invitrogen) was used. Up to 1 µg total RNA was used as template in a final reaction of 20 µl. qPCR reactions were carried out 384-well plates in an ABI PRISM 7900HT system (Applied Biosystems) using GoTaq qPCR Master Mix (Promega).

TaqMan Low Density Arrays (TLDA)

Precursor B populations (prepro-B, pro-B, pre-B and immature B cells) were obtained by cell sorting from bone marrow of wt and *Dido1*ΔE16 mice, RNA was extracted from these cell populations as described above, and mRNA was retro-transcribed with SuperScript III (Invitrogen); the resulting cDNA was amplified in TaqMan Universal Master Mix II solution, not UNG (2x) (Applied Biosystems), with a pre-amplification step using TaqMan Custom PreAmp Pool (P/N 4441859; Applied Biosystems). Data were analyzed with ExpressionSuite v. 1.1 (Applied Biosystems). The level of significance for Student's t-test was established at $p<0.05$.

Assay for transposase-accessible chromatin using sequencing (ATAC-seq)

The LSK cell samples obtained by sorting were processed with the DNA Library Prep Kit (Illumina). The tagged DNA was purified with the DNA Clean ConcentratorTM5 Kit (Zymo Research). The samples were pre-amplified with the Nextera Index kit and the Nextera DNA Library Prep kit (both from Illumina), incorporating index sequences at the ends. DNA from the PCR reaction was purified using the DNA Clean ConcentratorTM5 Kit. To quantify tagged DNA, the 1x dsDNA HS Assay kit (Qubit) was used. Samples were then enriched in DNA sizes between 200 and 600 bp (corresponding to 1 to 3 nucleosomes) using AMPure XP magnetic beads (Beckman-Coulter), following the manufacturer's guidelines. To analyze size distribution, DNA analysis was performed by electropherogram as above. To sequence

tagged DNA, a mixture was used of libraries with a balanced proportion of three samples each of LSK-wt cells and LSK-*Dido1*ΔE16 cells, each with ~100,000 pmol/l tagged DNA fragments. After samples were sequenced, fragment size distribution was determined to have maxima corresponding to the lengths of two nucleosomes (~350 bp), one nucleosome (~180 bp), and <1 nucleosome, the last compatible with that expected for naked DNA. Massive sequencing was performed by the CNIC Genomics Service on a HiSeq 2500 platform using a Hi-Seq-Rapid PE Flowcell 2x50 kit.

Sequencing data processing: FASTQ files with the paired-end sequences were aligned to the UCSC mm10 mouse reference genome (genome.ucsc.edu) using Bowtie2 (bowtie-bio.sourceforge.net/bowtie2/) and BWA-MEM 0.7.15 (bio−bwa.sourceforge.net) methods. Sequences aligned in blacklisted regions (sites.google.com/site/anshulkundaje/projects/blacklists) were removed with the Intersect tool from BEDTools (github.com/arq5x*f*bedtools2) before calculating accessible regions of chromatin using the MACS2 program (github.com/taoliu/MACS/tree/master/MACS2) used in the ENCODE project pipeline (www.encodeproject.org). In parallel, the HOMER tool (homer.ucsd.edu/homer/) was also used to calculate accessible regions of chromatin and to find differentially accessible regions between LSK-wt and LSK-*Dido1*ΔE16 cells (see below). The overlap between accessible regions identified by MACS2 and HOMER was 80-90% (see Supplementary Table 4).

Genomic annotations: The data were obtained, processed, and annotated using tools from R (www.r-project.org/) and Bioconductor (bioconductor.org). To determine the equivalent accessible regions in the replicas, the Intersect tool and the files produced by MACS2 were used. Genes, promoters, UTRs, introns, and exons were allocated to the accessible regions with the ChIPseeker program (github.com/GuangchuangYu/ChIPseeker).

Differential accessibility analysis of chromatin: The sequences (readings) in the accessible and equivalent regions of all replicates were counted and normalized with the StringTie 1.3.3 method (ccb.jhu.edu/software/stringtie). To calculate the differential accessibility of chromatin, the accessible and equivalent regions were analyzed with at least one reading in all replicas, with the DESeq2 (bioconductor.org/packages/DESeq2) and edgeR methods (bioconductor.org/packages/edgeR). Accessible regions with a fold change value >2 and a false discovery rate (FDR) <0.05 were considered statistically significant. We also used the HOMER tool in the differential accessibility analysis of chromatin. Gene Set Enrichment Analysis (GSEA, www.gsea-msigdb.org/) was used for the ATAC-seq data.

RNA-Seq

Pre-B cells extracted from the bone marrow of wt and *Dido1*ΔE16 mice were isolated by sorting. RNA was purified using the RNeasy mini plus kit (Qiagen) and massive sequencing was performed at BGI Genomics (Hong Kong) using the HiSeq 2000 platform.

RNA-seq data analysis. Sequenced reads were processed in parallel using the Galaxy RNA-seq pipeline (usegalaxy.org) and a combined approach with BWA-MEM 0.7.15, StringTie (ccb.jhu.edu/software/stringtie/) and edgeR. The combined approach was previously used to process RNA-seq data of *Dido1*ΔE16 in embryonic stem cells (GEO: GSE152346) Differentially expressed genes (DEG) were defined according to the absolute value of their log2 (fold change) ≥0.6 and FDR <0.05, unless otherwise stated. Gene ontology (GO), pathway annotation, and enrichment analyses were carried out using the Molecular Signatures Database (MSigDB) (go-basic.obo, downloaded Jan 15, 2020 by gsea-msigdb.org). A Venn diagram was constructed to obtain co-expressed DEG among samples using the webtool at http://bioinformatics.psb.ugent.be/webtools/Venn/, provided by Bioinformatics & Evolutionary Genomics (Gent, BE). The biological significance of DEG was explored using STRING v. 11.0 (string-db.org).

Supplementary Materials

Fig. S1: Dido1 expression in anatomical samples.

Fig. S2: Deletion of *Dido1* exon 16 in hematopoietic lineage.

Fig. S3: Clones obtained from lin$^-$ cells from wt and Dido1ΔE16 mice.

Fig. S4: Cell pool used in adoptive transfer experiments.

Fig. S5: STRING analysis and clustering of differentially expressed genes.

Table S1: GSEA analysis of ATAC-seq data.

Table S2: DEG from RNA-seq data.

Table S3: DEG in *Igh* locus.

Table S4: Accessible regions overlap enrichment analysis.

REFERENCES

1. M. A. Inlay, D. Bhattacharya, D. Sahoo, T. Serwold, J. Seita, H. Karsunky, S. K. Plevritis, D. L. Dill, I. L. Weissman, Ly6d marks the earliest stage of B-cell specification and identifies the branchpoint between B-cell and T-cell development. Genes Dev. **23**, 2376-2381 (2009). doi: 10.1101/gad.1836009. [Published erratum in: *Genes Dev*. **27**, 2063 (2013)]. PMID: 19833765; PMCID: PMC2764492.

2. S. H. M. Pang, C. A. de Graaf, D. J. Hilton, N. D. Huntington, S. Carotta, L. Wu, S. L. Nutt, PU.1 Is Required for the Developmental Progression of Multipotent Progenitors to Common Lymphoid Progenitors. *Front. Immunol*. **9**, 1264. (2018). doi: 10.3389/fimmu.2018.01264. PMID: 29942304; PMCID: PMC6005176.

3. M. Sellars, P. Kastner, S. Chan, Ikaros in B cell development and function. *World J. Biol. Chem*., **2**, 132-139, (2011). doi: 10.4331/wjbc.v2.i6.132. PMID: 21765979; PMCID: PMC3135860.

4. Y. C. Lin, S. Jhunjhunwala, C. Benner, S. Heinz, E. Welinder, R. Mansson, M. Sigvardsson, J. Hagman, C. A. Espinoza, J. Dutkowski, T. Ideker, C. K. Glass, C. Murre, A global network of transcription factors, involving E2A, EBF1 and Foxo1, that orchestrates B cell fate. *Nat. Immunol.* **11**, 635-643 (2010) doi: 10.1038/ni.1891. Epub 2010 Jun 13. PMID: 20543837; PMCID: PMC2896911.

5. T. Treiber, E. M. Mandel, S. Pott, I. Györy, S. Firner, E. T. Liu, R. Grosschedl, Early B cell factor 1 regulates B cell gene networks by activation, repression, and transcription- independent poising of chromatin. *Immunity*. **32**, 714-725 (2010). doi: 10.1016/j.immuni.2010.04.013. Epub 2010 May 6. PMID: 20451411.

6. S. L. Nutt, B. Heavey, A. G. Rolink, M. Busslinger, Commitment to the B-lymphoid lineage depends on the transcription factor Pax5. *Nature* **401**, 556-562 (1999). doi: 10.1038/44076. PMID: 10524622.

7. D. Allman, A. Sambandam, S. Kim, J. P. Miller, A. Pagan, D. Well, A. Meraz, A. Bhandoola, Thymopoiesis independent of common lymphoid progenitors. *Nat. Immunol.* **4**, 168-174 (2003). doi: 10.1038/ni878. Epub 2003 Jan 6. PMID: 12514733.

8. M. Kondo, I. L. Weissman, K. Akashi, Identification of clonogenic common lymphoid progenitors in mouse bone marrow. *Cell* **91**, 661-672 (1997). doi: 10.1016/s0092-8674(00)80453-5. PMID: 9393859.

9. M. G. Manz, D. Traver, T. Miyamoto, I. L. Weissman, K. Akashi K, Dendritic cell potentials of early lymphoid and myeloid progenitors. *Blood* **97**, 3333-3341 (2001). doi: 10.1182/blood.v97.11.3333. PMID: 11369621.

10. L. L. Rumfelt, Y. Zhou, B. M. Rowley, S. A. Shinton, R. R. Hardy, Lineage specification and plasticity in CD19- early B cell precursors. *J. Exp. Med.* **203**, 675-687 (2006). doi: 10.1084/jem.20052444. Epub 2006 Feb 27. PMID: 16505143; PMCID: PMC2118241.

11. H. E. Fleming, C. J. Paige, Pre-B cell receptor signaling mediates selective response to IL-7 at the pro-B to pre-B cell transition via an ERK/MAP kinase-dependent pathway. *Immunity* **15**, 521-531 (2001). doi: 10.1016/s1074-7613(01)00216-3. PMID: 11672535.

12. E. Bertolino, K. Reddy, K. L. Medina, E. Parganas, J. Ihle, H. Singh, Regulation of interleukin 7-dependent immunoglobulin heavy-chain variable gene rearrangements by transcription factor STAT5. *Nat. Immunol*. **6**, 836-843 (2005). doi: 10.1038/ni1226. Epub 2005 Jul 17. PMID: 16025120.

13. J. Lutz, M. R. Heideman, E. Roth, P. van den Berk, W. Müller, C. Raman,M. Wabl, H. Jacobs, H-M. Jäck, Pro-B cells sense productive immunoglobulin heavy chain rearrangement irrespective of polypeptide production. *Proc. Natl. Acad. Sci. U.S.A.* **108**, 10644-10649 (2011) DOI:10.1073/pnas.1019224108.

14. M. Berdasco, M. Esteller, Aberrant epigenetic landscape in cancer: how cellular identity goes awry. *Dev. Cell* **19**, 698-711 (2010). doi: 10.1016/j.devcel.2010.10.005. PMID: 21074720.

15. C. J. Petell, A. T. Pham, J. Skela, B. D. Strahl, Improved methods for the detection of histone interactions with peptide microarrays. *Sci. Rep*. **9**, 6265 (2019). doi: 10.1038/s41598-019-42711-y. PMID: 31000785; PMCID: PMC6472351.

16. H. C. Eberl, C. G. Spruijt, C. D. Kelstrup, M. Vermeulen, M. Mann, A map of general and specialized chromatin readers in mouse tissues generated by label-free interaction proteomics. *Mol. Cell*, **49**, 368-378 (2013). doi: 10.1016/j.molcel.2012.10.026. Epub 2012 Nov 29. PMID: 23201125.

17. A. A. Guerrero, M. C. Gamero, V. Trachana, A. Fütterer, C. Pacios-Bras, N. P. Díaz-Concha, J. C. Cigudosa, C. Martínez-A, K. H. van Wely. Centromere-localized breaks indicate the generation of DNA damage by the mitotic spindle. *Proc. Natl. Acad. Sci. U S A* **107**, 4159-4164 (2010). doi: 10.1073/pnas.0912143106. Epub 2010 Feb 8. PMID: 20142474; PMCID: PMC2840104.

18. A. Fütterer, M. R. Campanero, E. Leonardo, L. M. Criado, J. M. Flores, J. M. Hernández, J. F. San Miguel, C Martínez-A, Dido gene expression alterations are implicated in the induction of hematological myeloid neoplasms. *J. Clin. Invest*. **115**, 2351-2362 (2005). doi: 10.1172/JCI24177. Epub 2005 Aug 25. PMID: 16127461; PMCID: PMC1190370.

19. A. Fütterer, A. Raya, M. Llorente, J. C. Izpisúa-Belmonte, J. L. de la Pompa, P. Klatt, C. Martínez-A, Ablation of Dido3 compromises lineage commitment of stem cells in vitro and during early embryonic development. *Cell Death Differ*. **19**, 132-143 (2011). doi: 10.1038/cdd.2011.62. Epub 2011 Jun 10. PMID: 21660050; PMCID: PMC3252825.

20. C. Mora Gallardo, A. Sánchez de Diego, J. Gutiérrez Hernández, A. Talavera-Gutiérrez, T. Fischer, C. Martínez-A, K. H. van Wely, Dido3-dependent SFPQ recruitment maintains efficiency in mammalian alternative splicing. *Nucleic Acids Res*. **47**, 5381-5394 (2019). doi: 10.1093/nar/gkz235. PMID: 30931476; PMCID: PMC6547428.

21. N. Bosco, L. K. Swee, A. Bénard, R. Ceredig, A. Rolink, Auto-reconstitution of the T-cell compartment by radioresistant hematopoietic cells following lethal irradiation and bone marrow transplantation. *Exp. Hematol*. **38**, 222-232.e2 (2010). doi: 10.1016/j.exphem.2009.12.006. Epub 2010 Jan 4. PMID: 20045443.

22. M. R. Corces, A. E. Trevino, E. G. Hamilton, P. G. Greenside, N. A. Sinnott-Armstrong, S. Vesuna, A. T. Satpathy, A. J. Rubin, K. S. Montine, B. Wu, A. Kathiria, S. W. Cho, M. R. Mumbach, A. C. Carter, M. Kasowski, L. A. Orloff, V. I. RiscaI, A. Kundaje, P. A. Khavari, T. J. Montine, W. J. Greenleaf, H. Y. Chang, An improved ATAC-seq protocol reduces background and enables interrogation of frozen tissues. *Nat. Methods*. **14**, 959-962 (2017). doi: 10.1038/nmeth.4396. Epub 2017 Aug 28. PMID: 28846090; PMCID: PMC5623106.

23. G. Yu, L. G. Wang, Q. Y. He, ChIPseeker: an R/Bioconductor package for ChIP peak annotation, comparison and visualization. *Bioinformatics* **31**, 2382-2383 (2015). doi: 10.1093/bioinformatics/btv145. Epub 2015 Mar 11. PMID: 25765347.

24. E. Engelen, J. H. Brandsma, M. J. Moen, L. Signorile, D. H. Dekkers, J. Demmers, C. E. Kockx, Z. Ozgür, W. F. van IJcken, D. L. van den Berg, R. A. Poo, Proteins that bind regulatory regions identified by histone modification chromatin immunoprecipitations and mass spectrometry. *Nat. Commun.* **6**, 7155 (2015). doi: 10.1038/ncomms8155. PMID: 25990348; PMCID: PMC4455091.

25. A. Subramanian, P. Tamayo, V. K. Mootha, S. Mukherjee, B. L. Ebert, M. A. Gillette, A. Paulovich, S. L. Pomeroy, T. R. Golub, E. S. Lander, J. P. Mesiro,. Gene set enrichment analysis: a knowledge-based approach for interpreting genome-wide expression profiles. *Proc. Natl. Acad. Sci. U.S.A.* **102**,15545-15550 (2015). doi: 10.1073/pnas.0506580102. Epub 2005 Sep 30. PMID: 16199517; PMCID: PMC1239896.

26. A. Fütterer, J. de Celis, R Navajas, L. Almonacid, J. Gutiérrez, A. Talavera-Gutiérrez, C. Pacios-Bras, I. Bernascone, F. Martin-Belmonte, C. Martínez-A, DIDO as a Switchboard that Regulates Self-Renewal and Differentiation in Embryonic Stem Cells. *Stem Cell Reports* **8**, 1062-1075 (2017). doi: 10.1016/j.stemcr.2017.02.013. Epub 2017 Mar 16. PMID: 28330622; PMCID: PMC5390109.

27. H. Hirai, A. Yokota, A. Tamura, A. Sato, T. Maekawa, Non-steady-state hematopoiesis regulated by the C/EBPβ transcription factor. *Cancer Sci*. **106**, 797-802 (2015). doi: 10.1111/cas.12690. Epub 2015 Jun 1. PMID: 25940801; PMCID: PMC4520629.

28. A. Rolink, U. Grawunder, T. H. Winkler, H. Karasuyama, F. Melchers, IL-2 receptor alpha chain (CD25, TAC) expression defines a crucial stage in pre-B cell development. *Int. Immunol*. **6**, 1257-1264 (1994). doi: 10.1093/intimm/6.8.1257. PMID: 7526894.

29. H. von Boehmer, F. Melchers. Checkpoints in lymphocyte development and autoimmune disease. *Nat. Immunol*. **11**, 14-20 (2010). doi: 10.1038/ni.1794. Epub 2009 Dec 17. PMID: 20016505.

30. A. Grijzenhout, J. Godwin, H. Koseki, M. R. Gdula, D. Szumska, J. F. McGouran, S. Bhattacharya, B. M. Kessler, N. Brockdorff, S. Cooper, Functional analysis of AEBP2, a PRC2 Polycomb protein, reveals a Trithorax phenotype in embryonic development and in ESCs. *Development* **143**, 2716-2723 (2016). doi: 10.1242/dev.123935. Epub 2016 Jun 17. PMID: 27317809; PMCID: PMC5004903.

31. C. Pacios-Bras, T. Pons, A. Alonso-Guerrero, S. Román-García, J. Gutiérrez, P. Manrique, F. Gutiérrez del Burgo, R. Villares, C. Mora Gallardo, K. H. M. van Wely, Y. R. Carrasco, C. Martínez-A, DIDO3 Regulates Microtubule Stability at Transcriptional and Posttranslational Levels and is Needed for Fibroblast Adhesion and Movement (July 27, 2019). Available at SSRN: https://ssrn.com/abstract=3428482 or http://dx.doi.org/10.2139/ssrn.3428482.

32. J. Gatchalian, A. Fütterer, S. B. Rothbart, Q. Tong, H. Rincon-Arano, A. Sánchez de Diego, M. Groudine, B. D. Strahl, C. Martínez-A, K. H. van Wely, T. G. Kutateladze, Dido3 PHD modulates cell differentiation and division. *Cell Rep*. **4**, 148-58 (2013). doi: 10.1016/j.celrep.2013.06.014. Epub 2013 Jul 3. PMID: 23831028; PMCID: PMC3967714.

33. A. Sánchez de Diego, A. Alonso Guerrero, C. Martínez-A, K. H. van Wely, Dido3-dependent HDAC6 targeting controls cilium size. *Nat. Commun*. **5**, 3500 (2014). doi: 10.1038/ncomms4500. PMID: 24667272; PMCID: PMC3973121.

34. Z. Zhang, C. V. Cotta, R. P. Stephan, C. G. de Guzman, C. A. Klug, Enforced expression of EBF in hematopoietic stem cells restricts lymphopoiesis to the B cell lineage. *EMBO J*. **22**, 4759-4769 (2003). doi: 10.1093/emboj/cdg464. PMID: 12970188; PMCID: PMC212730.

35. H. Lin, R. Grosschedl, Failure of B-cell differentiation in mice lacking the transcription factor EBF. *Nature* **376**, 263-267 (1995). doi: 10.1038/376263a0. PMID: 7542362.

36. J. Åhsberg, J. Ungerbäck, T. Strid, E. Welinder, J. Stjernberg, M. Larsson, H. Qian, M. Sigvardsson, Early B-cell factor 1 regulates the expansion of B-cell progenitors in a dose-dependent manner. *J. Biol. Chem*. **288**, 33449-33461 (2013). doi: 10.1074/jbc.M113.506261. Epub 2013 Sep 27. PMID: 24078629; PMCID: PMC3829190.

37. B. L. Kee, E and ID proteins branch out. *Nat. Rev. Immunol*. **9**, 175-184 (2009). doi: 10.1038/nri2507. PMID: 19240756.

38. Y. Zhuang, P. Cheng, H. Weintraub, B-lymphocyte development is regulated by the combined dosage of three basic helix-loop-helix genes, E2A, E2-2, and HEB. *Mol. Cell. Biol.* **16**, 2898-2905 (1996). doi: 10.1128/mcb.16.6.2898. PMID: 8649400; PMCID: PMC231283.

39. E. Welinder, R. Mansson, E. M. Mercer, D. Bryder, M. Sigvardsson, C. Murre, The transcription factors E2A and HEB act in concert to induce the expression of FOXO1 in the common lymphoid progenitor. *Proc. Natl. Acad. Sci. U.S.A.* **108**, 17402-17407(2011). doi: 10.1073/pnas.1111766108. Epub 2011 Oct 4. PMID: 21972416; PMCID: PMC3198373.

40. G. Bain, E. C. Maandag, D. J. Izon, D. Amsen, A. M. Kruisbeek, B. C. Weintraub, I. Krop, M. S. Schlissel, A. J. Feeney, M. van Roon, M. van der Valk, H. P. J. te Riele, A. Berns, C. Murre, E2A proteins are required for proper B cell development and initiation of immunoglobulin gene rearrangements. *Cell* **79**, 885-892 (1994). doi: 10.1016/0092-8674(94)90077-9. PMID: 8001125.

41. E. Edry, H. Azulay-Debby, D. Melamed, TOLL-like receptor ligands stimulate aberrant class switch recombination in early B cell precursors. *Int. Immunol*. **20**, 1575-1585 (2008). doi: 10.1093/intimm/dxn117. Epub 2008 Oct 29. PMID: 18974086.

42. R. Riedel, R. Addo, M. Ferreira-Gomes, G. A. Heinz, F. Heinrich, J. Kummer, V. Greiff, D. Schulz, C. Klaeden, R. Cornelis, U. Menzel, S. Kröger, U. Stervbo, R. Köhler, C. Haftmann, S. Kühnel, K. Lehmann, P. Maschmeyer, M. McGrath, S. Naundorf, S. Hahne, Ö. Sercan-Alp, F. Siracusa, J. Stefanowski, M. Weber, K. Westendorf, J. Zimmermann, A. E. Hauser, S. T. Reddy, P. Durek, H. D. Chang, M. F. Mashreghi, A. Radbruch, Discrete populations of isotype-switched memory B lymphocytes are maintained in murine spleen and bone marrow. *Nat. Commun*. **11**, 2570 (2020). doi: 10.1038/s41467-020-16464-6. PMID: 32444631; PMCID: PMC7244721.

43. I. Velichutina, R. Shaknovich, H. Geng, N. A. Johnson, R. D. Gascoyne, A. M. Melnick, O. Elemento, EZH2-mediated epigenetic silencing in germinal center B cells contributes to proliferation and lymphomagenesis. *Blood* **116**, 5247-5255 (2010). doi: 10.1182/blood-2010-04-280149. Epub 2010 Aug 24. PMID: 20736451; PMCID: PMC3012542.

44. B. B. McConnell, F. J. Gregory, F. J. Stott, E. Hara, G. Peters, Induced expression of p16(INK4a) inhibits both CDK4- and CDK2-associated kinase activity by reassortment of cyclin-CDK-inhibitor complexes. *Mol. Cell. Biol.* **19**, 1981-1989 (1999). doi: 10.1128/mcb.19.3.1981. PMID: 10022885; PMCID: PMC83991.

45. J. A. Jacobsen, J. Woodard, M. Mandal, M. R. Clark, E. T. Bartom, M. Sigvardsson, B. L. Kee, EZH2 Regulates the Developmental Timing of Effectors of the Pre-Antigen Receptor Checkpoints. *J. Immunol*. **198**, 4682-4691 (2017). doi: 10.4049/jimmunol.1700319. Epub 2017 May 10. PMID: 28490575; PMCID: PMC5527689.

46. S. Swaminathan, C. Duy, M. Müschen, BACH2-BCL6 balance regulates selection at the pre-B cell receptor checkpoint. *Trends Immunol.* **35**, 131-137 (2014). doi: 10.1016/j.it.2013.11.002. Epub 2013 Dec 10. PMID: 24332591; PMCID: PMC3943645.

47. I. H. Su, A. Basavaraj, A. N. Krutchinsky, O. Hobert, A. Ullrich, B. T. Chait, A. Tarakhovsky, Ezh2 controls B cell development through histone H3 methylation and Igh rearrangement. *Nat. Immunol.* **4**, 124-131 (2003). doi: 10.1038/ni876. Epub 2002 Dec 23. PMID: 12496962.

48. M. G. Berzoti-Coelho, A. F. Ferreira, N. de Souza Nunes, M. T. Pinto, M. C. Júnior, B. P. Simões, C. Martínez-A, E. X. Souto, R. A. Panepucci, D. T. Covas, S. Kashima, F. A. Castro, The expression of Death Inducer-Obliterator (DIDO) variants in Myeloproliferative Neoplasms. *Blood Cells Mol. Dis.* **59**, 25-30 (2016). doi: 10.1016/j.bcmd.2016.03.008. Epub 2016 Apr 8. [Published erratum appears in *Blood Cells Mol. Dis.* **69**, 123 (2018). PMID: 27282563].

49. S. Kumar, R. Wuerffel, I. Achour, B. Lajoie, R. Sen, J. Dekker, A. J. Feeney, A. L. Kenter, Flexible ordering of antibody class switch and V(D)J joining during B-cell ontogeny. *Genes Dev.* **27**, 2439-2444 (2013). doi: 10.1101/gad.227165.113. PMID: 24240234; PMCID: PMC3841733.

50. M. Sattler, J. D.Griffin, Molecular mechanisms of transformation by the BCR-ABL oncogene. *Semin. Hematol*. **40**, Suppl. 2, 4-10 (2003).

51. Z. J. Kang, Y. F. Liu, L. Z. Xu, Z. J. Long, D. Huang, Y. Yang, B. Liu, J. X. Feng, Y. J. Pan, J. S. Yan, Q. Liu, The Philadelphia chromosome in leukemogenesis. *Chin. J. Cancer* **35**, 48 (2016). doi: 10.1186/s40880-016-0108-0. PMID: 27233483; PMCID: PMC4896164.

52. S. Tommasi, A. Zheng, J. I. Yoon, A. Besaratinia, Epigenetic targeting of the Nanog pathway and signaling networks during chemical carcinogenesis. *Carcinogenesis* **35**, 1726-1736 (2014). doi: 10.1093/carcin/bgu026. Epub 2014 Jan 30. PMID: 24480805.

53. M. Widschwendter. A. Teschendorff, I. Jacobs, Method for predicting risk of developing cancer - Google Patents WO2012104642A1 (2012).

ACKNOWLEDGEMENTS

We thank the Flow Cytometry and the Animal Facilities of the Spanish National Center of Biotechnology (CNB-CSIC). We thank also the Genomics Unit and the Service of Cardiovascular Physiology of the Animal Facility of the Spanish National Center for Cardiovascular Research (CNIC) for ATAC-seq and complete blood count processing, respectively, Dr María López-Bravo for B6-CD45.1 mice and C. Mark for editorial assistance.

Funding:

Spanish Ministerio de Ciencia e Innovación grant PID2019-110574RB-I00.
Spanish Ministerio de Ciencia e Innovación grant SAF2016-75456-R.
Fundación Ramón Areces XVIII Concurso Nacional para la Adjudicación de Ayudas a la Investigación en Ciencias de la Vida y de la Materia.

Author contributions:

Conceptualization: CMA, RV
Writing: FGB, CMA, RV
Funding acquisition: CMA, RV
Formal analysis: FGB, TP, EVdL, RV
Data curation: TP, EVdL
Methodology: FGB, RV
Supervision: RV

Competing interests

The authors declare no competing interests.

Data availability

ATAC-seq and RNA-seq data are deposited in the Gene Expression Omnibus under accession code GSE157228. Private access token: gpunwiqctludnib

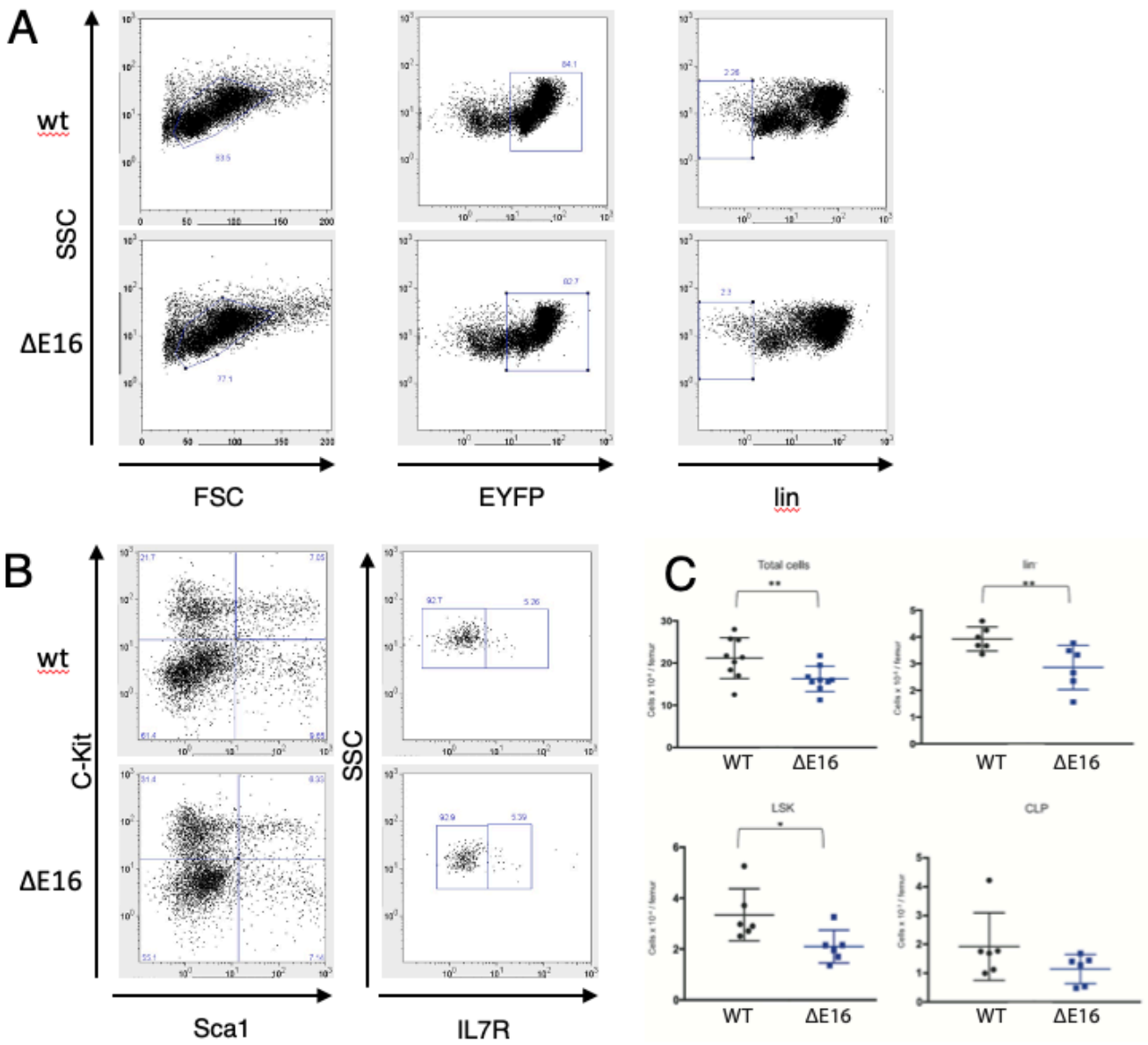

Figure 1. Characterization of hematopoietic progenitor cell populations. A. Total bone marrow cells in wt and *Dido1*ΔE16 mice were selected by EYFP$^+$ and lin$^-$ (Gr1$^-$ Ter119$^-$CD11b$^-$CD3$^-$B220$^-$) phenotype. **B.** Lin$^-$ cells were further analyzed for Sca1, c-Kit, and IL7R expression to characterize LSK (Sca1$^+$cKit$^+$IL7R$^-$) and CLP (Sca1$^+$cKit$^+$IL7R$^+$) populations. **C.** Quantification of total (wt n = 9, *Dido1*ΔE16 n = 9), lin$^-$, LSK and CLP cells (wt n = 6, *Dido1*ΔE16 n = 6) per single femur (t-test ** $p<0.01$, * $p<0.05$). Bars, mean ± SD.

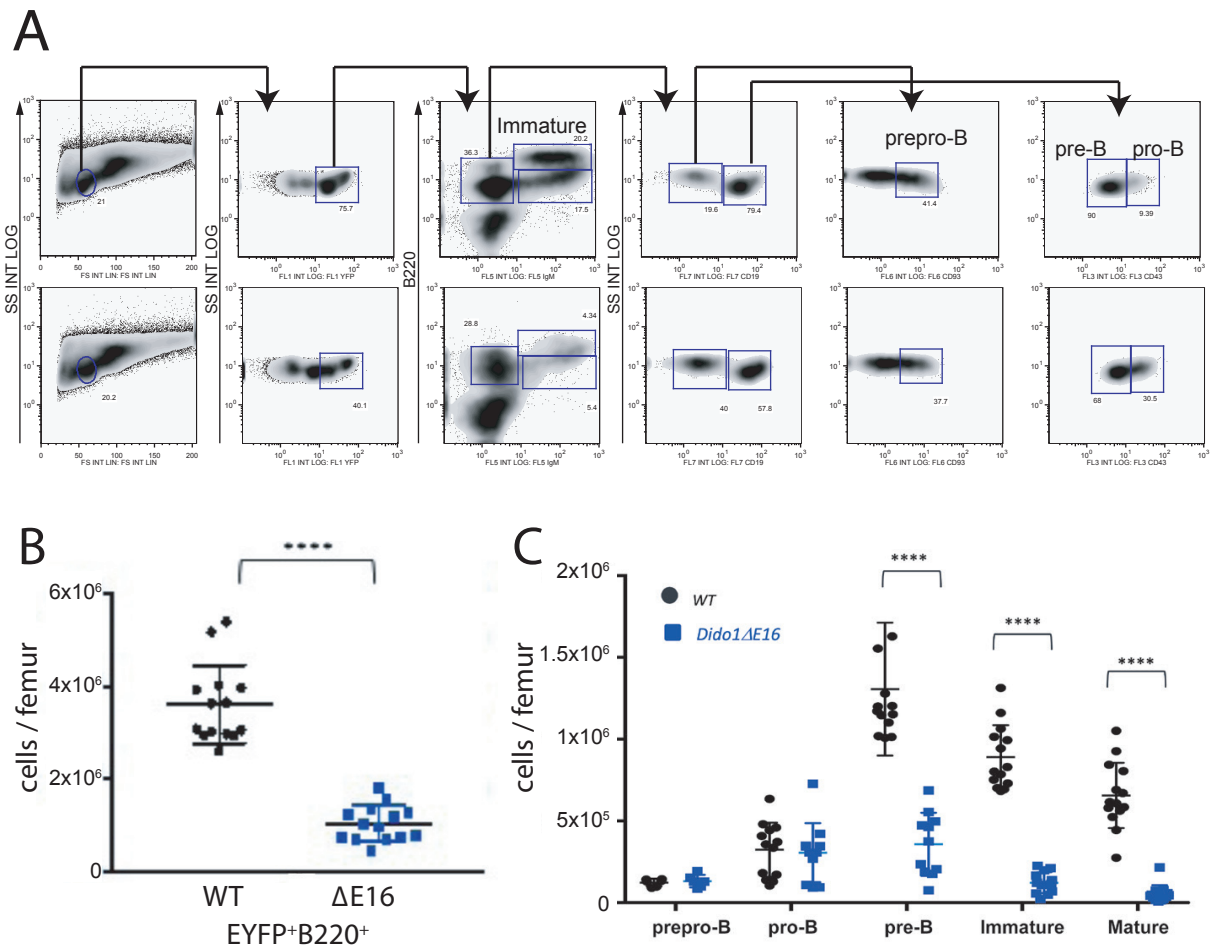

Figure 2. Characterization strategy by flow cytometry for lymphoid progenitor populations in mouse bone marrow. A. Total cells in wt and *Dido1*ΔEI6 mice cells were selected in FS/SS plot. EYFP^{+} cells were gated by IgM and B220 markers to distinguish populations of mature EYFP^{+}B220^{+}IgM^{high} cells and immature EYFP^{+}B220^{+}IgM^{low} cells. Of the EYFP^{+}B220^{+}IgM^{-} subpopulation, prepro-B cells were identified as CD19^{-}CD93^{+}, pre-B as CD19^{+}CD43^{-}, and pro-B as CD19^{+}CD43^{+}. **B.** Numbers of EYFP^{+}B220^{+} cells per femur in wt compared to *Dido1*ΔE16 mice (n = 14; ****, p<0.0001). **C.** Total bone marrow B precursors and mature recirculating B cells isolated from a single femur. Prepro-B (n = 6); pro-B, pre-B (wt n = 13, *Dido1*ΔE16 n = 11); immature and mature B cells (wt n = 14, *Dido1*ΔE16 n = 13). **B, C.** Mean ± SD are shown, t-test **** p<0.0001.

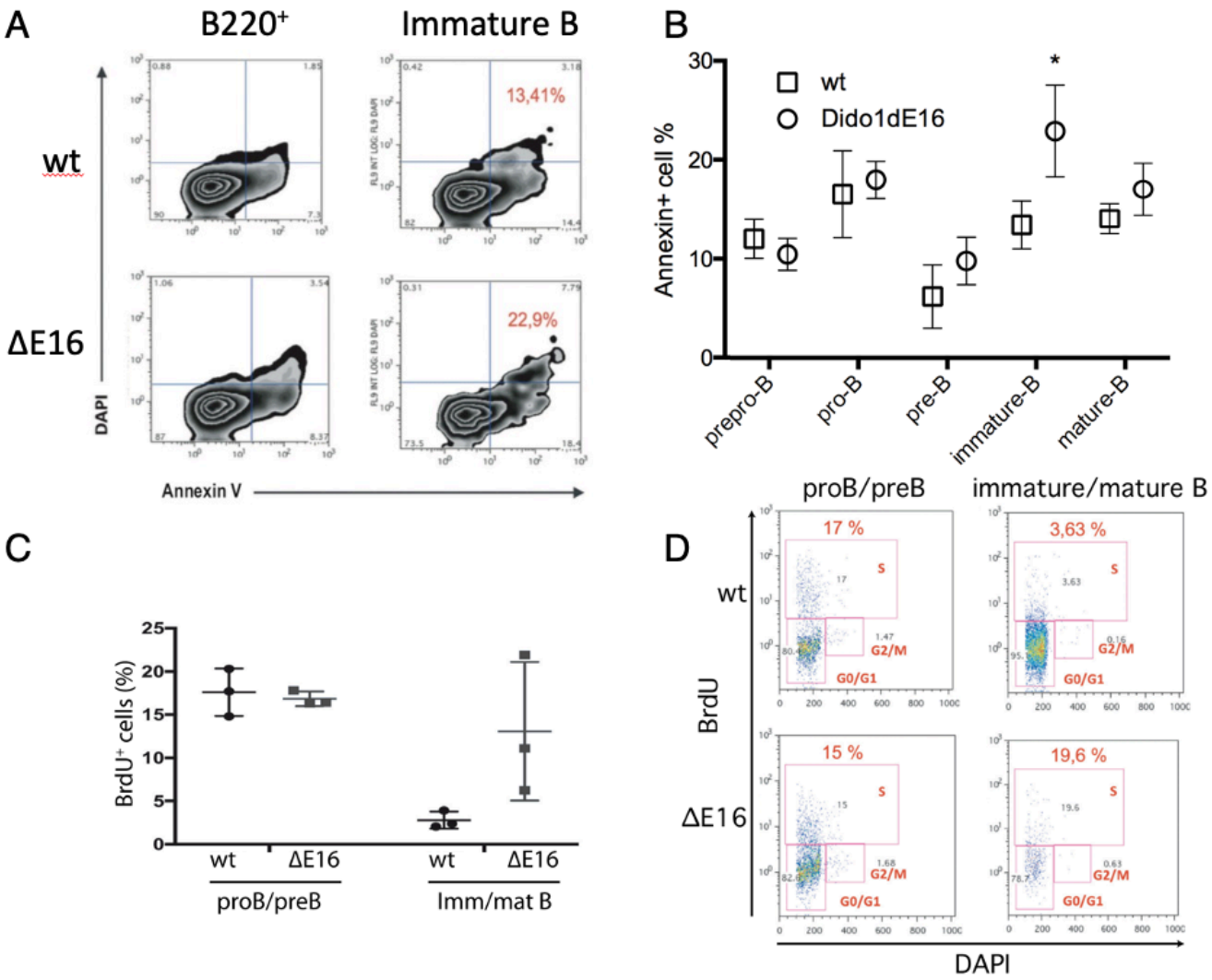

Figure 3. Effect of lack of DIDO3 on apoptosis and proliferation. **A**. Representative graphs of annexin V binding total B220+ and immature B cells from bone marrow of wt and Dido1ΔE16 mice. Lower left, viable cells. Lower right, cells in early apoptosis (which bind annexin V and exclude DAPI). Upper right, cells in late apoptosis (which bind annexin V and incorporate DAPI). Upper left, necrotic cells. **B**. Mean percentages of annexin V+ cells in different precursor subpopulations (mean ± SD, n = 3, t-test * $p<0.05$). **C.** Percentages (mean ± SD; n = 3) of cells incorporating BrdU in pro-B/pre-B and immature/mature B cell populations, from bone marrow of wt and Dido1ΔE16 mice 18 h after intraperitoneal BrdU injection. **D.** Representative flow cytometry analysis of the cell cycle in pro-B/pre-B precursors ($EYFP^+B220^+CD19^+IgM^-$) and immature/mature B cells ($EYFP^+B220^+CD19^+IgM^+$) from bone marrow of BrdU-treated WT and Dido1ΔE16 mice.

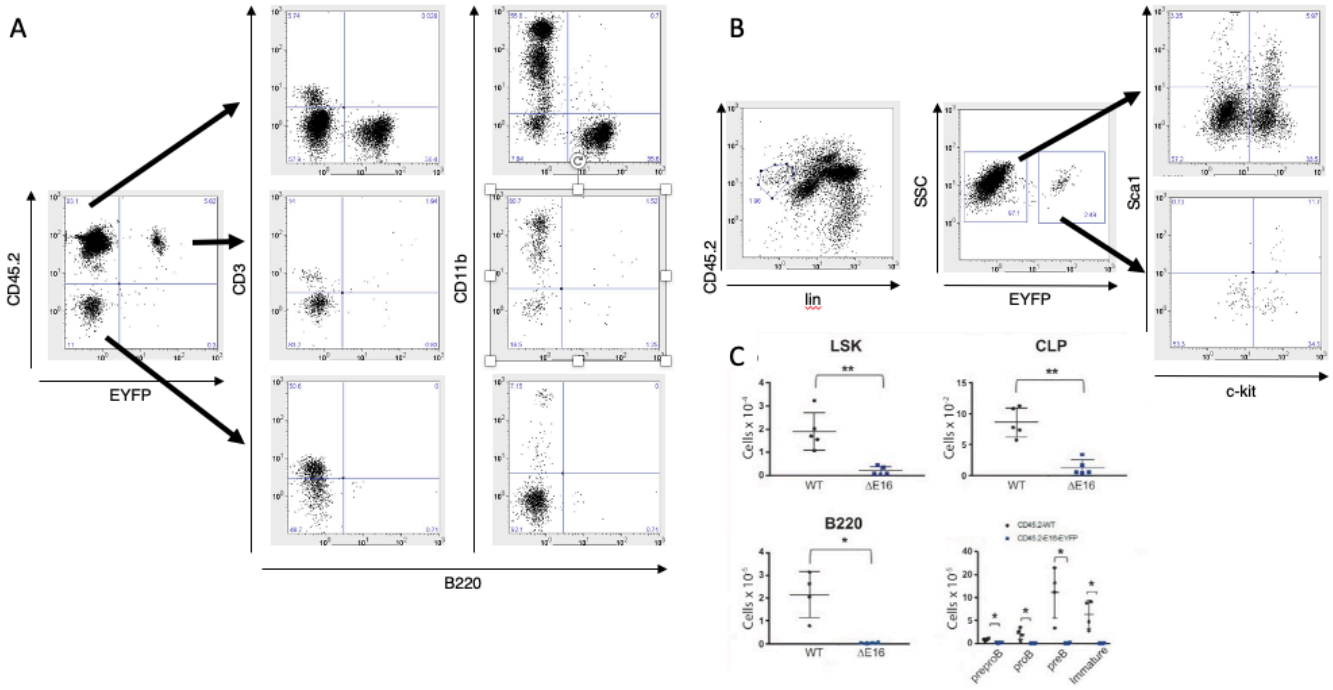

Figure 4. Effect of DIDO3 deficiency on bone marrow transplantation. A. Characterization of peripheral blood white cells in lethally irradiated mice at 21 days post-transplant; total CD45.1^{+} (host) and CD45.2^{+} (donor) cells in blood. *Dido1*ΔE16 cells were identified by EYFP expression. **B.** Representative analysis of flow cytometry data to quantify CD45.1^{+} (host) and CD45.2^{+} (*Dido1*ΔE16 (EYFP^{+}) and wt) populations of lin^{-} cells in transplanted mice. **C.** Total numbers of hematopoietic precursors per femur recovered from transplanted mice 40 days post-transplant. Student's t-tests compare CD45.2 wt and CD45.2^{+} EYFP^{+} *Dido1*ΔE16 LSK and CLP cells (** $p<0.01$; n = 5), and cells from different B cell precursor populations (*, $p<0.05$; n = 4).

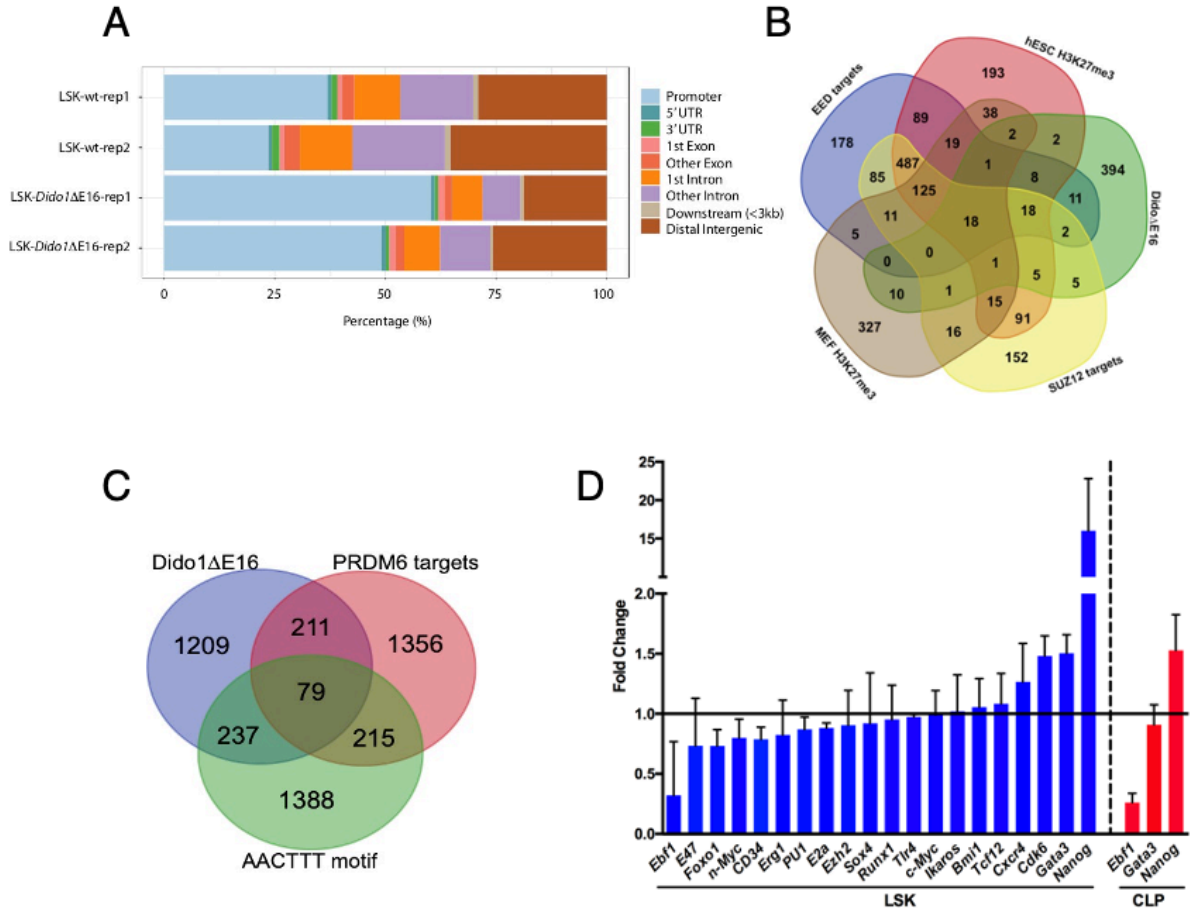

Figure 5. Effect of DIDO3 deficiency on chromatin accessibility. A. Distribution by distance to transcription start sites of chromatin open in wt and closed in *Dido1*ΔE16 LSK cells, as determined by ATAC-seq (mean values, n = 3). **B.** Venn diagrams show overlaps in promoter regions of differentially accessible chromatin with genesets associated with PRC2 activity. **C.** Overlap of differentially accessible chromatin in intronic and intergenic regions. **D.** Validation by real-time qPCR of the expression of potentially affected genes.

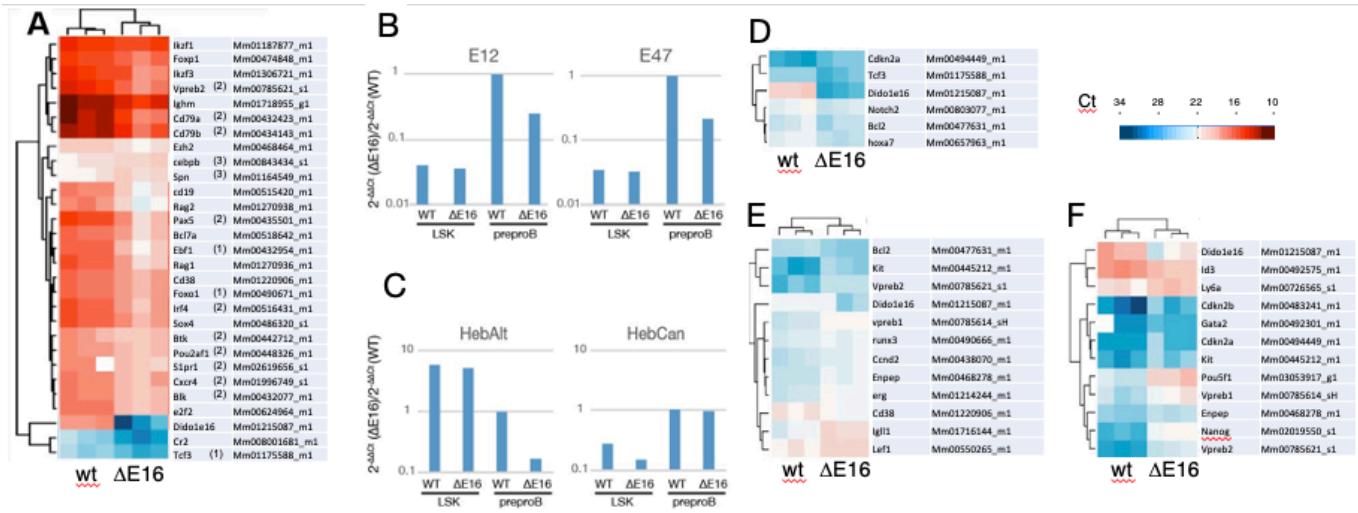

Figure 6. **Differences in gene transcription levels in distinct B cell precursor populations from bone marrow.** Three biological replicates were analyzed from wt and *Dido1*ΔE16 mice. Cells were sorted by flow cytometry. The RNA from each precursor population was extracted, preamplified, and used as template for the TLDA assay. Maximal expression is represented in dark red and minimal expression, dark blue **A.** Heatmap showing hierarchical clustering and expression of differentially expressed genes ($p < 0.05$) by the prepro-B population. **B.** Differential expression of Tcf3 and its two isoforms in prepro-B cells and in lin$^-$ precursors. Values are relative to wt prepro-B levels. **C**. Expression of various Tcf12 isoforms in *Dido1*ΔE16 prepro-B cells, each relative to expression of the same region in wt cells. **D-F**, heatmaps as in A, for other B progenitor subpopulations. **D.** Heatmap for the pro-B population. **E.** Heatmap of the pre-B population. **F**. Heatmap of the immature B cell population.

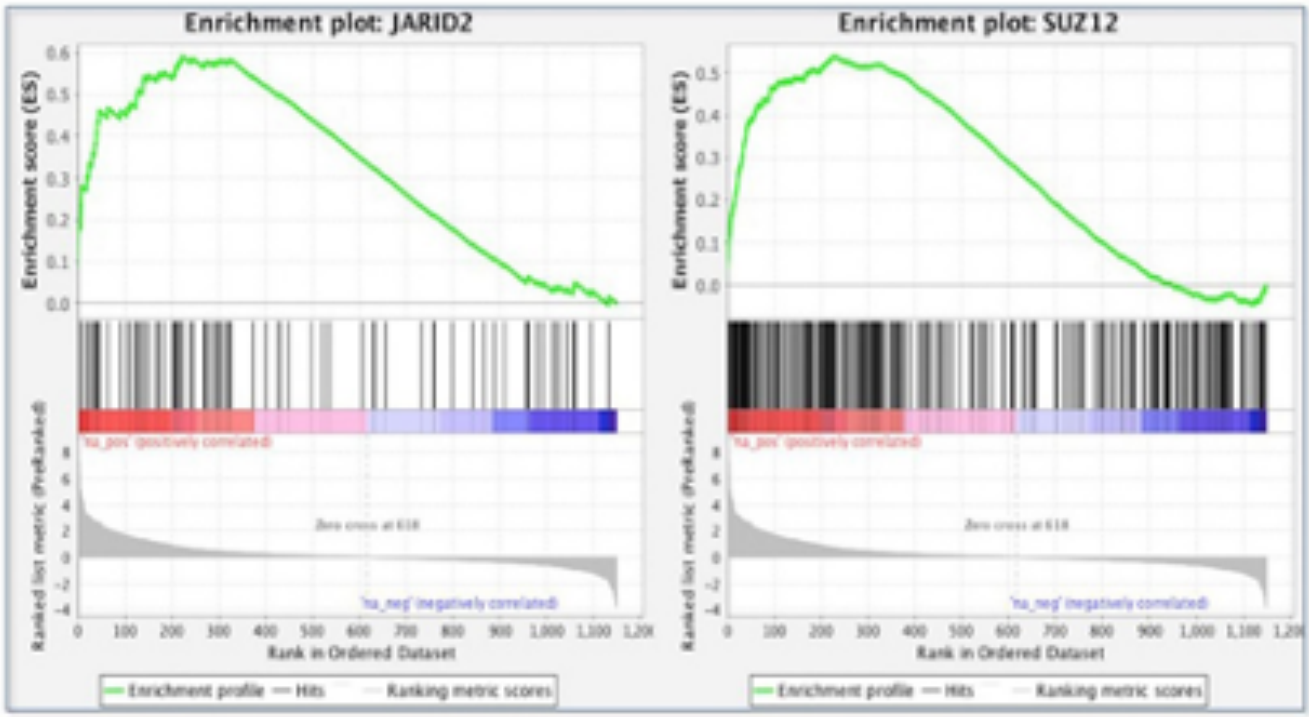

Figure 7. GSEA enrichment graphs of genesets relative to PRC2 activity and differentially expressed genes in pre-B cells. RNA-seq expression data ranked according to fold change in the transcription level in pre-B *Dido1*ΔE16 cells, relative to pre-B wt cells. Maximal correlation was observed between the expression of altered genes in pre-B *Dido1*ΔE16 cells and genes identified by ChIPseq as targets of PRC2 components JARID2 ($p < 0.001$; FDR = 0.213) and SUZ12 ($p < 0.001$: FDR = 0.217).

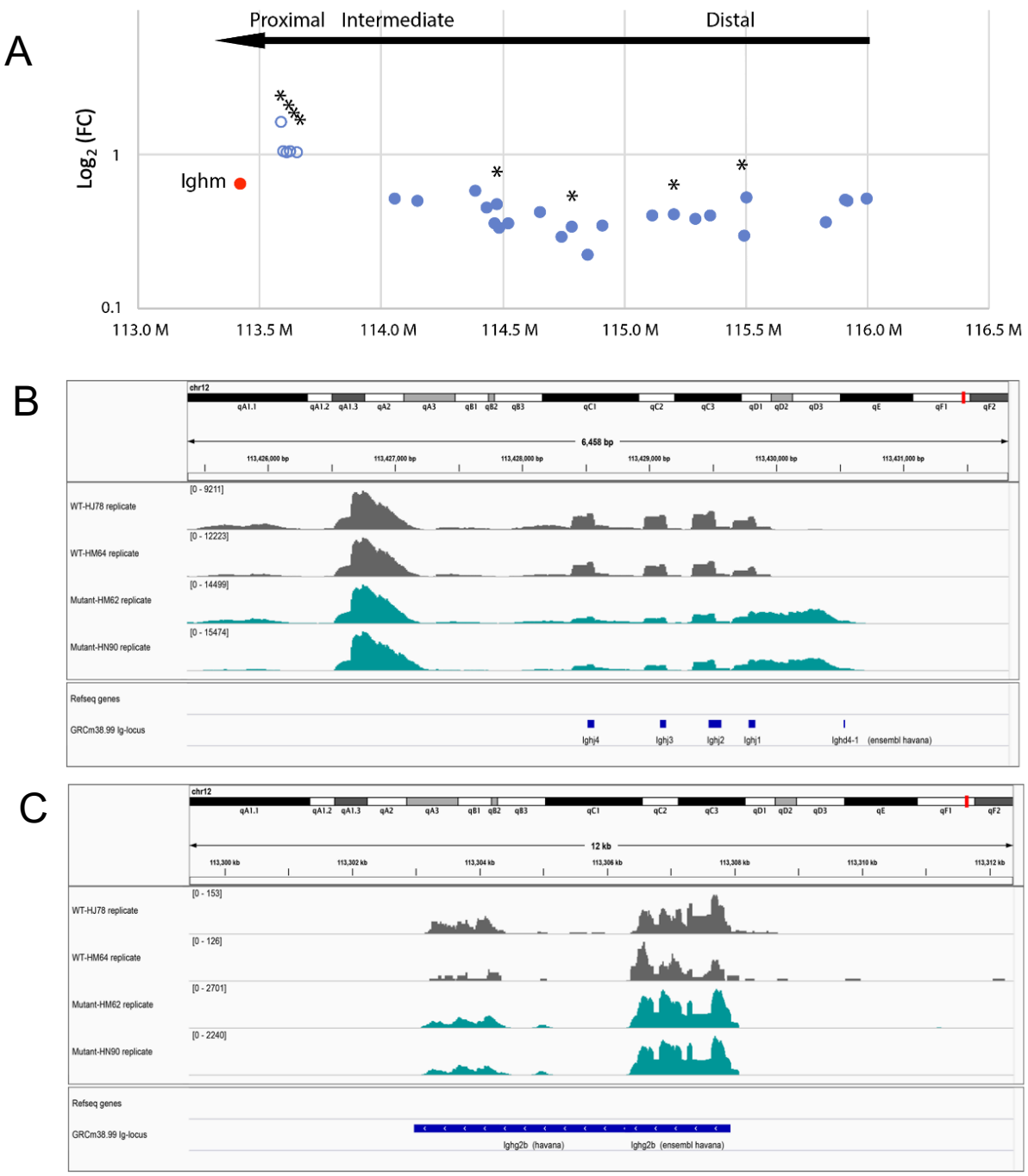

Figure 8. Analysis of the *Igh* locus in *Dido1*ΔE16 pre-B cells. A. Relative abundance of *Ighv* regions in the transcriptome of *Dido1*ΔE16 pre-B cells, shown as logFC of wt levels (*, p<0.05). Bottom, chromosome coordinates; top, the main regions (proximal, intermediate, distal) in which distinct V families map. **B**. Integrative Genomics Viewer (IGV; http://www.broadinstitute.org) plot with RNA-seq data showing transcription from the DNA region between D and J regions; J fragments and the more distal D fragment (D4) positions are represented. **C.** IGV plot with RNA-seq data showing transcription of the *Igg2b* gene in *Dido1*ΔE16 pre-B samples.

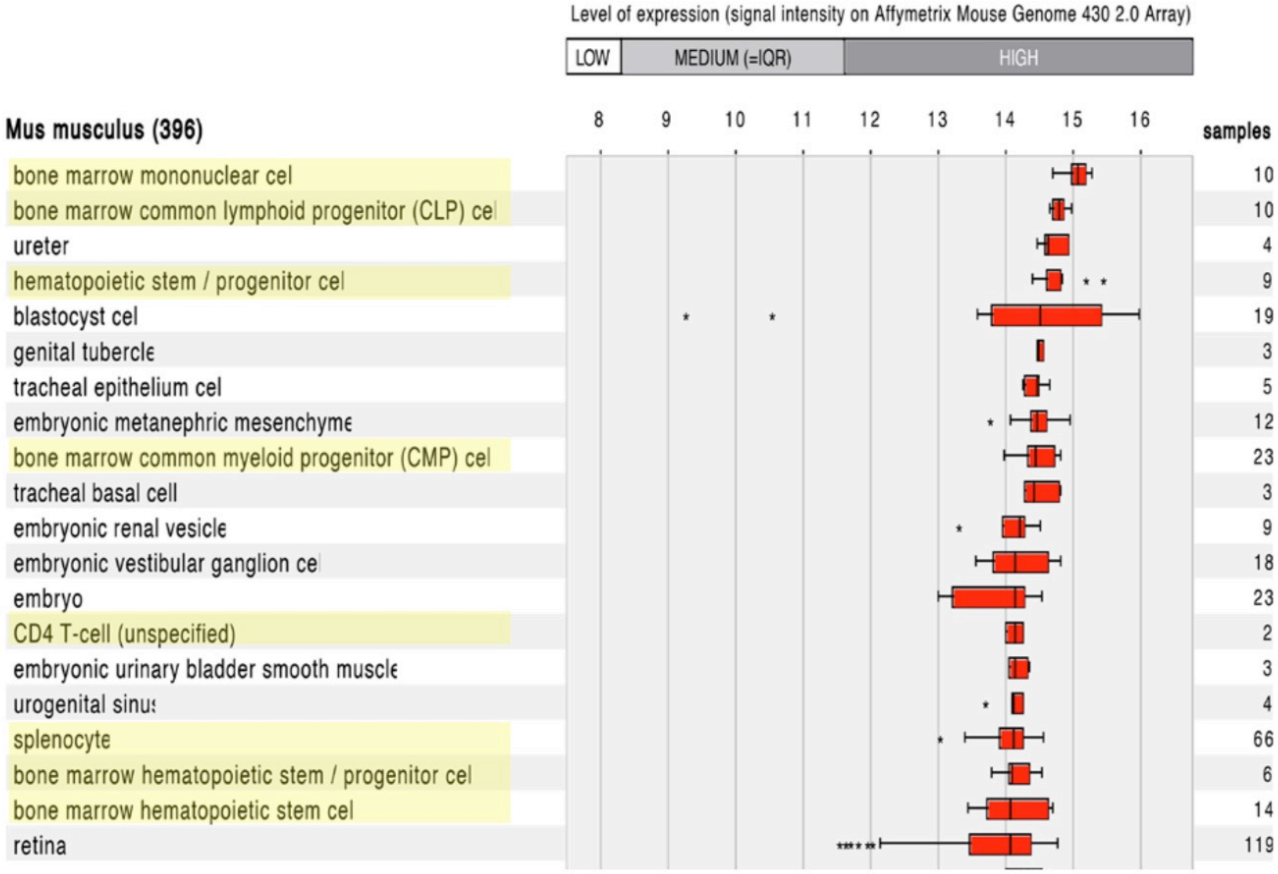

Supplementary figure 1. *Dido1* expression in anatomical samples (1456_at probe, across 396 anatomical samples tested by Genevestigator). The 20 top samples are shown.

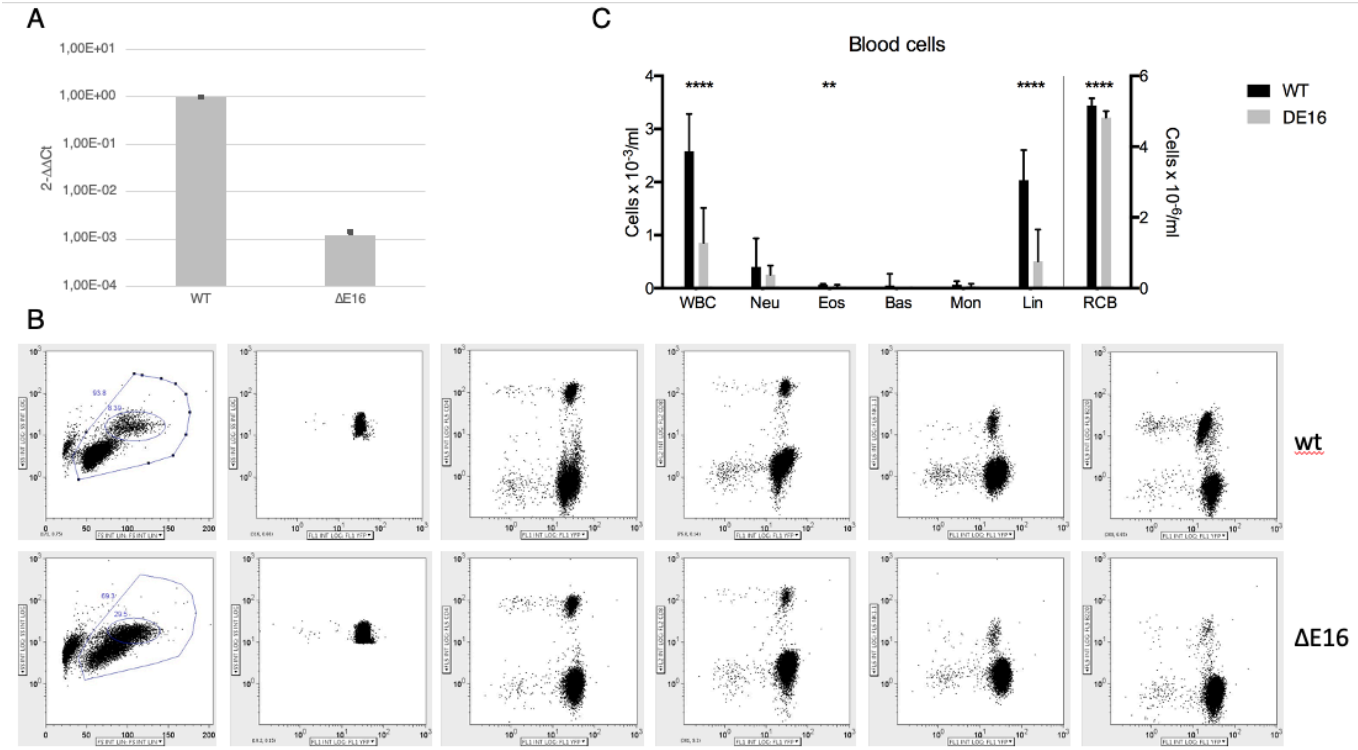

Supplementary figure 2. Deletion of *Dido1* exon 16 in hematopoietic lineage. **A.** Real-time qPCR of genomic DNA from bone marrow lin⁻ cells, normalized by ΔΔCt to the insulin gene (internal control) and wt exon 16 (reference). **B.** Complete blood count in wt (n = 18) and *Dido1*ΔE16 (n = 8) mice. Each column shows the mean number of leukocytes; bars indicate the standard error of the mean (SEM), t-test **** $p < 0.0001$, ** $p < 0.01$. **C.** Flow cytometry analysis of peripheral blood WBC from wt (top row) and *Dido1*ΔE16 (bottom row) mice, showing cells that express EYFP as reporter of recombinase activity and *Dido1* exon 16 deletion. Left to right: EYFP in the FSC vs. SSC myeloid gate and in $CD4^+$, $CD8^+$, $NK1.1^+$ and $B220^+$ cells.

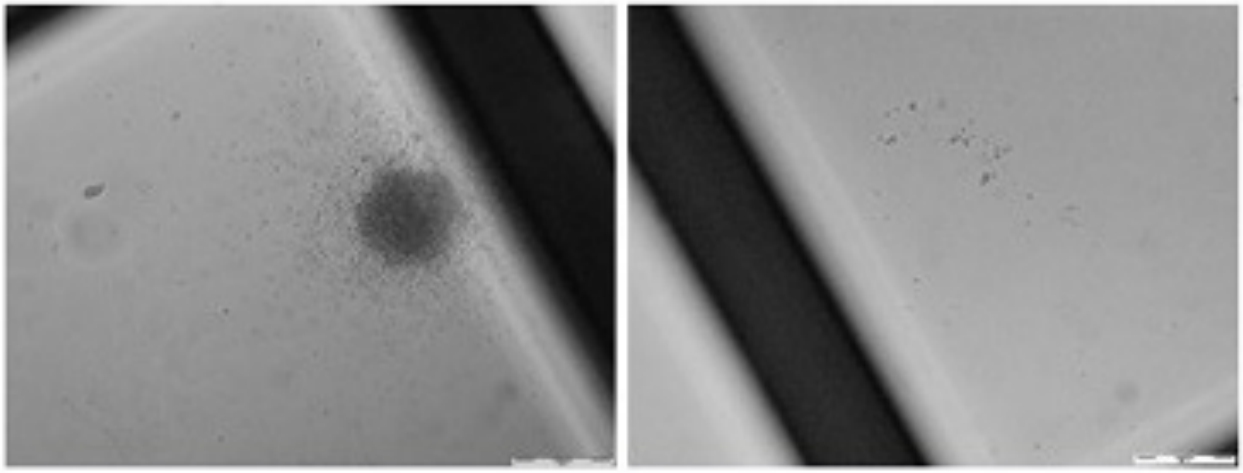

Supplementary figure 3. Clones obtained from lin⁻ cells from wt and *Dido1*ΔE16 mice. Representative micrographs of plated Lin⁻ cells in a semi-solid matrix and photographed after 10 days in culture. Progenitor cells able to generate pre-B colony-forming units gave rise to colonies in IL7-supplemented cultures.

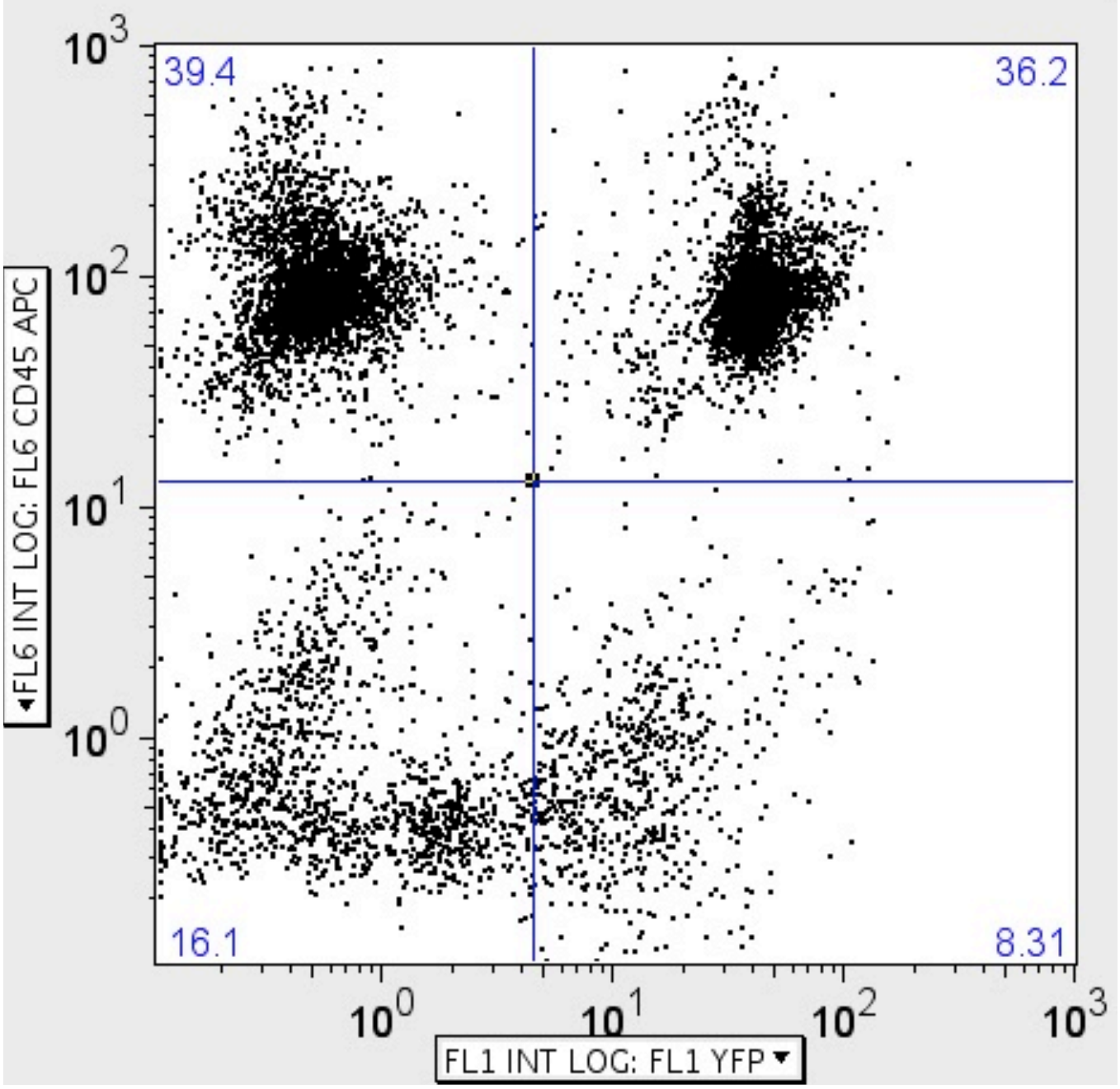

Supplementary figure 4. Cell pool used in adoptive transfer experiments. Flow cytometry analysis of the bone marrow cell pool used as inoculum in competitive adoptive transfer experiments, showing equivalent amounts of EYFP$^+$ (*Dido1*ΔE16) and EYFP$^-$ (wt) hematopoietic (CD45$^+$) cells.

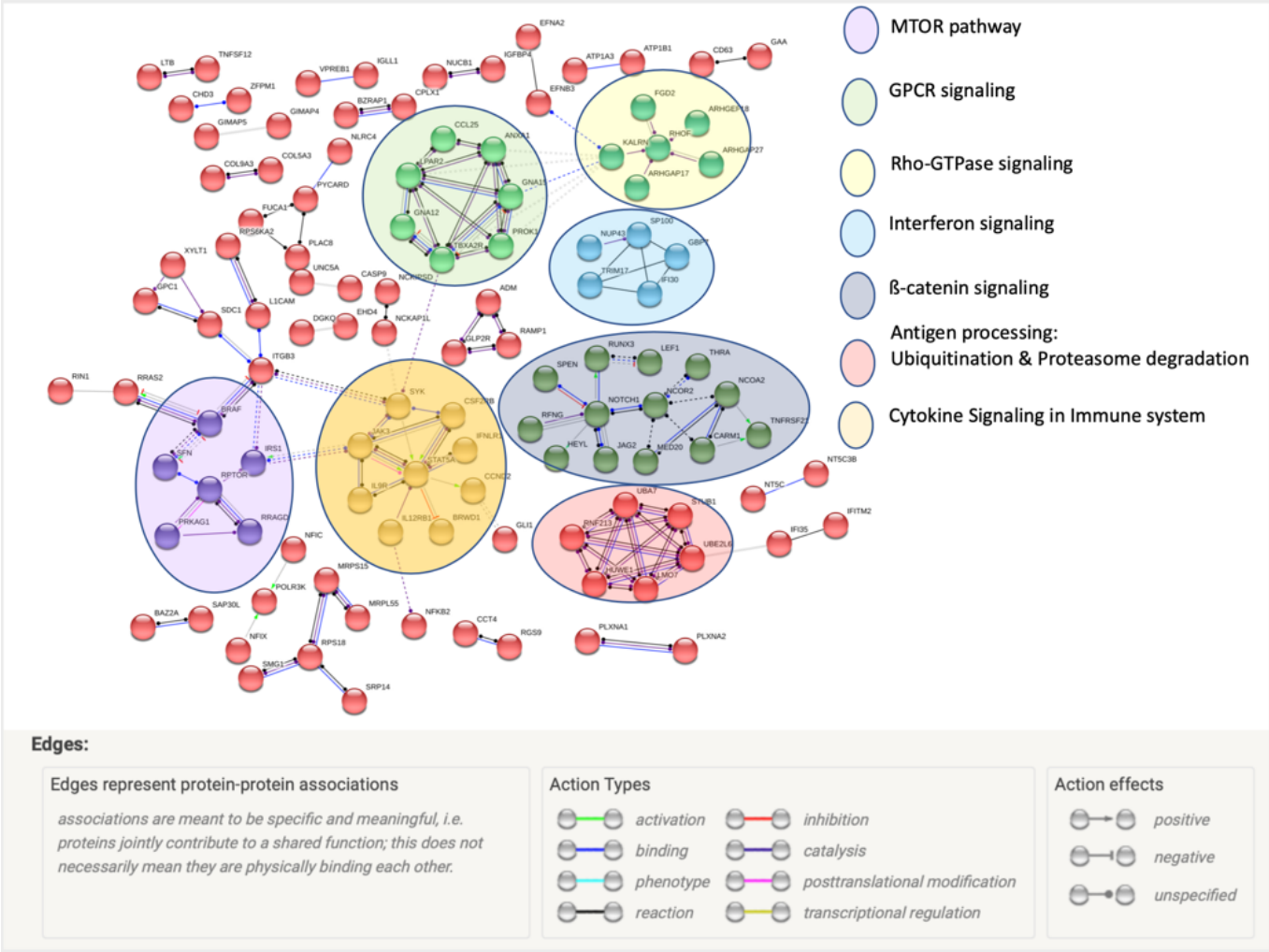

Supplementary figure 5. STRING analysis and clustering of differentially expressed genes between *Dido1*Δ16 and wt LSK cells.

Supplementary Table 1

GSEA analysis of ATAC-seq data

Overlap Results

Collection(s):	C2
# overlaps shown:	50
# genesets in collections:	4762
# genes in comparison (n):	1098
# genes in universe (N):	45956

Gene Set Name	# Genes in Gene Set (K)	Description	# Genes in Overlap (k)	k/K	p-value	FDR q-value
MEISSNER_BRAIN_HCP_WITH_H3K4ME3_AND_H3K27ME3	1069	H3 dimethylation at K4 (H3K4me2) and trimethylation at K27 (H3K27me3) in brain.	135	0,1263	2,66E-57	1,27E-53
BENPORATH_ES_WITH_H3K27ME3	1118	(H3K27me3) mark in their promoters in human embryonic stem cells, as identified by ChIP on chip.	113	0,1011	1,99E-38	4,74E-35
CHEN_METABOLIC_SYNDROM_NETWORK	1210	(MEMN) claimed to have a causal relationship with the metabolic syndrom traits.	111	0,0917	6,59E-34	1,05E-30
BENPORATH_EED_TARGETS	1062	the Polycomb protein EED [GeneID=8726] in human embryonic stem cells.	103	0,097	1,61E-33	1,91E-30
PEREZ_TP53_TARGETS	1174	epithelium) upon expression of TP53 [GeneID=7157] off	105	0,0894	3,65E-31	3,47E-28
BENPORATH_SUZ12_TARGETS	1038	of the Polycomb protein SUZ12 [GeneID=23512] in human embryonic stem cells.	98	0,0944	5,56E-31	4,42E-28
SCHAEFFER_PROSTATE_DEVELOPMENT_48HR_DN	428	females exposed to the androgen dihydrotestosterone [PubChem=10635] for 48 h.	63	0,1472	7,77E-31	5,28E-28
YOSHIMURA_MAPK8_TARGETS_UP	1305	MAPK8 (JNK1) [GeneID=5599].	107	0,082	1,42E-28	8,46E-26
NUYTTEN_EZH2_TARGETS_UP	1037	knockdown of EZH2 [GeneID=2146] by RNAi.	94	0,0906	2,12E-28	1,12E-25
BLALOCK_ALZHEIMERS_DISEASE_UP	1691	disease.	123	0,0727	5,72E-28	2,73E-25
WONG_ADULT_TISSUE_STEM_MODULE	721	regulated in a compendium of adult tissue stem cells.	76	0,1054	3,21E-27	1,39E-24
MEISSNER_NPC_HCP_WITH_H3K4ME2	491	H3 dimethylation mark at K4 (H3K4me2) in neural precursor cells (NPC).	62	0,1263	1,29E-26	5,12E-24
CUI_TCF21_TARGETS_2_DN	830	isolated from TCF21 [Gene ID=6943] knockout mice.	80	0,0964	5,08E-26	1,86E-23
LIM_MAMMARY_STEM_CELL_UP	489	mouse and human species.	60	0,1227	3,92E-25	1,33E-22
MIKKELSEN_NPC_ICP_WITH_H3K4ME3	445	histone H3 trimethylation mark at K4 (H3K4me3) in neural progenitor cells (NPC).	57	0,1281	7,01E-25	2,22E-22
KINSEY_TARGETS_OF_EWSR1_FLII_FUSION_DN	329	Genes down-regulated in TC71 and EWS502 cells (Ewing's sarcoma) by EWSR1-FLI1 [GeneID=2130;2314] as inferred from RNAi knockdown of this fusion protein.	48	0,1459	1,29E-23	3,83E-21
SMID_BREAST_CANCER_BASAL_DN	701	Genes down-regulated in basal subtype of breast cancer samles.	69	0,0984	4,22E-23	1,18E-20
BENPORATH_PRC2_TARGETS	652	Set 'PRC2 targets': Polycomb Repression Complex 2 (PRC) targets; identified by ChIP on chip on human embryonic stem cells as genes that: posess the trimethylated H3K27 mark in their promoters and are bound by SUZ12 [GeneID=23512] and EED [GeneID=8726] Polycomb proteins.	65	0,0997	4,00E-22	1,06E-19
LEE_BMP2_TARGETS_UP	745	Genes up-regulated in uterus upon knockout of BMP2 [GeneID=650].	69	0,0926	1,29E-21	3,23E-19
DODD_NASOPHARYNGEAL_CARCINOMA_UP	1821	Genes up-regulated in nasopharyngeal carcinoma (NPC) compared to the normal tissue.	114	0,0626	1,06E-20	2,52E-18
GOBERT_OLIGODENDROCYTE_DIFFERENTIATION_DN	1080	Genes down-regulated during differentiation of Oli-Neu cells (oligodendroglial precursor) in response to PD174265 [PubChem=4709].	83	0,0769	1,45E-20	3,30E-18
ZWANG_TRANSIENTLY_UP_BY_2ND_EGF_PULSE_ONLY	1725	Genes transiently induced only by the second pulse of EGF [GeneID =1950] in 184A1 cells (mammary epithelium).	109	0,0632	4,04E-20	8,74E-18
GOZGIT_ESR1_TARGETS_DN	781	Genes down-regulated in TMX2-28 cells (breast cancer) which do not express ESR1 [GeneID=2099]) compared to the parental MCF7 cells which do.	68	0,0871	7,21E-20	1,49E-17
GRAESSMANN_APOPTOSIS_BY_DOXORUBICIN_UP	1142	Genes up-regulated in ME-A cells (breast cancer) undergoing apoptosis in response to doxorubicin [PubChem=31703].	82	0,0718	1,51E-18	2,99E-16
SMID_BREAST_CANCER_LUMINAL_B_DN	564	Genes down-regulated in the luminal B subtype of breast cancer.	55	0,0975	1,78E-18	3,38E-16
SMID_BREAST_CANCER_BASAL_UP	648	Genes up-regulated in basal subtype of breast cancer samles.	59	0,091	2,63E-18	4,82E-16
LIU_PROSTATE_CANCER_DN	481	Genes down-regulated in prostate cancer samples.	50	0,104	4,61E-18	8,12E-16
DURAND_STROMA_S_UP	297	Genes up-regulated in the HSC supportive stromal cell lines.	39	0,1313	8,07E-18	1,37E-15
YANG_BCL3_TARGETS_UP	364	Genes up-regulated in neonatal cardiac myocytes upon knockdown of BCL3 [GeneID=602] by RNAi.	43	0,1181	9,24E-18	1,52E-15
CHICAS_RB1_TARGETS_CONFLUENT	567	Genes up-regulated in confluent IMR90 cells (fibroblast) after knockdown of RB1 [GeneID=5925] by RNAi.	54	0,0952	1,03E-17	1,64E-15
MEISSNER_NPC_HCP_WITH_H3_UNMETHYLATED	536	Genes with high-CpG-density promoters (HCP) that have no histone H3 methylation marks in neural precursor cells (NPC).	52	0,097	1,91E-17	2,88E-15
MIKKELSEN_ES_ICP_WITH_H3K4ME3	718	Genes with intermediate-CpG-density (ICP) promoters bearing histone H3 K4 trimethylation mark (H3K4me3) in embryonic stem cells (ES).	61	0,085	1,94E-17	2,88E-15
PLASARI_TGFB1_TARGETS_10HR_DN	244	Genes down-regulated in MEF cells (embryonic fibroblast) upon stimulation with TGFB1 [GeneID=7040] for 10 h.	35	0,1434	2,36E-17	3,40E-15
IVANOVA_HEMATOPOIESIS_STEM_CELL_AND_PROGENITOR	681	Genes in the expression cluster 'HSC and Progenitors Shared': up-regulated in hematopoietic stem cells (HSC) and progenitors from adult bone marrow and fetal liver.	59	0,0866	2,67E-17	3,74E-15
NUYTTEN_EZH2_TARGETS_DN	1024	Genes down-regulated in PC3 cells (prostate cancer) after knockdown of EZH2 [GeneID=2146] by RNAi.	74	0,0723	5,40E-17	7,35E-15
ZWANG_TRANSIENTLY_UP_BY_1ST_EGF_PULSE_ONLY	1839	Genes transiently induced only by the first pulse of EGF [GeneID =1950] in 184A1 cells (mammary epithelium).	106	0,0576	8,61E-17	1,13E-14

CREIGHTON_ENDOCRINE_THERAPY_RESISTANCE_3	720	The 'group 3 set' of genes associated with acquired endocrine therapy resistance in breast tumors expressing ESR1 and ERBB2 [GeneID=2099;2064].	60	0,0833	8,75E-17	1,13E-14
MCBRYAN_PUBERTAL_BREAST_4_5WK_UP	271	Genes up-regulated during pubertal mammary gland development between week 4 and 5.	36	0,1328	1,02E-16	1,27E-14
ONDER_CDH1_TARGETS_2_DN	464	Genes down-regulated in HMLE cells (immortalized nontransformed mammary epithelium) after E-cadhedrin (CDH1) [GeneID=999] knockdown by RNAi.	47	0,1013	1,28E-16	1,56E-14
LINDGREN_BLADDER_CANCER_CLUSTER_2B	392	Genes specifically up-regulated in Cluster IIb of urothelial cell carcinom (UCC) tumors.	43	0,1097	1,43E-16	1,71E-14
GRYDER_PAX3FOXO1_ENHANCERS_IN_TADS	975	Expressed genes (FPKM>1) associated with high-confidence PAX3-FOXO1 sites with enhancers in primary tumors and cell lines, restricted to those within topological domain boundaries	71	0,0728	1,60E-16	1,86E-14
RIGGI_EWING_SARCOMA_PROGENITOR_UP	430	Genes up-regulated in mesenchymal stem cells (MSC) engineered to express EWS-FLI1 [GeneID=2130;2321] fusion protein.	45	0,1047	1,68E-16	1,90E-14
WEST_ADRENOCORTICAL_TUMOR_DN	546	Down-regulated genes in pediatric adrenocortical tumors (ACT) compared to the normal tissue.	51	0,0934	1,87E-16	2,08E-14
NABA_MATRISOME	1028	Ensemble of genes encoding extracellular matrix and extracellular matrix-associated proteins	73	0,071	2,22E-16	2,41E-14
BAELDE_DIABETIC_NEPHROPATHY_DN	434	Genes down-regulated in glomeruli of kidneys from patients with diabetic nephropathy (type 2 diabetes mellitus).	45	0,1037	2,38E-16	2,52E-14
RODRIGUES_THYROID_CARCINOMA_POORLY_DIFFERENTIATED_DN	805	Genes down-regulated in poorly differentiated thyroid carcinoma (PDTC) compared to normal thyroid tissue.	63	0,0783	2,97E-16	3,07E-14
BLALOCK_ALZHEIMERS_DISEASE_DN	1237	Genes down-regulated in brain from patients with Alzheimer's disease.	81	0,0655	4,81E-16	4,87E-14
BOQUEST_STEM_CELL_CULTURED_VS_FRESH_UP	425	Genes up-regulated in cultured stromal stem cells from adipose tissue, compared to the freshly isolated cells.	44	0,1035	5,42E-16	5,37E-14
ACEVEDO_FGFR1_TARGETS_IN_PROSTATE_CANCER_MODEL_DN	308	Genes down-regulated during prostate cancer progression in the JOCK1 model due to inducible activation of FGFR1 [GeneID=2260] gene in prostate.	37	0,1201	1,04E-15	1,01E-13
BONOME_OVARIAN_CANCER_SURVIVAL_SUBOPTIMAL_DEBULKING	510	Genes whose expression in suboptimally debulked ovarian tumors is associated with survival prognosis.	48	0,0941	1,08E-15	1,03E-13

Supplementary Table 2

Differentially expresed genes. RNA-seq data

Upregulated in Dido1ΔE16 preB						
GeneID	Symbol	logFC	logCPM	F	PValue	FDR
ENSMUST00000054491.5	Sox18	8,857512753	1,34795791	77,4372545	1,37E-18	3,56E-15
ENSMUST00000030420.8	Epha8	8,802780653	1,308029304	75,36574302	3,92E-18	9,31E-15
ENSMUST00000127305.1	Epn3	8,460520852	1,009187845	61,83380794	3,74E-15	7,11E-12
ENSMUST00000045068.9	Cplx3	8,373271374	3,009840974	200,5853343	1,80E-45	5,13E-41
ENSMUST00000093832.10	Lman1l	8,327862413	2,278974964	129,007599	6,81E-30	5,10E-26
ENSMUST00000044123.1	Trhr2	8,178254997	3,689639849	291,5462108	2,38E-65	1,69E-60
ENSMUST00000176061.1	Gm20681	8,12726194	2,058727587	112,3932968	2,95E-26	1,61E-22
ENSMUST00000187142.2	Zfp469	7,556092546	2,19423831	116,6247506	3,49E-27	2,11E-23
ENSMUST00000069741.3	E130018O15Rik	7,328231004	3,400752558	227,4450916	2,97E-51	1,06E-46
ENSMUST00000231330.1	Gm35455	7,257248574	1,915417082	96,70873365	8,07E-23	3,28E-19
ENSMUST00000044970.6	Mgat3	7,248207023	1,912963946	96,40751334	9,39E-23	3,72E-19
ENSMUST00000166193.8	Igfn1	6,853215762	1,529374109	74,07841672	7,53E-18	1,73E-14
ENSMUST00000114574.2	Glp1r	6,747750682	2,213000516	108,8820554	1,73E-25	9,14E-22
ENSMUST00000181436.1	Gm26583	6,580283705	2,667763471	135,657234	3,65E-31	2,89E-27
ENSMUST00000196046.1	Gm43364	6,479984579	1,171433088	57,88118167	2,79E-14	4,97E-11
ENSMUST00000000199.7	Ncs1	6,476854223	3,228629155	186,3587587	2,01E-42	4,10E-38
ENSMUST00000149378.1	Gm13398	6,422683528	3,251844647	184,800757	5,98E-42	1,06E-37
ENSMUST00000046892.9	Cplx1	6,350367745	2,47891755	116,6594687	3,55E-27	2,11E-23
ENSMUST00000027533.8	Klhl30	6,312169778	1,524034391	68,46552634	1,29E-16	2,79E-13
ENSMUST00000003501.8	Elavl3	6,145498595	3,091770125	164,8498319	9,99E-38	1,42E-33
ENSMUST00000100396.3	4930407I10Rik	6,007672773	3,012110222	152,6974129	4,51E-35	5,35E-31
ENSMUST00000088904.9	Espnl	5,864652669	2,312617787	100,0042741	1,53E-23	6,59E-20
ENSMUST00000126198.2	Fam78b	5,812836728	1,343676636	58,01062587	2,61E-14	4,71E-11
ENSMUST00000140833.1	Gm15728	5,546501016	2,104448451	82,37768727	1,13E-19	3,28E-16
ENSMUST00000207625.1	A930030B08Rik	5,274463635	2,786384842	113,8938095	1,38E-26	7,88E-23
ENSMUST00000030677.6	Map3k6	5,128849384	1,20890097	47,07878579	6,83E-12	9,26E-09
ENSMUST00000036215.7	Foxj1	5,05070799	4,24479595	240,3549946	3,38E-54	1,60E-49
ENSMUST00000057831.7	Cilp2	5,029747674	2,245706746	81,06735435	2,19E-19	6,11E-16
ENSMUST00000051765.8	Glp2r	4,982508838	1,935230947	65,5190259	5,80E-16	1,18E-12
ENSMUST00000039752.3	Slc16a8	4,955339846	1,298610136	46,7491308	8,08E-12	1,08E-08
ENSMUST00000145549.1	B230312C02Rik	4,950126862	4,267465985	215,6493373	4,32E-37	5,59E-33
ENSMUST00000201921.1	4930478P22Rik	4,849938561	3,724752284	171,9832757	2,77E-39	4,38E-35
ENSMUST00000080368.12	Atp8a2	4,772741967	2,689835341	95,81534358	1,27E-22	4,81E-19
ENSMUST00000238352.1	Gm10570	4,65685676	1,140663365	40,24497226	2,24E-10	2,37E-07
ENSMUST00000073935.6	Gsg1l	4,583973176	2,863310035	99,65603652	1,82E-23	7,63E-20
ENSMUST00000053926.11	Gm49486	4,520082979	1,257922682	40,51833229	1,95E-10	2,10E-07
ENSMUST00000057612.8	Ssc5d	4,502593079	3,19675086	117,2099648	2,60E-27	1,68E-23
ENSMUST00000168386.8	Prr36	4,461707258	1,163163503	38,15753377	6,53E-10	6,33E-07
ENSMUST00000055436.4	Hpdl	4,395973385	1,110148268	35,18551657	3,00E-09	2,56E-06
ENSMUST00000025805.7	Cnih2	4,390761895	1,571238692	46,78615298	7,93E-12	1,06E-08
ENSMUST00000050519.7	Elfn1	4,348535247	1,06872759	33,9158706	5,77E-09	4,64E-06
ENSMUST00000202026.3	4930478P22Rik	4,326020601	1,697352809	47,61659668	5,20E-12	7,34E-09
ENSMUST00000040059.8	Hyal3	4,306498157	1,494729643	43,48327016	4,28E-11	5,04E-08
ENSMUST00000114973.8	Kalrn	4,193488629	3,806229123	144,124296	3,37E-33	3,20E-29
ENSMUST00000179520.1	Ighd4-1	4,181337013	2,652040852	77,36235869	1,43E-18	3,63E-15
ENSMUST00000046937.3	Tssk1	4,152835828	1,611894621	43,99331675	3,30E-11	3,95E-08
ENSMUST00000103430.1	Ighj1	4,142917982	3,161137658	101,0360908	9,07E-24	4,17E-20
ENSMUST00000232008.1	4933432I09Rik	4,123826935	1,644247453	43,5698768	4,09E-11	4,86E-08
ENSMUST00000095360.10	Igf1	4,022933516	3,03523223	89,80536709	2,64E-21	8,94E-18
ENSMUST00000150442.1	Gm11642	3,953466338	1,331947062	34,99043619	3,32E-09	2,76E-06
ENSMUST00000030585.7	A3galt2	3,901896341	1,92571106	47,4104692	5,78E-12	8,07E-09
ENSMUST00000009875.4	Kcnd1	3,878502091	3,060776876	86,71730507	1,26E-20	3,98E-17
ENSMUST00000238703.1	Gm50464	3,843958267	1,322656373	33,29999737	7,90E-09	6,22E-06
ENSMUST00000231439.1	Igll1	3,654322209	3,723318304	109,8775049	5,94E-25	2,92E-21
ENSMUST00000132562.1	Wrap73	3,651890768	2,045044936	44,96172096	2,01E-11	2,47E-08
ENSMUST00000045085.7	Grin3b	3,645437838	3,469184124	95,7902219	1,28E-22	4,81E-19
ENSMUST00000067458.6	Sema5a	3,639412476	4,416924321	34,1782988	0,000204773	0,04689568
ENSMUST00000052528.4	Gm9847	3,624529389	2,40044788	52,78942758	3,73E-13	6,17E-10
ENSMUST00000145401.7	Il9r	3,600406092	3,923795062	100,1664368	6,83E-18	1,59E-14
ENSMUST00000204971.1	Pyroxd1	3,535965666	1,681534547	35,46673706	2,60E-09	2,23E-06

ENSMUST00000103091.8	Elmo2	3,524071926	2,440161058	52,32854761	4,70E-13	7,52E-10
ENSMUST00000095076.9	Epb41l4b	3,467940505	1,959970582	39,68324766	2,99E-10	3,06E-07
ENSMUST00000225289.1	Rab24	3,467489401	1,933190752	38,68112905	4,99E-10	4,94E-07
ENSMUST00000206494.1	Unc45a	3,446151321	3,057578002	70,31115962	5,08E-17	1,13E-13
ENSMUST00000054487.9	Ajuba	3,432751962	1,148390741	25,21224091	5,14E-07	0,000278234
ENSMUST00000142367.7	Palm3	3,415190644	1,474732627	30,13047218	4,05E-08	2,80E-05
ENSMUST00000185943.1	5031425E22Rik	3,323723001	3,043311935	65,79335522	5,04E-16	1,06E-12
ENSMUST00000124126.1	Polr1c	3,319268229	1,183690409	23,8860097	1,02E-06	0,000514616
ENSMUST00000053856.5	Pcdhb17	3,31656198	2,705065885	53,65228999	2,40E-13	4,06E-10
ENSMUST00000103105.9	Aoc3	3,313840055	1,722766459	32,07082628	1,49E-08	1,15E-05
ENSMUST00000204059.2	Add2	3,308950451	2,010560846	37,76298621	7,99E-10	7,54E-07
ENSMUST00000028689.3	Lrp4	3,288327318	3,094569561	65,64168988	5,42E-16	1,12E-12
ENSMUST00000132422.1	Gps1	3,284351465	2,758402058	54,54650402	1,52E-13	2,64E-10
ENSMUST00000122882.1	2210406O10Rik	3,271197846	1,046784841	22,15524491	2,52E-06	0,001144697
ENSMUST00000065587.4	Ackr3	3,26082333	3,812359919	93,99867194	3,47E-22	1,24E-18
ENSMUST00000093369.4	Nefh	3,255859372	1,408825797	26,37595979	2,81E-07	0,000162776
ENSMUST00000144818.1	Gm14168	3,243553083	4,087137291	107,3749792	3,70E-25	1,88E-21
ENSMUST00000152138.7	Casc1	3,209823198	1,201112581	22,7080501	1,89E-06	0,000883833
ENSMUST00000037007.3	Evpl	3,199786031	2,525025391	45,620841	1,44E-11	1,85E-08
ENSMUST00000104937.1	Ankrd63	3,182732563	1,266945918	23,91952368	1,00E-06	0,000509172
ENSMUST00000051259.9	Adgrg3	3,149464432	1,582950951	27,5342098	1,54E-07	9,60E-05
ENSMUST00000055619.4	Hic1	3,146427583	2,54680267	45,31331751	1,68E-11	2,10E-08
ENSMUST00000193194.1	AA914427	3,146122504	1,118916616	20,98483954	4,63E-06	0,001923849
ENSMUST00000211939.1	Polr2c	3,127553302	2,612228058	46,30081159	1,02E-11	1,34E-08
ENSMUST00000099373.11	Cnnm2	3,11348923	2,358574148	40,20048908	2,29E-10	2,40E-07
ENSMUST00000122029.1	Gm6939	3,104980149	2,396644455	41,14392486	1,42E-10	1,58E-07
ENSMUST00000133221.2	Trp53cor1	3,098395699	1,320261454	23,37125186	1,34E-06	0,000656207
ENSMUST00000055872.2	Galr2	3,091181839	2,541521959	43,07381194	5,28E-11	6,11E-08
ENSMUST00000016172.8	Celsr1	3,06916754	2,851172513	51,14074038	8,61E-13	1,35E-09
ENSMUST00000187230.1	Begain	3,058379859	1,290756938	22,67051025	1,92E-06	0,000898314
ENSMUST00000217282.1	Gm38431	3,047412451	2,155405091	35,14967029	3,05E-09	2,59E-06
ENSMUST00000039178.11	Tnn	3,021037311	1,966058195	30,76333939	2,92E-08	2,08E-05
ENSMUST00000236745.1	Ubash3a	3,015582757	3,297585315	63,06607012	2,00E-15	3,91E-12
ENSMUST00000149932.1	Gm13184	3,001670523	1,615375774	25,43483112	4,58E-07	0,000252715
ENSMUST00000051442.6	Pcdhb16	2,981830872	2,384961332	37,70910916	8,22E-10	7,70E-07
ENSMUST00000145988.8	Dnhd1	2,979992739	5,009071296	137,1784691	1,11E-31	9,90E-28
ENSMUST00000098778.2	Gm10676	2,975303294	5,190339212	145,529287	1,66E-33	1,69E-29
ENSMUST00000204482.2	Tmem176a	2,954310878	1,69945943	26,26396613	2,98E-07	0,000169733
ENSMUST00000022699.9	Gfra2	2,926129741	3,827212439	78,58993845	7,71E-19	2,07E-15
ENSMUST00000127208.7	Lrrc14	2,921898408	2,831551061	46,08399964	1,13E-11	1,47E-08
ENSMUST00000132080.1	Tmem259	2,905692276	3,118682753	53,42706116	2,69E-13	4,50E-10
ENSMUST00000180252.2	Tmem151b	2,902782205	1,092301247	18,5867386	1,62E-05	0,005826049
ENSMUST00000180852.1	2610037D02Rik	2,883952188	1,80721041	26,32098562	2,89E-07	0,000165457
ENSMUST00000017637.12	Igfbp4	2,865737935	4,840380216	120,4695138	5,03E-28	3,41E-24
ENSMUST00000003154.6	Efna2	2,856305497	1,64539989	23,91329801	1,01E-06	0,000509172
ENSMUST00000139210.7	Socs2	2,851757636	1,221918022	18,96721204	1,33E-05	0,004908384
ENSMUST00000231640.1	Gm49745	2,835067494	2,0716474	29,54989546	5,45E-08	3,75E-05
ENSMUST00000025830.8	Apba1	2,83487618	3,933545204	77,33293058	1,47E-18	3,68E-15
ENSMUST00000203350.1	Gm44067	2,829409924	5,51242358	148,3735112	3,97E-34	4,35E-30
ENSMUST00000141708.1	Plxdc1	2,818761143	1,055704752	16,95217177	3,83E-05	0,011950139
ENSMUST00000039840.14	Enpp6	2,810178276	2,502889818	36,13162121	1,85E-09	1,64E-06
ENSMUST00000047309.5	Nat14	2,795271917	2,755541996	40,68164561	1,79E-10	1,98E-07
ENSMUST00000071135.5	Tubb4a	2,778146887	3,099110788	48,58844318	3,16E-12	4,59E-09
ENSMUST00000192126.1	Gm18407	2,775747462	3,512532719	59,74526766	1,08E-14	2,00E-11
ENSMUST00000193564.1	Gm37736	2,774531055	1,80628983	24,78582995	6,41E-07	0,000339357
ENSMUST00000179531.1	Rnpepl1	2,766281975	5,374760616	135,2117135	2,99E-31	2,51E-27
ENSMUST00000070328.9	Sh2d4b	2,756022319	4,209991815	84,79227113	3,32E-20	1,01E-16
ENSMUST00000033054.9	Adm	2,745857335	4,051061047	77,31621369	1,52E-18	3,73E-15
ENSMUST00000201142.3	1700028E10Rik	2,743697883	2,808371646	40,61036861	1,86E-10	2,04E-07
ENSMUST00000105572.2	Perm1	2,736342512	4,010776099	76,00926352	2,83E-18	6,83E-15
ENSMUST00000211974.1	Adgrg3	2,726435361	1,610165285	21,80186389	3,02E-06	0,001337643
ENSMUST00000154277.1	Galr2	2,720036002	1,686457289	22,47970309	2,12E-06	0,000979268
ENSMUST00000183583.7	Ntng2	2,713081499	1,010883844	15,50033431	8,25E-05	0,022513142
ENSMUST00000075827.4	Jag2	2,709793846	3,29670242	51,52895184	7,06E-13	1,12E-09
ENSMUST00000028403.2	Cybrd1	2,701860557	2,708552249	36,43646512	1,87E-09	1,65E-06
ENSMUST00000201164.1	4930553P18Rik	2,691706319	2,400043714	31,37788503	2,12E-08	1,55E-05
ENSMUST00000060125.6	Scn4b	2,689071631	5,386890346	128,0014945	5,13E-29	3,65E-25

ENSMUST00000180430.1	Ksr2	2,687576574	1,31561539	17,82193914	2,43E-05	0,008074414
ENSMUST00000149137.2	Gm13270	2,675173489	1,389537889	18,17959909	2,01E-05	0,00688442
ENSMUST00000043315.14	Serpina3g	2,670885696	6,717498823	193,9837055	4,37E-44	1,04E-39
ENSMUST00000014118.3	Mcemp1	2,659118377	1,757489807	22,08215972	2,61E-06	0,001182165
ENSMUST00000108288.8	Lrfn1	2,648980494	2,118020507	26,87884245	2,17E-07	0,00012915
ENSMUST00000159004.1	Mrgpra2a	2,648018483	1,876412857	22,36282257	2,92E-06	0,001304577
ENSMUST00000165968.1	Serpina3e-ps	2,644285216	2,411907374	30,63693545	3,11E-08	2,21E-05
ENSMUST00000203263.1	Gm44066	2,643559159	4,429725713	87,93388583	6,79E-21	2,20E-17
ENSMUST00000224954.1	Daam2	2,639852539	3,123062049	44,50121968	2,54E-11	3,10E-08
ENSMUST00000033915.8	Gpm6a	2,631341363	1,334824432	17,16215365	3,44E-05	0,011019398
ENSMUST00000058479.6	Drc7	2,627568213	2,080968669	25,83238963	3,73E-07	0,000208904
ENSMUST00000046383.11	Tnfsf10	2,627373387	4,558816641	92,17799591	1,56E-21	5,42E-18
ENSMUST00000231568.1	Ermard	2,613916207	1,065845372	14,68957757	0,000126759	0,032014705
ENSMUST00000035672.4	Ppl	2,60080229	1,597221282	19,6156583	9,47E-06	0,003626536
ENSMUST00000132882.1	Hyi	2,585618917	1,637535361	19,80162095	8,59E-06	0,003326038
ENSMUST00000234131.1	Slc8a1	2,580137573	1,850693752	21,79559037	3,03E-06	0,001337869
ENSMUST00000233692.1	Lrrc73	2,578944247	1,6071816	19,47485064	1,02E-05	0,003872694
ENSMUST00000028780.3	Chac1	2,542078207	1,852268354	21,47526434	3,59E-06	0,001528955
ENSMUST00000020549.3	Gzmm	2,539601573	2,0484197	23,59066076	1,19E-06	0,000593671
ENSMUST00000212276.1	2900026A02Rik	2,519530348	1,106689538	14,31217287	0,000154876	0,037971555
ENSMUST00000029658.13	Enpep	2,509797611	3,483001415	49,1351093	2,39E-12	3,59E-09
ENSMUST00000134982.7	Gm14296	2,488825159	1,326195281	15,95959731	6,48E-05	0,018525725
ENSMUST00000019068.6	Alox15	2,4872212	1,833073366	20,19116051	7,41E-06	0,002922246
ENSMUST00000049614.12	B430306N03Rik	2,477422298	4,677193091	85,91677149	1,88E-20	5,83E-17
ENSMUST00000022304.9	Thrb	2,465009772	1,332511772	15,48328466	8,32E-05	0,022673688
ENSMUST00000059026.9	Abi3	2,459223566	2,102308684	22,78780396	1,81E-06	0,000856356
ENSMUST00000209248.1	Rnf223	2,456071228	2,702815818	31,03311763	2,54E-08	1,82E-05
ENSMUST00000027952.11	Plxna2	2,451827751	2,679388168	30,55589348	3,25E-08	2,29E-05
ENSMUST00000144897.1	Slx1b	2,44672511	4,826217701	88,32164445	5,58E-21	1,85E-17
ENSMUST00000194216.1	Gm37795	2,443973485	3,052818063	37,35251713	9,87E-10	8,95E-07
ENSMUST00000159977.1	Pcmt1	2,424066666	1,933994746	20,35431869	6,44E-06	0,002568039
ENSMUST00000040128.11	Atp8b4	2,417728374	2,038192274	20,24541723	8,85E-06	0,003407539
ENSMUST00000200257.1	Gm19710	2,389135468	2,183344783	22,75505761	1,84E-06	0,000865322
ENSMUST00000096338.4	Gpr152	2,382783071	1,262397684	13,86321668	0,000196628	0,045468949
ENSMUST00000090246.4	Sgms2	2,375894668	1,583909448	15,85498177	7,62E-05	0,021131314
ENSMUST00000212475.1	Gm7807	2,354005543	1,500624243	15,34909554	8,94E-05	0,024157467
ENSMUST00000218571.1	Map2k2	2,343529236	2,300906166	23,26372174	1,41E-06	0,000689183
ENSMUST00000134427.1	Gm11613	2,334296872	3,824140741	50,75561061	1,05E-12	1,60E-09
ENSMUST00000043400.7	Asprv1	2,309018389	1,791814166	17,09104218	3,67E-05	0,011591079
ENSMUST00000179719.1	Hyi	2,303165648	3,285830862	37,63990033	8,51E-10	7,92E-07
ENSMUST00000105818.7	Kif17	2,290716976	1,498257089	14,61700719	0,000131734	0,032978986
ENSMUST00000018711.14	Gabarap	2,282096628	4,308942553	62,17482126	3,15E-15	6,06E-12
ENSMUST00000062211.3	Gpat2	2,272488105	1,443188796	13,97570754	0,000185206	0,043462699
ENSMUST00000208023.1	Slc35a2	2,259435725	1,824266541	17,00877201	3,72E-05	0,011727463
ENSMUST00000050020.7	Jaml	2,252198496	2,089603582	19,1849666	1,19E-05	0,004459996
ENSMUST00000048923.6	Spred3	2,233625227	2,883617794	28,47234464	9,51E-08	6,22E-05
ENSMUST00000097474.8	Rcsd1	2,233583036	4,159368437	54,99921882	1,21E-13	2,12E-10
ENSMUST00000060524.10	Trim10	2,23280333	2,290065577	21,04537315	4,50E-06	0,001881433
ENSMUST00000086281.4	Zfp599	2,204170722	3,581558944	40,03868374	2,49E-10	2,57E-07
ENSMUST00000156839.1	Ttpal	2,198145953	1,565111647	13,85379841	0,000197616	0,045623333
ENSMUST00000208686.1	Prcp	2,196527545	2,490823108	22,42829885	2,18E-06	0,001002584
ENSMUST00000094897.4	Dnaaf3	2,194825466	1,820541701	15,86551964	6,80E-05	0,019299718
ENSMUST00000232529.1	Car15	2,190762771	2,816033678	26,49825842	2,64E-07	0,000154042
ENSMUST00000144519.1	Gps1	2,190738575	1,729844653	15,29938823	9,18E-05	0,024668887
ENSMUST00000050511.6	Kynu	2,18494778	2,078697419	18,0026277	2,21E-05	0,007447531
ENSMUST00000074408.6	Ifnlr1	2,184659642	2,438989006	21,6521755	3,27E-06	0,001419737
ENSMUST00000045487.3	Rhou	2,175048853	2,104316282	16,1961656	7,60E-05	0,021097427
ENSMUST00000198190.4	Rnf216	2,1680711	1,738065333	14,84510431	0,000116723	0,030212319
ENSMUST00000029158.3	Aar2	2,141757873	1,767565526	14,88871784	0,000114056	0,029865364
ENSMUST00000132092.1	1110051M20Rik	2,140659711	1,926134182	15,85193673	6,85E-05	0,019390703
ENSMUST00000097648.5	Ramp1	2,138698729	4,519124664	60,58985181	7,04E-15	1,32E-11
ENSMUST00000017561.14	Plxdc1	2,130467259	4,719182841	64,85862685	8,06E-16	1,62E-12
ENSMUST00000156997.7	Dvl1	2,123140792	1,823795163	14,84503948	0,000116727	0,030212319
ENSMUST00000204498.1	Gm44280	2,10551515	2,15921874	17,52632093	2,83E-05	0,009216716
ENSMUST00000165559.2	Ctif	2,102857236	2,200264373	17,60586527	2,72E-05	0,008870608
ENSMUST00000159283.7	Manf	2,099437434	3,071940068	27,73969493	1,39E-07	8,75E-05
ENSMUST00000003561.9	Phyhip	2,096810671	1,721291854	13,77959715	0,000205576	0,046928667

ENSMUST00000173127.2	Gm9574	2,090222372	2,324130758	18,82405284	1,43E-05	0,005183463
ENSMUST00000108567.8	Zfp444	2,085246088	4,243471562	50,20504135	1,39E-12	2,10E-09
ENSMUST00000206275.1	Bola2	2,04896394	3,857536965	40,12932128	2,38E-10	2,47E-07
ENSMUST00000040821.4	Heyl	2,045638174	5,54571685	79,12551615	1,17E-18	3,07E-15
ENSMUST00000024774.13	Guca1b	2,026143064	2,60078282	20,21724586	6,91E-06	0,002751059
ENSMUST00000030551.10	Alpl	2,024903863	6,33004764	100,9736693	9,76E-24	4,34E-20
ENSMUST00000165838.8	Metrn	2,013891208	3,934040724	40,28601272	2,20E-10	2,33E-07
ENSMUST00000082432.4	Dio2	2,000961368	2,76544012	21,60887215	3,34E-06	0,001443352
ENSMUST00000094451.3	Gpr157	2,000914006	2,899214486	23,10041596	1,54E-06	0,00074516
ENSMUST00000153578.7	Tspoap1	1,991732965	3,934592249	39,14459395	5,11E-10	5,02E-07
ENSMUST00000098513.5	Plekhf1	1,96504943	2,049646196	14,4279329	0,000145641	0,035958993
ENSMUST00000052457.14	Mtss2	1,960211438	2,117583032	14,79164572	0,000120079	0,030693586
ENSMUST00000028179.14	Fcnb	1,946885528	2,322166731	16,07037795	6,25E-05	0,017998063
ENSMUST00000208484.1	D7Bwg0826e	1,940997967	2,034448473	13,976648	0,000185113	0,043462699
ENSMUST00000087497.10	Col11a2	1,918409716	3,511668596	29,49297622	5,61E-08	3,83E-05
ENSMUST00000066386.5	Lysmd1	1,916718853	3,643093553	31,3707699	2,13E-08	1,55E-05
ENSMUST00000036248.12	Pmepa1	1,889435097	3,406260219	27,11245222	1,92E-07	0,000116893
ENSMUST00000137906.1	Arid5a	1,883715516	4,820906235	52,59156905	4,11E-13	6,66E-10
ENSMUST00000077502.4	Dqx1	1,869603207	3,750285324	31,75555964	1,75E-08	1,33E-05
ENSMUST00000177908.1	Cfap73	1,863204877	3,343751007	25,25257978	5,03E-07	0,0002737
ENSMUST00000234364.1	1810073O08Rik	1,838884233	2,505484297	15,92594077	6,59E-05	0,018805713
ENSMUST00000211765.1	Nucb1	1,823622664	4,731981699	47,86251092	4,58E-12	6,52E-09
ENSMUST00000062117.13	Rap2a	1,823566263	4,054593856	35,0695298	3,18E-09	2,67E-06
ENSMUST00000000188.11	Ccnd2	1,818841158	6,329194025	81,45457634	1,83E-19	5,21E-16
ENSMUST00000111881.3	Nfkb2	1,812067868	2,871430599	18,70725661	1,52E-05	0,005496874
ENSMUST00000023072.6	Parvb	1,80953032	3,435541445	25,33830344	4,82E-07	0,00026396
ENSMUST00000110218.8	Spef1	1,779618352	3,473243744	24,82857175	6,27E-07	0,000333154
ENSMUST00000101339.7	Nhsl2	1,775886223	3,947564817	31,42541421	2,07E-08	1,52E-05
ENSMUST00000020537.8	Nsg2	1,765745532	6,112490555	71,46610797	2,83E-17	6,39E-14
ENSMUST00000069324.6	Zfp580	1,759429981	3,099546922	19,90546691	8,14E-06	0,003167394
ENSMUST00000192173.1	Gm37233	1,756222894	3,963099576	31,10297182	2,45E-08	1,76E-05
ENSMUST00000044384.4	Aldh1b1	1,75479016	7,28316449	94,78412823	2,15E-22	7,85E-19
ENSMUST00000205979.1	Qpctl	1,751379181	2,438628057	13,94372899	0,000188383	0,043875928
ENSMUST00000109764.7	Nfix	1,7474685	4,639411263	42,50577762	7,05E-11	8,10E-08
ENSMUST00000112682.3	Slc25a18	1,746638239	4,461506871	39,37063282	3,51E-10	3,56E-07
ENSMUST00000102942.7	Psd4	1,726891331	5,629282353	58,2842288	2,27E-14	4,15E-11
ENSMUST00000024575.7	Rps6ka2	1,724961592	4,949365839	46,22813017	1,05E-11	1,38E-08
ENSMUST00000047282.11	Mthfsd	1,706383836	4,895833979	44,40456761	2,67E-11	3,23E-08
ENSMUST00000237716.1	Gramd3	1,704791207	3,267133208	20,41862597	6,22E-06	0,002504222
ENSMUST00000081649.9	Ifitm2	1,675778866	2,842725493	15,79724437	7,05E-05	0,019819627
ENSMUST00000128342.1	Gm16576	1,670149231	4,238729656	32,30430049	1,32E-08	1,02E-05
ENSMUST00000091288.12	Prnp	1,667251143	2,917886515	16,39102658	5,16E-05	0,015235528
ENSMUST00000130268.7	Mypop	1,651725153	3,9274394	26,93075453	2,11E-07	0,000126255
ENSMUST00000119494.2	Plk-ps1	1,649705765	4,078484833	29,00786005	7,21E-08	4,87E-05
ENSMUST00000049787.2	Lrrn4	1,633936313	3,07014468	16,99350495	3,75E-05	0,011783735
ENSMUST00000028593.10	Prrg4	1,623305896	2,919716397	15,45181677	8,46E-05	0,02296651
ENSMUST00000169652.2	Tifab	1,622130984	3,485237747	20,70558945	5,36E-06	0,002193104
ENSMUST00000142665.1	Wrap73	1,614515928	3,569008251	21,40444732	3,72E-06	0,001581742
ENSMUST00000028223.8	Kynu	1,607251987	3,812534738	24,11986018	9,05E-07	0,00046902
ENSMUST00000210581.1	Gm45353	1,605477738	3,045566074	16,09415714	6,03E-05	0,017487316
ENSMUST00000006669.5	Pdk1	1,598024162	3,934299237	25,38804423	4,69E-07	0,000258066
ENSMUST00000190826.1	Ly6m	1,59735376	2,861653911	14,46330722	0,000142931	0,035554569
ENSMUST00000190196.4	Prob1	1,596870647	3,300553402	18,32104184	1,87E-05	0,006469501
ENSMUST00000180086.2	H1f0	1,595263421	7,333076762	78,90285205	6,54E-19	1,79E-15
ENSMUST00000004036.5	Efnb3	1,593601349	3,729015516	22,77231922	1,82E-06	0,000860425
ENSMUST00000024708.5	Tnfrsf21	1,584030434	3,229964413	17,37891121	3,06E-05	0,009892078
ENSMUST00000123349.1	Gramd4	1,580677503	4,425720133	31,62199216	1,87E-08	1,41E-05
ENSMUST00000075317.11	Pdzd2	1,577930631	6,475284059	63,91053675	1,41E-15	2,79E-12
ENSMUST00000094303.5	Fcrl6	1,573454053	2,967723721	14,86673159	0,000115393	0,030049776
ENSMUST00000059341.4	Zc2hc1c	1,568068621	2,864413198	13,8423194	0,000198883	0,045841677
ENSMUST00000105545.11	Phactr2	1,552111795	3,596681038	20,06800061	7,48E-06	0,002941441
ENSMUST00000159547.2	Vamp1	1,542047785	6,889653481	67,41663009	2,20E-16	4,68E-13
ENSMUST00000026315.7	Dnase1l3	1,541661805	6,019372997	52,69721816	3,90E-13	6,38E-10
ENSMUST00000060474.13	Septin6	1,537678051	5,80830831	48,91053335	2,68E-12	3,98E-09
ENSMUST00000032877.10	Ddias	1,522241681	5,29710636	40,41477923	2,06E-10	2,21E-07
ENSMUST00000232332.2	Gm1043	1,515355313	4,323381884	27,56396107	1,52E-07	9,50E-05
ENSMUST00000020768.3	Pgam2	1,511219167	5,805748496	47,19041525	6,45E-12	8,83E-09

ENSMUST00000201742.1	Gm43860	1,504986218	5,056842678	36,35552456	1,65E-09	1,47E-06
ENSMUST00000178353.1	Gm21992	1,498680905	3,067317817	14,20554851	0,000163903	0,039564816
ENSMUST00000073109.11	Ctdspl	1,492178379	3,093966786	14,30662304	0,000155411	0,03803725
ENSMUST00000217354.1	Ppp2r3d	1,490085117	3,979783517	22,51386827	2,09E-06	0,000965129
ENSMUST00000170998.8	Scn2b	1,489581799	3,331547338	15,4954795	9,07E-05	0,024477231
ENSMUST00000125447.2	Macf1	1,488815289	4,207830645	25,15140066	5,31E-07	0,000286305
ENSMUST00000027809.7	Opn3	1,488250879	4,718897142	31,57717888	1,92E-08	1,42E-05
ENSMUST00000058154.14	Tmtc3	1,475000559	3,093075609	13,9460486	0,000188151	0,043875928
ENSMUST00000041124.12	Zfp704	1,471828907	4,208156849	24,66828683	6,82E-07	0,000359985
ENSMUST00000138611.7	Ino80dos	1,464950471	3,210541081	14,66560241	0,000128381	0,032309915
ENSMUST00000064187.11	Thra	1,46464195	3,245568694	14,93263581	0,000111431	0,029394289
ENSMUST00000118960.1	Car15	1,450243285	3,149629562	13,94249496	0,000188507	0,043875928
ENSMUST00000135229.7	Dgcr2	1,443464753	3,684723069	18,13202921	2,06E-05	0,007024777
ENSMUST00000180612.2	9330175E14Rik	1,438984143	5,022930753	32,87358614	9,84E-09	7,70E-06
ENSMUST00000135091.1	Mtln	1,405864455	3,247832623	13,75955962	0,000207781	0,047280357
ENSMUST00000045713.3	Nacad	1,397895867	4,270906699	22,90602162	1,70E-06	0,000816118
ENSMUST00000123325.8	Ankrd33b	1,385163378	4,612731563	26,3481133	2,85E-07	0,000163808
ENSMUST00000226062.1	Psd	1,382994821	4,796589922	28,04201831	1,19E-07	7,62E-05
ENSMUST00000160523.7	Vamp1	1,381188592	3,541026352	15,41915374	8,61E-05	0,023322464
ENSMUST00000026565.6	Ifitm3	1,375575329	3,426334712	14,2246013	0,00016576	0,039750707
ENSMUST00000193350.1	Gm37120	1,369415633	4,236353842	21,57156364	3,41E-06	0,001463789
ENSMUST00000022921.6	Angpt1	1,366028426	4,423730217	23,43669635	1,29E-06	0,000638663
ENSMUST00000029875.3	Pip4p2	1,332829542	3,840615409	16,72690092	4,32E-05	0,013139886
ENSMUST00000000153.8	Gna12	1,332689888	6,748772682	48,70528104	2,98E-12	4,37E-09
ENSMUST00000056890.9	Fbxl22	1,324652146	5,787102885	35,89699984	2,08E-09	1,83E-06
ENSMUST00000024860.8	Ehd3	1,300951319	4,815575882	24,90150471	6,04E-07	0,000321987
ENSMUST00000163139.7	Plxna1	1,300548345	4,708694186	23,97406199	9,77E-07	0,000498658
ENSMUST00000057311.3	Sfn	1,293032336	6,207664903	39,23106449	3,79E-10	3,80E-07
ENSMUST00000004565.14	Ralb	1,261448967	4,195447806	17,86523433	2,37E-05	0,007929837
ENSMUST00000181211.1	Gm17552	1,245442491	3,877798069	14,90655133	0,000113264	0,029712636
ENSMUST00000066330.14	Mprip	1,240870191	5,813474083	31,70793684	1,79E-08	1,36E-05
ENSMUST00000086040.5	F5	1,239453192	7,159198127	41,20653877	7,58E-10	7,20E-07
ENSMUST00000082152.4	Ube2o	1,238773818	4,283131946	18,00507573	2,20E-05	0,007447531
ENSMUST00000231165.1	Nfam1	1,226158307	4,800452911	21,91974	2,84E-06	0,001273771
ENSMUST00000030949.3	Tas1r3	1,222001363	4,147078432	16,33049231	5,32E-05	0,015628693
ENSMUST00000110052.1	Ocel1	1,202401787	5,630785468	28,02148255	1,20E-07	7,67E-05
ENSMUST00000058524.2	Zc3hav1l	1,191379259	4,019837718	14,61840745	0,000131637	0,032978986
ENSMUST00000184613.1	Mrip-ps	1,188132892	7,181988937	42,07389417	8,81E-11	9,97E-08
ENSMUST00000026886.7	Itih5	1,178633588	5,016252047	21,81641371	3,00E-06	0,001331674
ENSMUST00000070084.10	Ticam2	1,160760069	5,086970346	21,67381182	3,23E-06	0,001408107
ENSMUST00000165774.7	Gbp2	1,119464739	4,302242568	14,78943983	0,00012022	0,030693586
ENSMUST00000120430.1	Gm7901	1,119022712	7,808153921	42,14990359	8,46E-11	9,64E-08
ENSMUST00000030142.3	Epb41l4b	1,114166377	7,034874192	35,83237583	2,15E-09	1,88E-06
ENSMUST00000053078.4	Map10	1,113478994	4,180729456	13,75524674	0,000208258	0,047313452
ENSMUST00000087867.5	Uprt	1,090461689	4,368119862	14,44429954	0,000144381	0,035767856
ENSMUST00000119613.1	Gm5939	1,081571173	5,721270725	23,24257768	1,43E-06	0,000694423
ENSMUST00000050234.3	Jrk	1,078053278	5,135798253	18,95126244	1,34E-05	0,004924073
ENSMUST00000211473.1	Gm9347	1,07377183	4,506600577	15,01030004	0,000106938	0,028313904
ENSMUST00000172910.2	Crybg3	1,05867018	5,158532199	18,40626317	1,78E-05	0,006278167
ENSMUST00000021028.4	Itgb3	1,052570974	4,979349472	17,14037813	3,47E-05	0,011089499
ENSMUST00000005671.9	Igf1r	1,049573733	4,43546616	13,83779409	0,000199349	0,045874786
ENSMUST00000113658.7	Gfpt1	1,043398623	5,24004564	18,38379541	1,81E-05	0,006336984
ENSMUST00000057561.8	Wwc2	1,036929522	4,968346886	16,51719599	4,82E-05	0,014399082
ENSMUST00000023487.4	Arhgap31	1,011545585	5,439308958	18,44933609	1,75E-05	0,006158626
ENSMUST00000029078.8	Car2	0,998261627	5,158079653	16,33032816	5,32E-05	0,015628693
ENSMUST00000065793.11	Phgdh	0,978825536	6,451178839	24,04023603	9,44E-07	0,00048529
ENSMUST00000044195.5	Tmc7	0,972133477	5,633514391	18,17140072	2,02E-05	0,006897539
ENSMUST00000040971.13	Capn5	0,965678577	5,691155889	18,26944101	1,92E-05	0,006598963
ENSMUST00000182751.1	Rbpj-ps3	0,962880195	5,957685839	19,81859605	8,52E-06	0,003305615
ENSMUST00000199915.1	Gm43737	0,959646607	5,304041997	15,84909436	6,86E-05	0,019390703
ENSMUST00000231574.1	Gm2792	0,953075215	4,927914037	13,72149338	0,000212034	0,048009217
ENSMUST00000119848.7	Eme2	0,944359867	4,972499349	13,70129894	0,000214326	0,04830686
ENSMUST00000069817.14	Prrc2b	0,921954593	6,411183435	20,99414127	4,62E-06	0,001923849
ENSMUST00000024779.14	Usp49	0,921717753	5,877910248	17,66871917	2,63E-05	0,008610777
ENSMUST00000231927.1	Rnaset2a	0,915389624	5,625877892	16,01204011	6,29E-05	0,018078259
ENSMUST00000051803.7	Aldh3b1	0,912361699	5,236743549	13,95996895	0,000186763	0,043684131
ENSMUST00000115421.2	Steap4	0,906258524	9,153220041	34,91076411	3,45E-09	2,86E-06

ENSMUST00000056977.13	Runx3	0,904869666	5,476641029	14,90572358	0,000113032	0,029712636
ENSMUST00000023259.14	Lynx1	0,872210902	9,622204881	34,75964575	3,76E-09	3,06E-06
ENSMUST00000105617.7	Ipcef1	0,864975741	6,386381639	18,29696272	1,89E-05	0,006529436
ENSMUST00000033495.14	Pim2	0,844940609	7,347218913	21,6973006	3,19E-06	0,001398219
ENSMUST00000045281.12	Smg6	0,833354923	6,301554491	16,49661935	4,87E-05	0,014495414
ENSMUST00000038053.13	Lpp	0,817505107	6,091819532	14,83191869	0,000117542	0,030253495
ENSMUST00000041093.5	Creb3l2	0,815078195	7,689664066	21,57031547	3,41E-06	0,001463789
ENSMUST00000052678.8	Flnb	0,806014717	6,064554135	14,27437444	0,000158017	0,038586161
ENSMUST00000053686.8	Uck2	0,790459387	6,064749939	13,71885993	0,000212332	0,048009217
ENSMUST00000023105.4	Endou	0,787140835	6,800767368	16,81315244	4,13E-05	0,012664233
ENSMUST00000026985.8	Cplx2	0,786366167	11,12044583	35,08636215	3,16E-09	2,66E-06
ENSMUST00000027752.14	Lamc1	0,776612345	6,874243376	16,61247848	4,59E-05	0,013780172
ENSMUST00000112707.2	Lrrc8b	0,770240361	6,244318037	13,7875638	0,00020531	0,046928667
ENSMUST00000120711.1	Gm1848	0,760785311	6,414004482	14,20654002	0,000163817	0,039564816
ENSMUST00000044492.9	Akap9	0,760705726	6,422783521	14,2357382	0,000161295	0,039207817
ENSMUST00000020350.14	Lgr5	0,756865418	6,39686742	13,98456814	0,000184372	0,043462699
ENSMUST00000046206.4	Rprd1a	0,740099793	6,758436388	14,70886236	0,000125469	0,031858334
ENSMUST00000055475.8	Gpr18	0,71191288	8,061417842	17,60409652	2,72E-05	0,008870608
ENSMUST00000192833.1	(None) lncRNA	0,701764191	7,061849304	14,03283519	0,000179664	0,042583006
ENSMUST00000089510.4	Cenpb	0,691954558	8,828774413	19,12108393	1,23E-05	0,004575567
ENSMUST00000127984.8	Cbfa2t3	0,691218048	8,775555733	18,91562972	1,37E-05	0,005004006
ENSMUST00000049931.5	Spn	0,678072467	7,511650538	14,32202139	0,000154121	0,037892903
ENSMUST00000099858.3	Prep	0,658705716	9,17719194	18,2942255	1,89E-05	0,006529436
ENSMUST00000037099.8	Clic4	0,643789061	8,882647916	16,65300859	4,49E-05	0,013574763
ENSMUST00000119978.1	Gm12671	0,638325412	7,902025085	13,66813018	0,000218145	0,049089967
ENSMUST00000060148.5	Hivep1	0,627201462	8,653686716	15,21455299	9,60E-05	0,025648846
ENSMUST00000178993.2	Gm4617	0,621350107	9,037674858	15,88756742	6,72E-05	0,01915249
ENSMUST00000034983.6	Atp1b3	0,616451805	9,068331327	15,70587445	7,41E-05	0,020660522
ENSMUST00000098799.4	Ehd2	0,591317189	9,243669189	14,84331481	0,000116865	0,030212319

Downregurated in Dido1ΔE16 preB						
GeneID	Symbol	logFC	logCPM	F	PValue	FDR
ENSMUST00000159080.5	Clec2i	-7,983593355	1,558483814	33,37174352	7,62E-09	6,03E-06
ENSMUST00000139071.7	Iffo1	-7,890355654	1,463687259	31,36565171	2,14E-08	1,55E-05
ENSMUST00000219633.1	Icosl	-7,525804932	1,161075383	25,31362351	4,90E-07	0,000267191
ENSMUST00000087517.9	Dido1	-6,321931699	6,127988892	360,3444673	2,51E-80	3,57E-75
ENSMUST00000222616.1	Gm19951	-4,80983627	3,183063661	56,41428902	5,84E-12	8,07E-09
ENSMUST00000138127.7	Zfp318	-4,442870304	1,956464378	29,51947886	5,54E-08	3,80E-05
ENSMUST00000135559.7	Iffo1	-4,15081223	2,8172429	45,28881682	1,70E-11	2,11E-08
ENSMUST00000063140.14	Hcrtr2	-4,031617164	1,218501868	16,50007809	4,87E-05	0,014495414
ENSMUST00000087543.4	B3gatl4	-3,661303587	4,557737119	102,7008546	3,92E-24	1,86E-20
ENSMUST00000127842.7	Ctsh	-3,440887594	1,979518078	22,14112208	2,54E-06	0,001150331
ENSMUST00000191475.1	Gm8369	-3,285587564	1,914526522	19,76182214	8,77E-06	0,003386816
ENSMUST00000207327.1	Fcer2a	-3,283156331	1,372850445	14,44130764	0,000145658	0,035958993
ENSMUST00000098486.3	Bcl2a1d	-3,109744396	2,036965161	20,12783914	7,27E-06	0,002883393
ENSMUST00000089688.5	Mmp14	-3,049193137	2,042926237	19,38315756	1,07E-05	0,004041594
ENSMUST00000219038.1	Icosl	-3,030945151	1,624124969	15,22695931	9,53E-05	0,025528804
ENSMUST00000124563.7	Napa	-2,896490967	2,171873297	19,93717851	8,02E-06	0,003136808
ENSMUST00000105520.7	Enpp1	-2,7745023	2,294940484	19,70209371	9,05E-06	0,003475495
ENSMUST00000139806.1	Casz1	-2,62217115	3,113146752	28,85298785	7,81E-08	5,23E-05
ENSMUST00000001327.10	Itgb7	-2,61163875	3,107993862	26,35748488	4,57E-07	0,000252715
ENSMUST00000025266.5	Lta	-2,498746182	2,32040539	16,90669591	3,96E-05	0,012262889
ENSMUST00000032288.5	Klra1	-2,381443479	2,679955902	19,16790685	1,20E-05	0,004488191
ENSMUST00000072729.9	Ms4a4c	-2,331771874	2,251738081	14,33233054	0,000158196	0,038586161
ENSMUST00000015460.4	Slamf1	-2,286564693	2,455558045	15,87475288	6,78E-05	0,019273272
ENSMUST00000194738.5	Igha	-2,28159457	2,761208115	19,01513182	1,30E-05	0,004802556
ENSMUST00000200926.1	Nabp2l1	-2,27234845	2,326272308	14,88002122	0,000114583	0,029948313
ENSMUST00000112751.1	Bcl2	-2,270625247	4,416905344	44,30505812	5,20E-11	6,07E-08
ENSMUST00000108846.1	Galnt10	-2,251345495	3,090909269	22,57263474	2,03E-06	0,000942717
ENSMUST00000123453.1	Gmip	-2,080640912	2,83817036	17,09162441	3,56E-05	0,011327043
ENSMUST00000048935.5	DMrt3	-2,045531931	4,255897118	34,85501199	3,59E-09	2,96E-06
ENSMUST00000190715.6	Cep70	-2,040272535	2,979809197	17,91385147	2,31E-05	0,007766293
ENSMUST00000144920.3	Cmas	-2,003662183	3,954036653	29,30672633	6,31E-08	4,28E-05
ENSMUST00000060185.2	Fndc9	-1,953593451	6,973307638	83,07163692	7,94E-20	2,36E-16
ENSMUST00000124462.2	Arhgap27os3	-1,889261018	4,729862382	37,95072549	7,32E-10	6,99E-07
ENSMUST00000033056.4	Pycard	-1,883482372	5,753463343	54,41246882	1,63E-13	2,79E-10
ENSMUST00000033611.4	Xkrx	-1,877057128	4,45365182	22,18038806	1,65E-05	0,005898442
ENSMUST00000052124.8	Nlrc4	-1,870336605	4,02341972	26,68329429	2,40E-07	0,00014055
ENSMUST00000038552.12	Coro7	-1,869896301	6,500700051	68,86100539	1,06E-16	2,32E-13
ENSMUST00000103369.1	Igkv12_41	-1,843511231	3,176795449	16,64238842	4,51E-05	0,013622056
ENSMUST00000102600.3	Fndc5	-1,837701248	4,602258186	34,4097588	4,47E-09	3,62E-06
ENSMUST00000173103.1	H2-Ab1	-1,822872128	3,052427033	15,58433112	7,92E-05	0,021770549
ENSMUST00000236643.1	H2-Ab1	-1,809995864	3,510553429	19,50810809	1,01E-05	0,003834755
ENSMUST00000200318.1	Reln	-1,801471893	3,508443606	19,06073033	1,27E-05	0,004699707
ENSMUST00000103507.1	Ighv1-22	-1,800719921	4,202435221	27,47968675	1,59E-07	9,84E-05
ENSMUST00000119311.7	Auh	-1,774167059	3,641515153	20,09724599	7,36E-06	0,002912898
ENSMUST00000103534.1	Ighv1-63	-1,756876208	3,266879808	15,83304593	6,93E-05	0,019498865
ENSMUST00000164035.7	Arid3b	-1,747583514	3,159753895	15,22848471	9,53E-05	0,025528804
ENSMUST00000159745.1	Pip4p1	-1,716446429	4,448499287	28,85859076	7,82E-08	5,23E-05
ENSMUST00000110031.3	Auh	-1,699163386	3,82382454	20,55017493	5,81E-06	0,002357878
ENSMUST00000025786.8	Pacs1	-1,692871768	5,242494037	37,59600881	8,90E-10	8,18E-07
ENSMUST00000103328.2	Igkv10-96	-1,692240036	5,090174833	35,70522519	2,30E-09	1,99E-06
ENSMUST00000054279.14	Sp100	-1,679650835	4,002008163	21,97562283	2,76E-06	0,001241119
ENSMUST00000154177.1	Gm12678	-1,655462674	5,889877298	45,31532015	1,68E-11	2,10E-08
ENSMUST00000123602.1	Dctn5	-1,632783615	3,336595336	14,90422859	0,000113244	0,029712636
ENSMUST00000103493.2	Ighv1_4	-1,602674675	3,567852863	15,9900552	6,37E-05	0,01825261
ENSMUST00000030417.9	Cdc42	-1,590191046	4,399796876	23,90182956	1,21E-06	0,000602967
ENSMUST00000103330.1	Igkv10-94	-1,581022172	3,863354835	18,47096412	1,73E-05	0,006113882
ENSMUST00000185851.1	Ms4a1	-1,574366466	3,801611177	17,7073616	2,58E-05	0,008535729
ENSMUST00000103510.1	Ighv-26	-1,56806827	6,193893519	45,3781159	1,63E-11	2,07E-08
ENSMUST00000103515.1	Ighv1-39	-1,547760676	4,378250288	23,00184139	1,62E-06	0,000781701
ENSMUST00000171415.7	Ndufb8	-1,546232139	3,937086795	18,44760915	1,75E-05	0,006158626
ENSMUST00000136582.1	Dpm1	-1,543326311	4,409283137	23,36333687	1,34E-06	0,000656648
ENSMUST00000088785.5	Zfp566	-1,521634845	3,830695557	16,99129999	3,76E-05	0,011783735
ENSMUST00000195325.1	Ighv1_2	-1,506154793	3,650215269	14,99575642	0,000107765	0,028480012
ENSMUST00000103495.2	Ighv10-3	-1,495800386	4,954604049	27,25163869	1,79E-07	0,000110187
ENSMUST00000150208.7	Napa	-1,487700985	3,537511902	13,9375477	0,000190788	0,044299427
ENSMUST00000103544.2	Ighv1-75	-1,464349621	5,054374643	27,18513212	1,85E-07	0,000113064
ENSMUST00000192106.1	Gm8146	-1,425706995	3,686588118	13,98002222	0,000184781	0,043462699
ENSMUST00000117906.1	Gm14127	-1,420073761	5,320221421	28,24872281	1,07E-07	6,91E-05
ENSMUST00000140896.1	Coro1a	-1,402439401	3,905593784	15,2313424	9,66E-05	0,025761121
ENSMUST00000192591.1	Ighv8-8	-1,398220873	5,268371238	26,98035366	2,06E-07	0,000123576
ENSMUST00000232755.1	Brwd1	-1,388856764	6,525235209	40,566014	1,90E-10	2,07E-07
ENSMUST00000103386.2	Igkv6-23	-1,356995082	4,870950986	22,1892887	2,47E-06	0,001128871

ENSMUST00000130486.1	Gm15675	-1,339694373	5,647834982	28,47516073	9,58E-08	6,23E-05
ENSMUST00000103521.2	Ighv1-50	-1,339319172	4,520063	18,8886975	1,39E-05	0,005037705
ENSMUST00000108809.7	Trim11	-1,328841978	6,363271883	31,2363446	8,09E-08	5,36E-05
ENSMUST00000149244.7	Lrmp	-1,320774437	4,50840102	18,5478536	1,66E-05	0,005919815
ENSMUST00000070720.7	Sorcs2	-1,316907882	4,181814742	15,51468541	8,19E-05	0,022385759
ENSMUST00000103384.1	Igkv8_24	-1,313846169	4,059313433	14,53626051	0,000137502	0,034362495
ENSMUST00000103526.2	Ighv1-55	-1,310757938	5,559107453	26,45566013	2,70E-07	0,000156834
ENSMUST00000189288.1	F730311O21	-1,301374978	4,811238435	18,38186761	2,59E-05	0,008572595
ENSMUST00000035218.8	Nckipsd	-1,283554478	5,317747107	23,40961893	1,31E-06	0,000645474
ENSMUST00000026408.6	Gdf11	-1,261248622	5,657364824	25,54015348	4,34E-07	0,000241657
ENSMUST00000224965.1	Blk	-1,250333269	5,365670422	22,82565724	1,78E-06	0,000845437
ENSMUST00000229230.1	Gm18724	-1,248267124	5,065038697	20,40789211	6,26E-06	0,002511213
ENSMUST00000103321.2	Igkv1-110	-1,244154495	4,83149238	18,69219071	1,54E-05	0,005531082
ENSMUST00000029569.8	Slc35a3	-1,230029896	5,472174724	22,83947362	1,76E-06	0,000841061
ENSMUST00000161705.2	Mcoln1	-1,22439226	4,453059577	15,67899419	7,51E-05	0,020896092
ENSMUST00000106357.7	Ypel3	-1,209641194	4,602325694	16,37671719	5,19E-05	0,015313957
ENSMUST00000186927.1	Ly6e	-1,186612293	4,339905695	13,99950832	0,000182937	0,04321498
ENSMUST00000201831.3	Gm20559	-1,182468775	6,205358653	26,98167247	2,22E-07	0,000131625
ENSMUST00000076957.6	Zdhhc8	-1,179685888	6,382338265	28,64868403	8,68E-08	5,72E-05
ENSMUST00000049872.8	Gpr183	-1,171565745	5,567322821	18,39201523	3,19E-05	0,010252892
ENSMUST00000034466.9	Gnpat	-1,1617632	4,901555007	16,86739962	4,01E-05	0,01236066
ENSMUST00000171330.6	Slamf6	-1,13563657	6,058165089	24,0025037	9,62E-07	0,000493113
ENSMUST00000153442.7	Hnrnpdl	-1,096473772	5,059817253	16,08560917	6,06E-05	0,017500942
ENSMUST00000096243.6	B3gat3	-1,085825454	5,11984947	16,08608819	6,05E-05	0,017500942
ENSMUST00000103492.1	Ighv10_1	-1,084158731	5,162109654	16,20811053	5,68E-05	0,016567508
ENSMUST00000124485.7	Fam129c	-1,066469298	6,676448923	24,608023	9,92E-07	0,000504511
ENSMUST00000143378.7	RIKEN cDNA 4930426D05	-1,063285171	5,357939252	16,77561341	4,22E-05	0,012867344
ENSMUST00000028205.9	BC005624	-1,062442735	5,875275434	19,95054576	7,95E-06	0,003119156
ENSMUST00000177669.1	Pfn1	-1,038391608	6,305071193	22,02354857	2,70E-06	0,001218565
ENSMUST00000103548.2	Ighv1_81	-1,022871062	5,272466495	15,10425623	0,000101745	0,027039536
ENSMUST00000128652.1	RIKEN cDNA 4930597A21	-1,00947143	5,618464323	16,30293479	5,72E-05	0,016656537
ENSMUST00000089497.6	Lsy1	-1,005583807	5,690951661	16,88235191	3,98E-05	0,012290273
ENSMUST00000028928.7	Gzf1	-1,002841441	6,123570802	19,40183321	1,06E-05	0,004012909
ENSMUST00000204885.1	Hnrnpa2b1	-0,994640097	5,339542027	14,72942994	0,000124107	0,031625416
ENSMUST00000049295.14	Ehbp1l1	-0,986878979	5,72915136	16,49113643	4,89E-05	0,014507106
ENSMUST00000094646.5	Vps4b	-0,9528883	6,769731742	21,2618847	4,01E-06	0,001683743
ENSMUST00000168846.2	Prkag1	-0,95133699	5,941714353	16,53153497	4,79E-05	0,01435078
ENSMUST00000027266.3	Ormdl1	-0,9487111	5,913806377	16,29367741	5,43E-05	0,015901113
ENSMUST00000059644.12	Rbm33	-0,933005737	6,391954558	18,50911402	1,69E-05	0,006016918
ENSMUST00000120267.8	Atg16l2	-0,927330632	5,944811642	15,76609552	7,17E-05	0,020061185
ENSMUST00000119728.1	Npm3-ps1	-0,924176794	5,638522107	14,15437794	0,000168422	0,040274585
ENSMUST00000077605.11	Eif4a2	-0,857011307	6,70463286	17,09189787	3,65E-05	0,011557296
ENSMUST00000107802.7	Trim59	-0,855661493	6,779539165	17,35938084	3,09E-05	0,009971639
ENSMUST00000037913.8	Rmi2	-0,853572767	6,324823147	15,08240218	0,000106569	0,028268881
ENSMUST00000028755.7	Ehd4	-0,852689493	7,956604028	21,84851254	2,95E-06	0,001313675
ENSMUST00000113481.8	Zfp318	-0,799788028	6,608211956	14,71730276	0,000125115	0,031825347
ENSMUST00000057725.9	Samhd1	-0,792015264	9,539454369	24,98671412	5,77E-07	0,000310391
ENSMUST00000117892.1	Slc48a1	-0,771435071	6,987704437	14,85486262	0,000116121	0,030184274
ENSMUST00000074259.14	Nrm	-0,765176205	7,74999753	17,0492499	3,64E-05	0,011556825
ENSMUST00000074733.10	Sept11	-0,708824	8,200756884	16,06479354	6,12E-05	0,017652724
ENSMUST00000172057.7	Ralgps2	-0,67314841	8,049282892	14,1192891	0,000171592	0,040942466
ENSMUST00000035842.6	Rassf1	-0,654480122	8,580568303	14,80443381	0,000119268	0,030611202
ENSMUST00000030964.5	CD38	-0,651117231	9,203340782	16,23521185	5,60E-05	0,016365734
ENSMUST00000014597.4	Blk	-0,648216171	9,463687199	16,77374043	4,21E-05	0,012867344
ENSMUST00000001455.12	Mef2d	-0,595348928	9,43343979	14,15338483	0,000168511	0,040274585

Supplementary Table 3

Differentially expresed Ighv (variable) regions in pre B cells. RNA-seq data.

	logFC	logCPM	LR	PValue	FDR
ENSMUSG00000076613_Ighg2b	5,177375763	11,0114599	201,453585	1,01E-45	2,80E-43
ENSMUSG00000094028_Ighd4-1	3,435788362	11,6479589	114,786492	8,76E-27	1,22E-24
ENSMUSG00000094057_Ighd2-7	4,13279968	8,67285432	92,4153468	7,03E-22	6,51E-20
ENSMUSG00000095897_Ighd2-5	2,705912053	9,02573405	60,6345883	6,87E-15	4,78E-13
ENSMUSG00000095444_Ighd2-4	2,203923512	9,67438993	54,5985616	1,48E-13	8,22E-12
ENSMUSG00000076630_Ighd1-1	1,793919186	11,253159	30,6397651	3,11E-08	1,44E-06
ENSMUSG00000096568_Ighd2-3	1,798574118	9,51005007	29,510394	5,56E-08	2,21E-06
ENSMUSG00000096150_Ighv1-85	2,001683257	8,37291067	21,7637665	3,08E-06	0,00010716
ENSMUSG00000093955_Ighv1-34	-1,683806396	8,63910452	20,0707275	7,46E-06	0,00023052
ENSMUSG00000076633_Ighv5-2	1,149102373	10,7760075	18,7699476	1,47E-05	0,00040997
ENSMUSG00000096464_Ighv2-2	1,196086747	11,7479314	17,8036236	2,45E-05	0,00061897
ENSMUSG00000094117_Igkv3-12	1,177994346	11,2784643	16,1877401	5,74E-05	0,00132894
ENSMUSG00000095416_Ighv1-12	-1,180049493	9,75657498	15,9939	6,35E-05	0,00135893
ENSMUSG00000103439_Gm7019	1,111729657	12,0007745	15,0978134	0,00010208	0,00202705
ENSMUSG00000095130_Ighv1-39	-1,073056122	10,0470355	14,7446491	0,0001231	0,00228139
ENSMUSG00000105630_Gm42543	1,958377857	7,62244402	13,8997266	0,00019283	0,00331427
ENSMUSG00000094051_Ighv1-36	-1,729868909	8,40680503	13,7040139	0,000214	0,00331427
ENSMUSG00000076620_Ighj2	1,173126641	9,80407887	13,6987894	0,00021459	0,00331427
ENSMUSG00000094561_Ighv1-22	-0,968802278	10,0309777	11,9406639	0,00054922	0,00803594
ENSMUSG00000076531_Igkv4-92	0,947768886	9,64418052	11,4133208	0,00072919	0,01013579
ENSMUSG00000094940_Ighv1-84	-1,569747231	7,86347906	11,0600177	0,00088209	0,01167723
ENSMUSG00000076598_Igkv3-7	0,974039758	11,8250008	10,7807443	0,00102561	0,01296004
ENSMUSG00000096074_Ighv1-72	1,078454326	9,63555533	10,0677939	0,00150884	0,01823723
ENSMUSG00000095866_Ighv2-4	0,955057938	9,2066517	9,66627868	0,00187681	0,02173973
ENSMUSG00000096649_Ighv1-31	-1,603278868	7,74617826	9,53362458	0,00201741	0,02243363
ENSMUSG00000094652_Ighv1-42	-0,975189499	9,26275221	9,32514755	0,0022603	0,02379573
ENSMUSG00000076695_Ighv1-18	-0,92584829	10,3922373	9,2754911	0,0023224	0,02379573
ENSMUSG00000095863_Ighv1-67	-1,144229293	8,51612379	9,21783174	0,00239669	0,02379573
ENSMUSG00000093896_Ighv1-76	-0,834787482	10,7236013	8,36705245	0,00382085	0,03662744
ENSMUSG00000094546_Ighv1-26	-0,911194794	11,9062431	8,2095574	0,00416703	0,03857043
ENSMUSG00000106124_Gm42539	1,869388279	6,46688357	8,15214777	0,00430102	0,03857043
ENSMUSG00000103537_Gm37838	1,567022347	6,59522279	7,97100381	0,00475326	0,04129392
ENSMUSG00000094694_Ighv1-9	-0,759644961	11,0040389	7,40626887	0,0064997	0,05475503
ENSMUSG00000094951_Ighv5-6	0,726667156	11,0872131	7,30006217	0,00689522	0,05490461
ENSMUSG00000095700_Ighv10-3	-0,783609818	10,5656279	7,29557865	0,00691245	0,05490461
ENSMUSG00000095612_Ighv5-4	0,74439873	11,5734534	7,11169352	0,00765827	0,05913888
ENSMUSG00000000001_Gm30996	2,102964555	4,81116565	6,75350437	0,00935637	0,07029924
ENSMUSG00000103297_Ighv3-2	-1,472817484	7,33039719	6,6933679	0,00967722	0,07079652
ENSMUSG00000104760_Igkv3-8	1,658945266	5,00512581	6,47040267	0,01096857	0,0781862
ENSMUSG00000102942_Ighv1-33	-2,126420546	3,91093715	6,39753437	0,0114279	0,07942388
ENSMUSG00000094533_Ighv11-1	-1,669326819	5,8759403	6,31963143	0,01194084	0,08005876
ENSMUSG00000076596_Igkv3-10	0,673171372	10,4226837	6,29685931	0,01209521	0,08005876
ENSMUSG00000106098_Igkv14-118-2	1,495531483	5,31228066	6,05846689	0,01383978	0,08947577
ENSMUSG00000076501_Igkv2-137	0,646926589	10,8553969	5,99636998	0,01433534	0,08980706
ENSMUSG00000095197_Ighv1-59	-0,721533304	9,91442933	5,94771485	0,01473638	0,08980706
ENSMUSG00000102654_Ighv1-21	-1,201134567	7,45384167	5,93297185	0,01486016	0,08980706
ENSMUSG00000094087_Ighv1-61	-0,759887613	9,16421927	5,71295115	0,01684021	0,09960803

ENSMUSG00000094164_Ighv2-3	0,685587426	9,60526463	5,34609232	0,02076877	0,12028578
ENSMUSG00000103168_Gm30948	2,033469731	3,00730278	5,22282817	0,02229227	0,12408686
ENSMUSG00000106601_Ighv1-70	-1,381132688	5,69079483	5,22083902	0,02231778	0,12408686
ENSMUSG00000096594_Igkv8-19	0,632206719	11,1831626	5,11593087	0,02370714	0,12805691
ENSMUSG00000095170_Ighv8-11	-1,36949941	6,25424398	5,09802581	0,02395309	0,12805691
ENSMUSG00000094075_Ighv1-80	-0,620116103	10,0480177	4,95710873	0,02598362	0,13629142
ENSMUSG00000095981_Ighv10-1	-0,588829595	10,554939	4,81117145	0,02827582	0,1455681
ENSMUSG00000102888_Ighv1-11	-0,92138606	8,27124633	4,77202889	0,02892572	0,14620636
ENSMUSG00000095442_Ighv1-4	-0,663938949	9,15982116	4,71780225	0,02985187	0,14819323
ENSMUSG00000076589_Igkv8-18	0,947540018	8,36825993	4,62057115	0,03159072	0,15407403
ENSMUSG00000102952_Ighv1-25	-1,307576367	5,74547552	4,29499462	0,03822472	0,18321502
ENSMUSG00000095771_Igkv14-111	0,533274469	10,2864999	4,17979124	0,04090874	0,19275643
ENSMUSG00000105462_Igkv4-77	0,531311477	9,93846955	4,13771285	0,0419378	0,19431179
ENSMUSG00000076676_Ighv12-3	-0,687180345	9,13269173	4,10008879	0,04288096	0,19542471
ENSMUSG00000094198_Ighv1-50	-0,585001217	10,1161914	4,01208031	0,04517538	0,2005046
ENSMUSG00000094689_Ighv1-81	-0,584217099	10,9978384	3,99755463	0,04556633	0,2005046
ENSMUSG00000076621_Ighj1	0,884264822	14,4042261	3,97577047	0,04615933	0,2005046
ENSMUSG00000095589_Ighv1-55	-0,555040787	10,9645996	3,94440051	0,04702761	0,20113346
ENSMUSG00000094552_Ighd3-2	0,773590698	8,43986094	3,91042688	0,04798741	0,20212877
ENSMUSG00000096672_Ighv1-63	-0,763362468	8,82568421	3,76300446	0,05239835	0,21741404
ENSMUSG00000106599_Ighv1-73	-1,398410132	4,48734055	3,71656662	0,05387505	0,22025386
ENSMUSG00000102301_Ighv8-2	-0,936167637	7,69514926	3,5994213	0,05779969	0,23287411
ENSMUSG00000104213_Ighd	-0,659177666	9,88175883	3,47103318	0,06245229	0,24647816
ENSMUSG00000104769_Igkv8-34	0,941357387	7,02804306	3,443371	0,063506	0,24647816
ENSMUSG00000104452_Ighv8-8	-0,527043772	11,3098304	3,43480628	0,06383607	0,24647816
ENSMUSG00000095429_Ighv5-12	0,49803958	10,6063664	3,34159822	0,06754897	0,25724128
ENSMUSG00000076680_Ighv6-6	-0,527580202	9,7000838	3,21736697	0,07286074	0,27067816
ENSMUSG00000073028_Igkv4-71	-0,679573852	8,77448633	3,18170461	0,07446701	0,27067816
ENSMUSG00000076581_Igkv8-26	1,030033169	6,3041543	3,16804027	0,0750925	0,27067816
ENSMUSG00000096250_Ighd2-6	-0,587084644	10,4542299	3,10255832	0,07816936	0,27067816
ENSMUSG00000076606_Igkj3	0,640924259	11,5116641	3,09446147	0,07855914	0,27067816
ENSMUSG00000095127_Ighv1-82	-0,504245407	11,5938878	3,08994271	0,07877758	0,27067816
ENSMUSG00000102678_Ighv1-21-1	-1,004043452	5,873329	3,08886053	0,07882999	0,27067816
ENSMUSG00000094787_Ighv1-54	-0,5071661	9,60429213	3,08810393	0,07886666	0,27067816
ENSMUSG00000094420_Igkv10-96	-0,453739549	10,5607213	3,06213137	0,08013649	0,27168225
ENSMUSG00000095571_Ighv5-17	0,463357616	10,6474763	2,91762159	0,08761692	0,29001116
ENSMUSG00000094262_Igkv4-62	0,874528166	7,16048478	2,9054264	0,0882819	0,29001116
ENSMUSG00000106403_Igkv20-101-2	-1,082974466	6,07234901	2,88025985	0,08967155	0,29001116
ENSMUSG00000095761_Ighv1-20	-1,055689119	7,01745686	2,8776134	0,08981905	0,29001116
ENSMUSG00000103203_Gm37327	1,326136828	5,73368861	2,85504232	0,09108784	0,29001116
ENSMUSG00000103271_Ighv4-2	-0,806116273	7,60655197	2,80778994	0,09380753	0,29001116
ENSMUSG00000096078_Ighv1-62-2	1,001763931	7,45787547	2,80751714	0,09382348	0,29001116
ENSMUSG00000095794_Igkv6-17	0,429882915	10,4922438	2,79456216	0,0945846	0,29001116
ENSMUSG00000094134_Ighv5-15	0,492452966	9,2415781	2,78869158	0,09493171	0,29001116
ENSMUSG00000076731_Ighv8-12	-0,505490423	10,6615352	2,76956572	0,09607222	0,2903052
ENSMUSG00000076666_Ighv14-4	-0,439885409	10,9026793	2,64081998	0,10414978	0,31132944
ENSMUSG00000096844_Igkv6-14	0,598552395	8,88294692	2,58305221	0,10801321	0,31944331
ENSMUSG00000095630_Igkv6-23	-0,436742903	9,76588655	2,49506662	0,11420354	0,33403597
ENSMUSG00000094502_Ighv1-69	-0,406074466	10,2378681	2,47934131	0,11535055	0,33403597
ENSMUSG00000103873_Ighv1-38	-0,847369758	7,1242255	2,44680215	0,11776457	0,33688302
ENSMUSG00000104103_Gm9517	0,568057076	8,59524348	2,43363375	0,11875732	0,33688302
ENSMUSG00000093838_Ighv3-1	-0,524645867	8,89825088	2,36655136	0,12396063	0,34809146
ENSMUSG00000094094_Igkv5-45	0,397046687	10,0367108	2,30828563	0,12868591	0,35774684

ENSMUSG00000094345_Igkv14-126	-0,501278722	9,03501953	2,27166813	0,13175802	0,36266068
ENSMUSG00000096499_Ighv1-5	-0,41639089	11,0010588	2,2420177	0,13430563	0,36604867
ENSMUSG00000105906_Iglc1	0,697952416	15,6446864	2,2132972	0,13682596	0,36929724
ENSMUSG00000103989_Ighv5-21	1,185740316	3,696691	2,18464116	0,13939355	0,37260968
ENSMUSG00000095335_Igkv3-5	0,404687686	9,63444883	2,11418872	0,14593937	0,38639186
ENSMUSG00000095285_Ighv5-9	0,490247096	8,82247985	2,09121541	0,14814817	0,3869217
ENSMUSG00000076672_Ighv3-6	-0,439935206	11,6608676	2,08324695	0,1489231	0,3869217
ENSMUSG00000095204_Ighv1-52	-0,383154594	9,90330242	2,05735825	0,15147257	0,38990163
ENSMUSG00000105955_Igkv12-40	-0,831343442	7,37205575	2,01372719	0,15588195	0,39520584
ENSMUSG00000094993_Igkv4-51	0,54121124	8,50420195	2,00809557	0,15646162	0,39520584
ENSMUSG00000076543_Igkv4-74	-0,517388412	8,59620808	1,99520211	0,15779801	0,39520584
ENSMUSG00000105757_Ighv1-83	-0,840099243	5,46038142	1,97360712	0,16006551	0,39730545
ENSMUSG00000096498_Ighv2-5	0,376127475	9,99479459	1,93448397	0,16426871	0,4041301
ENSMUSG00000106668_Iglj1	0,65977613	16,2949127	1,8530564	0,17342833	0,42292173
ENSMUSG00000104712_Igkv4-75	-0,776275593	6,01635123	1,81471057	0,17794418	0,43016072
ENSMUSG00000076934_Iglv1	0,621829349	15,5288016	1,79752389	0,18001213	0,43140839
ENSMUSG00000103254_Ighv1-15	-0,420562261	9,70403143	1,6777382	0,19522526	0,46370708
ENSMUSG00000094433_Igkv5-43	0,335543925	10,727831	1,65992101	0,19761399	0,46370708
ENSMUSG00000076578_Igkv6-29	-0,702788094	7,42870741	1,65342567	0,19849332	0,46370708
ENSMUSG00000096355_Ighv8-4	-0,679160692	6,59248066	1,60774962	0,20480843	0,47447285
ENSMUSG00000095519_Ighv1-66	-0,500453107	8,57595717	1,57623443	0,20930393	0,4808801
ENSMUSG00000095889_Ighv1-58	-0,361396915	9,36345882	1,54469072	0,21392095	0,48435744
ENSMUSG00000076534_Igkv12-89	-0,410829361	8,95769102	1,54201517	0,2143181	0,48435744
ENSMUSG00000094174_Ighv6-4	0,870134735	4,21543851	1,52390026	0,21703022	0,48435744
ENSMUSG00000102765_Ighv1-62	-0,586863251	7,43619533	1,50140182	0,2204558	0,48435744
ENSMUSG00000105599_Gm9238	-0,786277568	5,27895761	1,46407662	0,2262826	0,48435744
ENSMUSG00000076940_Iglv2	0,535480051	13,8034696	1,46273654	0,22649521	0,48435744
ENSMUSG00000094319_Igkv4-54	0,346279984	9,38795044	1,45309118	0,22803259	0,48435744
ENSMUSG00000096108_Ighv11-2	-0,720556782	8,95932044	1,4509443	0,22837649	0,48435744
ENSMUSG00000076607_Igkj4	0,531183988	14,8029883	1,42745702	0,2321799	0,48435744
ENSMUSG00000093906_Igkv9-129	0,331344172	10,0123279	1,41938817	0,23350413	0,48435744
ENSMUSG00000104575_Igkv9-119	1,009895791	4,47058237	1,41429226	0,23434516	0,48435744
ENSMUSG00000076532_Igkv4-91	0,43127226	8,69238204	1,40767817	0,23544221	0,48435744
ENSMUSG00000076526_Igkv12-98	0,471417481	8,36153569	1,39581348	0,23742579	0,48435744
ENSMUSG00000076505_Igkv1-131	0,413437289	8,77375358	1,39337613	0,23783578	0,48435744
ENSMUSG00000105928_Gm9256	0,711054143	6,66474411	1,38232606	0,23970533	0,48435744
ENSMUSG00000104422_Ighv1-14	-0,92659312	3,8392428	1,38067141	0,23998681	0,48435744
ENSMUSG00000076733_Ighv8-13	-0,90725106	3,57763276	1,37803332	0,24043643	0,48435744
ENSMUSG00000076535_Igkv1-88	0,334989463	9,52801973	1,3625797	0,2430909	0,48494172
ENSMUSG00000093894_Ighv1-53	-0,331863888	10,3608133	1,35609585	0,24421525	0,48494172
ENSMUSG00000076583_Igkv8-24	-0,30269033	9,87016226	1,33342668	0,24819652	0,48882087
ENSMUSG00000094322_Ighv9-4	0,350445863	9,15944924	1,32506266	0,24968548	0,48882087
ENSMUSG00000096490_Igkv10-94	-0,364783491	9,55513238	1,2797716	0,25794151	0,49923956
ENSMUSG00000106428_Gm42667	0,596237557	6,8861137	1,27213745	0,25936608	0,49923956
ENSMUSG00000076533_Igkv4-90	-0,677187307	6,17758504	1,26657052	0,26041104	0,49923956
ENSMUSG00000096020_Ighv1-75	-0,323557453	10,70344	1,25715362	0,26219056	0,49923956
ENSMUSG00000076514_Igkv17-121	0,308582629	11,3131073	1,24171107	0,26514154	0,50142414
ENSMUSG00000094356_Igkv8-28	-0,310896373	9,53487803	1,21455404	0,27043208	0,50797377
ENSMUSG00000076550_Igkv4-63	0,347530991	8,90454381	1,12611662	0,28860519	0,53513966
ENSMUSG00000076522_Igkv16-104	0,271050448	10,2715059	1,12546645	0,28874442	0,53513966
ENSMUSG00000106039_Iglc4	0,626748129	6,10958567	1,08547482	0,29747602	0,54428012
ENSMUSG00000106372_Igkv14-126-1	0,640671539	5,10650691	1,08495374	0,29759201	0,54428012
ENSMUSG00000076580_Igkv8-27	0,315112972	10,7556421	1,06093665	0,30300165	0,55055202

ENSMUSG00000103290_Ighv1-23	-0,552986541	6,51221135	0,97457853	0,32354096	0,57933155
ENSMUSG00000106494_Igkv2-107	-0,679545597	4,49058185	0,97354072	0,32379872	0,57933155
ENSMUSG00000076652_Ighv7-3	-0,255794517	10,0408208	0,96834802	0,32509252	0,57933155
ENSMUSG00000094088_Ighv1-64	-0,276951909	10,8868825	0,95644203	0,32808494	0,5809402
ENSMUSG00000094124_Ighv1-74	-0,256971563	10,1565174	0,9407982	0,33207265	0,58263025
ENSMUSG00000105231_Iglj3	0,445552361	15,6411654	0,92919457	0,3350723	0,58263025
ENSMUSG00000079543_Igkv13-85	0,263507337	9,54336062	0,92231842	0,33686697	0,58263025
ENSMUSG00000094194_Ighv5-16	0,26056316	9,81106463	0,92019966	0,33742255	0,58263025
ENSMUSG00000094797_Igkv6-15	0,271672034	10,5824756	0,89871219	0,34312725	0,58882331
ENSMUSG00000076562_Igkv4-50	-0,24157172	10,1554421	0,87299281	0,3501281	0,597151
ENSMUSG00000095079_Igha	0,622972057	7,81467079	0,84951311	0,35669011	0,60358819
ENSMUSG00000096452_Ighv1-77	-0,290538096	9,18020159	0,84403681	0,35824479	0,60358819
ENSMUSG00000095592_Ighd5-7	-0,649330507	5,00801704	0,81973547	0,36525752	0,61064709
ENSMUSG00000095200_Ighv1-7	-0,260085741	10,1568173	0,80668439	0,36910233	0,61064709
ENSMUSG00000076564_Igkv12-46	-0,244995	9,76198843	0,80287265	0,37023588	0,61064709
ENSMUSG00000076594_Igkv6-13	0,272287622	9,23379843	0,79116689	0,37374752	0,61064709
ENSMUSG00000094505_Ighv8-6	0,472182721	6,48449882	0,78362143	0,37603586	0,61064709
ENSMUSG00000096805_Ighv9-1	0,259736521	10,0325341	0,77611813	0,37833099	0,61064709
ENSMUSG00000076523_Igkv15-103	0,241075804	9,57426012	0,77426322	0,37890141	0,61064709
ENSMUSG00000076577_Igkv8-30	0,251965001	9,6721933	0,77067926	0,380007	0,61064709
ENSMUSG00000095007_Igkv12-41	-0,233280903	9,65325154	0,73154946	0,39238141	0,62690823
ENSMUSG00000076538_Igkv13-84	0,308077386	8,80405391	0,69754677	0,40360925	0,6348118
ENSMUSG00000076525_Igkv1-99	-0,481681387	6,00351146	0,69718639	0,40373073	0,6348118
ENSMUSG00000105123_Ighv1-79	-0,491407698	5,3351094	0,69326074	0,40505749	0,6348118
ENSMUSG00000094006_Igkv4-59	0,21216088	10,3393884	0,68912478	0,40646223	0,6348118
ENSMUSG00000076709_Ighv1-47	-0,229032973	9,68623755	0,67518375	0,41125013	0,63707238
ENSMUSG00000076608_Igkj5	0,377073531	15,486796	0,67160409	0,41249291	0,63707238
ENSMUSG00000102524_Ighv1-2	-0,254762567	9,13168914	0,64354316	0,42243067	0,64881617
ENSMUSG00000118182_Gm50427	-0,442921533	6,01716163	0,61649833	0,43235151	0,65967763
ENSMUSG00000096638_Ighv2-9	0,234766291	9,19876365	0,60414049	0,43700259	0,65967763
ENSMUSG00000076615_Ighg3	-0,561090699	4,2901392	0,60395397	0,43707337	0,65967763
ENSMUSG00000104975_Iglj2	0,753599928	14,6635427	0,59375423	0,44097104	0,65967763
ENSMUSG00000095682_Igkv3-1	0,312557013	8,17792018	0,59272568	0,44136705	0,65967763
ENSMUSG00000076518_Igkv2-112	0,263756771	8,85308283	0,57980687	0,44638803	0,66361429
ENSMUSG00000094478_Igkv3-3	0,416937855	5,93614304	0,55996014	0,4542763	0,6665364
ENSMUSG00000104679_Igkv4-60	0,31541137	7,98018412	0,55786806	0,45512051	0,6665364
ENSMUSG00000105781_Igkv8-31	-0,558734137	3,96971686	0,55489596	0,45632408	0,6665364
ENSMUSG00000076591_Igkv8-16	0,20319541	10,7337683	0,55091499	0,45794407	0,6665364
ENSMUSG00000105547_Iglc3	0,339635191	15,1081855	0,54347477	0,46099623	0,66748412
ENSMUSG00000094315_Igkv4-78	0,248892032	8,89086979	0,5287429	0,46713585	0,67286925
ENSMUSG00000076617_Ighm	0,348183033	17,3514804	0,51663129	0,47228223	0,67677556
ENSMUSG00000095565_Ighv2-9-1	0,184258808	10,0521685	0,48983886	0,48399919	0,6861848
ENSMUSG00000106630_Igkv2-116	0,338122031	7,19670815	0,4792497	0,48876237	0,6861848
ENSMUSG00000106256_Igkv12-47	0,405542736	5,95829757	0,47543499	0,49049739	0,6861848
ENSMUSG00000104533_Igkv5-40-1	0,375379991	6,26698921	0,47494428	0,49072132	0,6861848
ENSMUSG00000076540_Igkv4-80	-0,281333597	8,40302214	0,47191206	0,49210884	0,6861848
ENSMUSG00000105606_Igkv2-109	0,245014201	8,63256957	0,4685432	0,49365813	0,6861848
ENSMUSG00000096715_Igkv3-4	0,198274599	9,23296256	0,45416514	0,5003636	0,68954181
ENSMUSG00000076710_Ighv1-49	-0,340366322	7,30480647	0,45274563	0,50103397	0,68954181
ENSMUSG00000076547_Igkv4-70	0,246010923	8,4109251	0,41864495	0,51761396	0,70727918
ENSMUSG00000096326_Ighv1-78	-0,317656718	11,8539838	0,41585893	0,51901062	0,70727918
ENSMUSG00000076609_Igkc	0,291222181	16,7502319	0,37662463	0,53941523	0,73149968
ENSMUSG00000094102_Ighv9-2	-0,170329386	9,43557026	0,34528378	0,55679508	0,75140308

ENSMUSG00000076512_Igkv9-123	0,271666192	7,48862618	0,33483406	0,56282639	0,75352941
ENSMUSG00000076556_Igkv4-57	0,154728655	10,5094676	0,33318133	0,56379179	0,75352941
ENSMUSG00000105432_Gm43218	0,148564981	10,3498374	0,30389826	0,58144882	0,76992341
ENSMUSG00000096833_Igkv4-55	0,14409403	10,0273607	0,30214115	0,58254321	0,76992341
ENSMUSG00000076549_Igkv4-68	-0,141048878	10,5684415	0,29922876	0,58436633	0,76992341
ENSMUSG00000076555_Igkv4-57-1	-0,262436959	7,71067725	0,2867031	0,59234105	0,77674911
ENSMUSG00000076552_Igkv4-61	-0,186117332	8,66037059	0,2755353	0,59964258	0,7826321
ENSMUSG00000094509_Ighv14-1	-0,189970368	8,69376466	0,26431842	0,60716874	0,78875192
ENSMUSG00000105605_Ighv1-86	-0,361815371	4,23368518	0,2555706	0,61317967	0,79285558
ENSMUSG00000076688_Ighv15-2	-0,149383467	9,48570109	0,24924357	0,61760821	0,79488464
ENSMUSG00000076563_Igkv5-48	-0,139570571	9,40559736	0,24004421	0,62417419	0,79963329
ENSMUSG00000106239_Gm9260	0,287001875	5,16385006	0,21634036	0,64184264	0,81408531
ENSMUSG00000102364_Ighv8-5	-0,161869405	8,99789554	0,21510133	0,64279808	0,81408531
ENSMUSG00000076655_Ighv4-1	-0,121571431	10,5384202	0,20891783	0,64761693	0,81408531
ENSMUSG00000105363_Igkv11-114	0,240278976	6,34800144	0,20184216	0,653238	0,81408531
ENSMUSG00000098814_Igkv19-93	0,124634903	11,778665	0,19659474	0,65748363	0,81408531
ENSMUSG00000096670_Ighv2-6	0,155854184	8,76412662	0,19629158	0,65773097	0,81408531
ENSMUSG00000076677_Ighv6-3	-0,120845008	11,0785089	0,19193504	0,66131095	0,81408531
ENSMUSG00000076618_Ighj4	-0,186959068	14,1884986	0,1901091	0,66282583	0,81408531
ENSMUSG00000094335_Igkv1-117	0,114967801	10,8050238	0,18932363	0,66348015	0,81408531
ENSMUSG00000094491_Igkv1-133	0,139406554	9,00614621	0,18474283	0,66732862	0,81408531
ENSMUSG00000093876_Ighd5-3	0,276261958	6,71784344	0,18210758	0,66956824	0,81408531
ENSMUSG00000076665_Ighv7-1	-0,120348616	9,50395325	0,1809064	0,67059545	0,81408531
ENSMUSG00000106387_Igkv4-73	-0,137780003	9,07078641	0,17708438	0,67389094	0,81452905
ENSMUSG00000076605_Igkj2	0,176885429	15,0225811	0,1568367	0,69208575	0,82639415
ENSMUSG00000076530_Igkv11-106	-0,18736427	7,45791349	0,15563006	0,6932121	0,82639415
ENSMUSG00000096632_Igkv9-124	-0,108582598	10,6291738	0,15468461	0,69409819	0,82639415
ENSMUSG00000095497_Igkv1-122	-0,12694671	9,0595918	0,14999015	0,69854477	0,82639415
ENSMUSG00000076587_Igkv6-20	-0,162908938	8,54752757	0,14996313	0,6985706	0,82639415
ENSMUSG00000096580_Igkv1-132	0,186139319	7,36224049	0,13940096	0,70887726	0,833794
ENSMUSG00000095753_Igkv4-53	-0,095777546	10,2749611	0,13745493	0,71082438	0,833794
ENSMUSG00000076541_Igkv4-79	0,121632105	8,9398792	0,12051305	0,72847871	0,85091211
ENSMUSG00000106405_Iglj3p	0,191227185	7,8650562	0,11487126	0,734665	0,85454758
ENSMUSG00000076573_Igkv1-35	0,209845865	4,76780112	0,11113314	0,73885774	0,85584355
ENSMUSG00000076576_Igkv6-32	-0,080550462	10,1078751	0,10026057	0,75151717	0,86499685
ENSMUSG00000105499_Igkv3-11	0,180479765	5,86457245	0,09896565	0,75307444	0,86499685
ENSMUSG00000076604_Igkj1	0,137928839	15,023093	0,09648083	0,75609437	0,86499685
ENSMUSG00000102381_Ighv8-7	0,18465745	5,86355052	0,08499911	0,77063371	0,8780171
ENSMUSG00000076548_Igkv4-69	-0,093399629	9,04179871	0,08116068	0,77573061	0,88021678
ENSMUSG00000096577_Ighv1-71	0,092346246	8,9955719	0,07753822	0,78066167	0,88037455
ENSMUSG00000095633_Igkv4-58	-0,094153211	9,70899731	0,076424	0,78220329	0,88037455
ENSMUSG00000076674_Ighv3-8	0,073361619	10,1637542	0,07076587	0,79022492	0,88581665
ENSMUSG00000095351_Igkv3-2	-0,065360601	10,2199948	0,06734516	0,79524219	0,88669299
ENSMUSG00000096767_Ighv1-62-3	-0,086999961	8,90785895	0,06591124	0,79738578	0,88669299
ENSMUSG00000076619_Ighj3	-0,101747365	14,1264234	0,05606735	0,81282324	0,89282621
ENSMUSG00000076571_Igkv5-37	-0,144791447	5,6630405	0,05508074	0,81444712	0,89282621
ENSMUSG00000095642_Ighv14-3	-0,059290379	10,1187981	0,05482572	0,81486936	0,89282621
ENSMUSG00000104742_Igkv9-128	-0,1921414	4,40318622	0,05429723	0,81574769	0,89282621
ENSMUSG00000076572_Igkv18-36	0,109422805	6,83412762	0,04664122	0,82901443	0,90073515
ENSMUSG00000091087_Ighv8-14	-0,185163176	2,99762025	0,046398	0,82945395	0,90073515
ENSMUSG00000094872_Igkv9-120	0,055844358	11,1235654	0,04353472	0,83472167	0,9029285
ENSMUSG00000076614_Ighg1	-0,138190691	3,9784508	0,03993818	0,8416015	0,90497231
ENSMUSG00000076536_Igkv4-86	-0,053758181	9,86559969	0,03916523	0,84312168	0,90497231

ENSMUSG00000096422_Igkv12-44	0,048912709	10,0671197	0,03659978	0,84828218	0,90700941
ENSMUSG00000094902_Igkv10-95	-0,049115534	10,055638	0,03466202	0,85230565	0,90781982
ENSMUSG00000093861_Igkv1-110	0,043759949	10,0831495	0,02841619	0,86613407	0,91902776
ENSMUSG00000106667_Igkv3-6	-0,105053915	4,13129792	0,02306254	0,87929456	0,92760834
ENSMUSG00000076508_Igkv17-127	0,03972502	11,4242513	0,02131987	0,88391092	0,92760834
ENSMUSG00000076586_Igkv8-21	0,04034298	9,71480056	0,01913409	0,88998276	0,92760834
ENSMUSG00000102901_Ighv5-1	0,071624359	6,66648494	0,01799088	0,89329972	0,92760834
ENSMUSG00000102535_Ighv1-41	-0,0722863	6,75060593	0,01768225	0,89421346	0,92760834
ENSMUSG00000076939_Iglv3	0,055580193	13,3533477	0,01767294	0,89424114	0,92760834
ENSMUSG00000103939_Ighv3-4	0,077553904	6,27476052	0,01499839	0,90252844	0,93272456
ENSMUSG00000096459_Ighv9-3	-0,029310753	12,2720502	0,00813855	0,92811722	0,95561699
ENSMUSG00000095210_Ighv5-9-1	0,022084337	9,94400644	0,00651178	0,93568404	0,959853
ENSMUSG00000076569_Igkv5-39	-0,013586154	11,1590319	0,00255699	0,95967083	0,98084003
ENSMUSG00000076545_Igkv4-72	-0,01190012	9,09632534	0,00147271	0,96938801	0,98401258
ENSMUSG00000106016_Igkv4-56	0,017566271	7,48033277	0,00142818	0,96985412	0,98401258
ENSMUSG00000095583_Ighv14-2	0,006201916	10,4775504	0,00052578	0,98170627	0,98975896
ENSMUSG00000076539_Igkv4-81	0,011010796	7,27230913	0,00047355	0,9826384	0,98975896
ENSMUSG00000094930_Igkv6-25	0,003325808	9,72610993	0,00015357	0,99011252	0,99366989
ENSMUSG00000076646_Ighv2-6-8	-0,003638691	7,72934721	6,29E-05	0,99366989	0,99366989

Supplementary Table 4. **Accessible regions overlap enrichment analysis**

qSample [a]	tSample [b]	qLen [c]	tLen [d]	N_OL [e]	N_OL (%qLen) [f]	p-value [g]	p-adjust [h]
HM19_MACS2	HM19_HOMER	13208	15373	11292	85%	9.9e-06	9.9e-06
HM21_MACS2	HM21_HOMER	16329	23839	13045	80%	9.9e-06	9.9e-06
HL89_MACS2	HL89_HOMER	27352	24700	21791	80%	9.9e-06	9.9e-06
HL90_MACS2	HL90_HOMER	57739	68357	52263	90%	9.9e-06	9.9e-06

[a] Query ATAC-seq sample, [b] Target ATAC-seq sample, [c] Number of query peaks, [d] Number of target peaks, [e] Number of overlapped peaks between query and target, [f] Percentage of overlapped peaks, [g] calculated p-value by ChIPseeker, [h] p-value correction (FDR) according to the Benjamini and Hochberg method. The values were obtained using the ChIPseeker command enrichPeakOverlap(queryPeak=file1, targetPeak=file-list, TxDb= TxDb.Mmusculus.UCSC.mm10.knownGene, pAdjustMethod="BH", nShuffle=10000, chainFile=NULL, verbose=FALSE) and a number of randomly permutations in the genomic locations of 10000.